Fakultät für Medizin

Institut für Pathologie

Cold atmospheric plasma decontamination against nosocomial bacteria

Tobias G. Klämpfl, Dipl.-Ing. (Univ.)

Vollständiger Abdruck der von der Fakultät für Medizin der Technischen Universität München zur Erlangung des akademischen Grades eines

Doctor of Philosophy (Ph.D.)

genehmigten Dissertation.

Vorsitzender: Univ.-Prof. Dr. Dr. Stefan Engelhardt

Betreuer: Univ.-Prof. Dr. Jürgen Schlegel

Prüfer der Dissertation:

1. apl. Prof. Dr. Dr. h.c. Gregor E. Morfill,

   Ludwig-Maximilians-Universität München

2. Univ.-Prof. Dr. Dirk Busch

Die Dissertation wurde am 15.01.2014 bei der Fakultät für Medizin der Technischen Universität München eingereicht und durch die Fakultät für Medizin am 14.02.2014 angenommen.

ABSTRACT

Nosocomial pathogens are a considerable public threat, which cause high morbidity, mortality and costs. In order to prohibit their spread, alternative and more efficient decontamination strategies are demanded. Cold atmospheric plasma (CAP) gains rising attention with its promising antimicrobial properties, appropriate also for the treatment of heat-sensitive materials. CAP is physical plasma containing a cocktail of chemically reactive species that is generated at ambient pressure.

My work addressed different important aspects of a CAP system based on the Surface micro-discharge (SMD) technology. This involved its development, characterization, decontaminating efficiency and factors influencing it. SMD air plasma showed bactericidal and sporicidal potential at the kinetic studies, according to European standard methods for sterilizing and disinfecting agents. Thereby, it was highly effective in the inactivation of conventional biological indicators as well as of endospores of *Clostridium difficile* due to the synergy between various plasma species (such as ROS/RNS, electric field). Furthermore, electron microscopy revealed that the microbicidal action was limited by the degree of contamination. For these reasons and due to the high toxic ozone concentration, the use of pre-cleaned instruments inside a closed volume is a prerequisite for adequate disinfection and safety.

In conclusion, my work improves strongly the understanding about the decontaminating action of SMD air plasma. It will serve as an alternative decontaminating agent and contribute to the prevention of nosocomial infections in the future. Important will be to validate an up-scaled device suitable for practical use, to solve handling issues and gain measurable additional effect compared to common methods.

ZUSAMMENFASSUNG

Nosokomiale Pathogene stellen eine ernsthafte öffentliche Bedrohung dar. Um ihre Ausbreitung zu verhindern, sind alternative und effiziente Dekontaminierungsstrategien notwendig. Kaltes atmosphärisches Plasma (CAP) erhält durch seine vielversprechenden antimikrobiellen Eigenschaften und der zugleich geeigneten Anwendung auf hitzeempfindlichen Materialen steigende Aufmerksamkeit. CAP ist physikalisches Plasma, das aus einem Cocktail von chemisch reaktiven Spezies besteht und bei Umgebungsdruck erzeugt wird.

Ich untersuchte unterschiedliche, wichtige Aspekte eines CAP Systems, basierend auf der Technologie von Oberflächenmikroentladungen (SMD). Dies umfasste ihre Entwicklung, Charakterisierung, dekontaminierende Effizienz und Faktoren, die diese beeinflussen. SMD Luftplasma bewies in kinetischen Studien, gemäß europäischer Standardmethoden, sein bakterizides und sporizides Potential. Dabei inaktivierte es sehr effektiv Bioindikatoren als auch *Clostridium difficile* Endosporen wegen der Synergie von verschiedenen Plasmaspezies (wie ROS/RNS, elektr. Feld). Zudem zeigten elektronmikroskopische Aufnahmen, dass die mikrobizide Wirkung von dem Grad der Kontaminierung abhängig war. Aus diesen Gründen und wegen der hohen toxischen Ozonkonzentration ist das Behandeln von vorgereinigten medizinischen Geräten in einem geschlossenen Raum für eine adäquate Desinfektion und Sicherheitsgewährleistung erforderlich.

Zusammenfassend verbessert meine Arbeit stark das Verständnis über die dekontaminierende Wirkung von SMD Luftplasma. Es könnte zukünftig alternativ eingesetzt werden und die Vermeidung von nosokomialen Infektionen unterstützen. Bedeutend werden dabei das Validieren eines für die Praxis geeigneten Plasmageräts, das Lösen von Handhabungsproblemen und das Erlangen eines messbaren zusätzlichen Nutzens gegenüber herkömmlichen Methoden sein.

TABLE OF CONTENTS

„All Ding‘ sind Gift und nichts ohn‘ Gift;
allein die Dosis macht,
dass ein Ding kein Gift ist.“
(Paracelsus, ca. 1538)

ABBREVIATIONS

APPJ	atmospheric pressure plasma jet
BSA	bovine serum albumin
CAP	cold atmospheric plasma
CDC	Center for Disease Control and Prevention
cfu	colony forming units
DBD	dielectric barrier discharge
DC	direct current
DIN	Deutsches Institut für Normierung
DLR	Deutsches Luft- und Raumfahrtzentrum
DSMZ	German Collection of Microorganisms and Cell Cultures
D-value	decimal reduction value
ECDC	European Center for Disease Control and Prevention
EDX	Energy-Dispersed X-Ray Spectroscopy
EN	European norm
ESBL	extended-spectrum β-lactamase
FE-DBD	floating-electrode DBD
FP2.0	FlatPlaSter 2.0
IHPH	Institute for Hygiene and Public Health
IPP	Max-Planck-Institute for Plasma Physics
MPE	Max-Planck-Institut for extraterrestrial Physics
MRSA	methicillin-resistant *Staphylococcus aureus*
MO	microorganism
MW	microwave
OES	Optical Emission Spectroscopy
PBS	phosphate buffered saline solution
PE	polyethylene
PET	polyethylene terephthalate
PP	polypropylene
PVC	polyvinylchloride
RF	radiofrequency
SAL	sterility assurance level
SASP	small acid-soluble protein
SEM	Scanning Electron Microscopy
SMD	surface micro-discharge
SS	physiological saline solution
TBS	tris buffered saline
TSB	tryptic soy broth
TUM	Technische Universität München
VRE	vancomycin-resistant Enterococcus
WD	working distance
UV	ultraviolet light

SYMBOLS

A	area
C	capacitance
c	concentration
d	dielectric thickness
d_A	length of electron avalanche
D_T	decimal reduction value at temperature T
E	electric field strength
e	elementary charge
f	repetition frequency (externally applied)
g	gap distance
h	Planck´s constant
I	current
I_0	transmitted light intensity without absorption
I_A	transmitted light intensity after absorption
L	absorption path length
N	number of bacteria
N_e	electron number
N_L	Loschmidt´s number
$Ø$	diameter
p	pressure
P	plasma power
Q	charge
r_A	head radius of an electron avalanche
t	treatment time
T	temperature
U	voltage
v	light frequency
α	ionization coefficient
ε_0	electric field constant
ε_r	relative dielectric permittivity
λ	wavelength
σ_λ	absorption cross-section at specific wavelength λ

1 INTRODUCTION

1.1 What is Physical Plasma?

The term “plasma” for an ionized gas was introduced in 1927, for the first time by Irving Langmuir (1881-1957) [1]. The American chemist, who won the Nobel Prize for his great achievements in surface chemistry in 1932, studied electric discharges and their fluid characteristics at General Electric Research and Development Center. The way these electrified fluids transported high-velocity electrons, molecules and ions of gas impurities reminded him of the transport process of red and white corpuscles and germs in blood plasma. Since that time plasma has also been used as a term in physics, which induced incomprehension and resistance in the medical field, and paved its determinant way through astrophysical science. It is assumed that 99% of the universe contains of plasma such as solar corona, solar wind, nebula, earth´s ionosphere and therefore, many physical processes require the understanding of terrestrial and extraterrestrial plasmas. Natural plasma phenomena occur on earth as lightning and the *aurora borealis*, a diffuse light displayed on the sky close to polar circles, when high energetic charged particles originating from solar wind and the magnetosphere collide with atoms in the atmosphere.

Conventionally, physical plasma is associated as the fourth state of matter. With rising energy input to a system such as by heating, matter can pass through states following higher degrees of freedom from the solid, through the liquid and to the gaseous state. Higher energy levels (e.g. by electric power) can even lead to the separation of gas molecule constituents in freely moving charged particles (electrons and ions) forming a quasi-neutral, though electrically conductive plasma with same densities of positive and negative charges (Figure 1.1). Accelerated electrons provide the basis for further excitation, dissociation and reaction processes upon collision

with other bodies that leads to the multicomponent nature of plasma: electrons, ions, excited molecules, neutrals like radicals and light. Further properties of plasma include a gas temperature range from room to solar temperature, electron densities from 10^6 - 10^{18} cm^{-3} and electron temperatures from 1 eV - 20 keV (1 eV ≈ 10^4 K) [2].

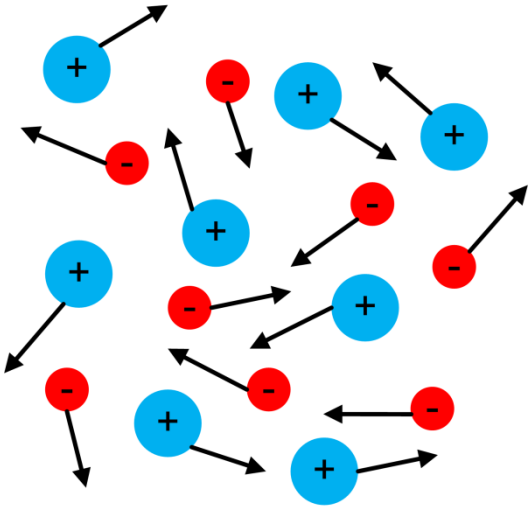

Figure 1.1: Schematic view of plasma with freely moving charges.

1.2 Cold Atmospheric Plasma (CAP)

There are two major categories of plasma systems: Thermal and non-thermal ones [3]. In thermal plasma, the gas temperature and the electron temperature are equal because of the complete ionization of a gas (T_e = T_g). This kind of plasma reaches very high temperatures and takes part for instance in natural thermonuclear fusion reactions of hydrogen nuclei into helium within the sun, from which it derives its energy. Arc discharges and microwave plasmas are derived from terrestrial plasma systems usually associated as thermal plasmas [4], since Joule heating and thermal ionization take place at high pressures [5]. In contrast, non-thermal plasma is a weakly ionized gas far from thermodynamic equilibrium. While electron temperature is 1-10 eV, electrons are not able to transfer their entire kinetic energy gained from

an externally applied electric field onto bigger particles and thus the gas remains non-thermal ($T_e >> T_g$; $T_g \approx$ 300 - 1000 K [4]). Non-thermal plasma can be generated in different ways: by the use of low pressure, low applied power, a pulsed discharge system and/or additional cooling of the gas. The term cold atmospheric plasma describes a sub-group of non-thermal plasma solely at atmospheric pressure with gas temperatures mainly below 425 K [6].

1.2.1 Discharges at atmospheric pressure

Atmospheric pressure plasmas can be classified into one of the three general discharge types (Figure 1.2):

- Corona discharges
- Glow discharges
- Arc discharges

Corona discharges (direct current (DC) or pulsed) are a typical source of non-thermal plasma. They have a weakly luminous and non-uniform appearance at atmospheric pressure preferably in the vicinity of sharp edges, points or thin wires that assure a high enough electric field. Their applications involve among many others ozone generation for water disinfection, removal of volatile organic compounds from waste gases and the enhancement of surface adhesion of thin polymer films. In contrast, glow discharges are luminous and characterized by a uniform and continuous glow. At atmospheric pressure, glow discharges are realized most of the time in form of plasma jets (DC to gigahertz), where electrodes are positioned inside a chamber, flow of a noble gas is ionized and transported outside the chamber forming a jet. Plasma-enhanced chemical vapour deposition of thin films is a particular process that utilizes plasma jets. As mentioned before, arc discharges are a source of thermal

plasma. Their discharges are usually self-sustaining discharges (DC or microwave) with low cathode fall voltage and an intensive thermionic field emission of electrons which causes very high current fluxes. Arcs have a long history in metallurgy (welding, cutting) and in illuminating devices.

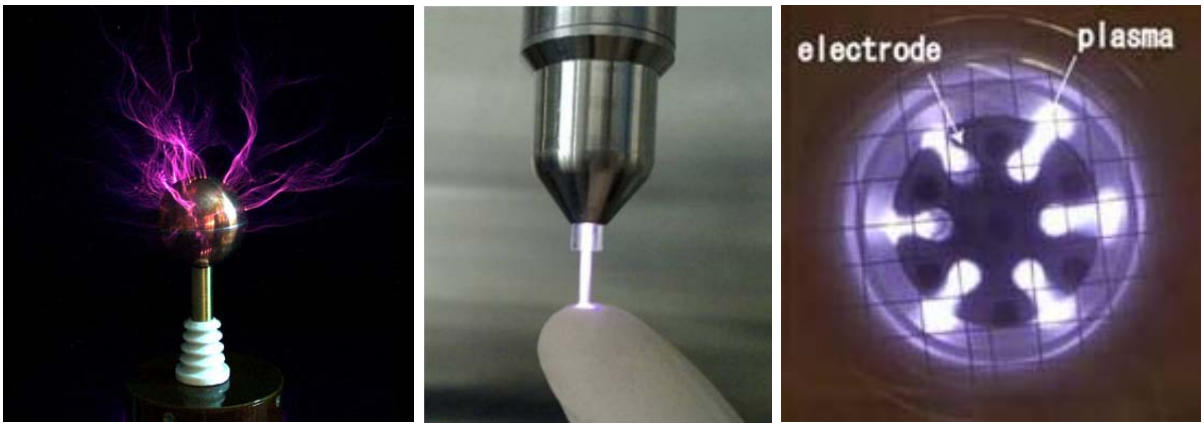

Figure 1.2: Atmospheric pressure discharges: corona [7], glow [8] and arc [9] (from left to right).

All three discharge types have been subject of inventions and investigations in regards of CAP devices aiming for biomedical applications for about fifteen years. Even plasma species from thermal arc or also glow discharges can be cooled down to such a degree that the remote treatment of thermo-sensitive organic matter like tissue or single cells does not result in thermal destruction. Topics and devices in the field of plasma medicine are introduced later (Section 1.3). In the following, the plasma technology used in this study is described in detail first.

1.2.2 Surface Micro-Discharge technology

Surface micro-discharges (SMDs) were used as non-thermal non-equilibrium plasma during this work. The generation of SMDs at ambient pressure is derived from the dielectric-barrier discharge (DBD) technology which is related to the corona discharge family and has been known for more than 150 years, notably much longer

than the term plasma itself. Many descriptions in this section are based on the review of Kogelschatz [10].

1.2.2.1 Historical background

Historically, Siemens was the first investigator that conducted experiments with DBDs in 1857 [11]. His goal was to produce ozone and he achieved it by implementing a novel set-up of discharge apparatus, which included the arrangement of the electrodes outside the plasma chamber and not in contact with the plasma. The discharge originated from a flow of oxygen or air at atmospheric pressure and was maintained in a narrow circular gap between two coaxial glass tubes by an alternating voltage of sufficiently high amplitude. Since the glass walls limited the electric current from passing as the dielectric barrier, this discharge type is commonly referred as DBD. It is also frequently assigned as silent discharge due to the absence of sparks, which are characterized by local overheating and the formation of local shock waves and noise [12]. Silent discharges became an important research field for the formation of ozone and nitrogen oxides for the next decades [13, 14]. Warburg investigated the nature of silent discharges during that period [15, 16]. Buss proved that numerous bright current filaments are characteristic for discharges, when atmospheric-pressure air breaks down between planar parallel electrodes covered by dielectric material [17]. He was also the first that recorded these micro-discharges photographically (Lichtenberg figures) as well as the current and voltage with an oscilloscope. Subsequently, many researchers devoted themselves to study the properties of these filamentary structures [18-23]. In 1943, Manley suggested a method for the determination of the power consumption in DBDs employing closed

voltage Lissajous figures and established an equation known as the power formula for ozonizers [24].

Becker and Otto laid with their important contributions the basis for the industrial application of DBDs as ozone generators in the first half of the 20th century [25-27], which had been the major application used mainly in water treatment until the '90s [10]. Nowadays, DBDs are utilized in a wide-ranged industrial scale. They combine the advantages of non-equilibrium plasma properties with the ease of being up-scaled under atmospheric pressure. At the same time power supplies become increasingly efficient and cost-effective. In addition, better understanding of the physical and chemical processes in ozonizers introduced beside improved ozone generators new industrial applications including surface treatment, pollution control, ultraviolet excimer lamps, excimer based mercury-free fluorescent lamps, high power CO_2 lasers and flat large-area plasma displays. More recently, research on atmospheric DBDs has been directed into biomedical applications by Kelly-Wintenberg et al. with the sterilization of matter [28], followed by initial and promising investigations on cells and living tissue by Fridman et al. [29].

1.2.2.2 Physical properties of barrier discharges

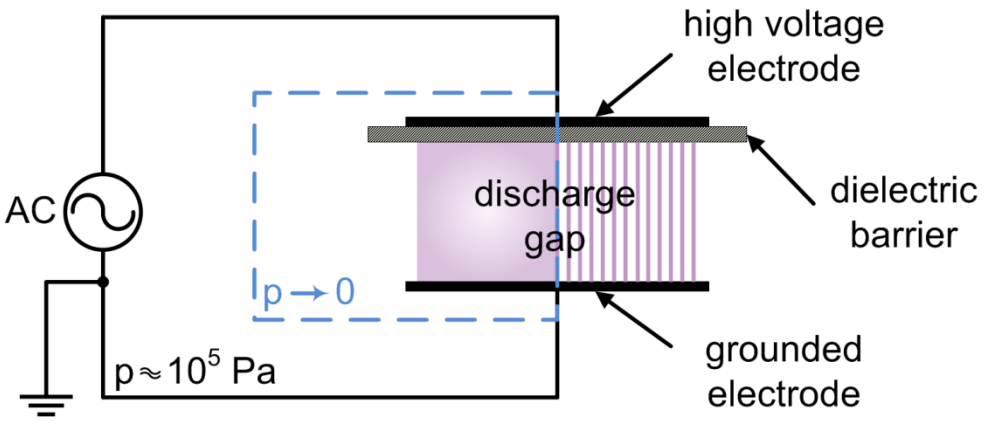

Figure 1.3: Typical basic configuration of a DBD system.

A typical DBD configuration is depicted in Figure 1.3 and typical operation conditions are summarized in Table 1.1. Two planar electrodes are positioned in parallel with a gap and at least one dielectric barrier in-between. The use of a dielectric barrier functioning as an insulator requires alternating current for the operation, since DC cannot be passed. The amount of current that can pass through a dielectric depends on the dielectric constant and thickness as well as the time derivative of the applied voltage. The electric field has to be sufficiently high to induce electrical breakdown in the gas (100 to 200 Td [30, 31]). The material of the dielectric vary from ceramic, glass, silica glass and other insulating materials such as thin polymer films. Since the dielectric property of current restriction declines at very high frequencies, DBDs are usually operated between low and high radiofrequency range. High voltage (kV range) is required to initiate gas discharges in the gap. As the electric field in the discharge gap reaches an adequately high level to induce breakdown, an abundant number of filamentary micro-discharges are observed in most gases at atmospheric pressures preferred for ozone generation and excimer discharges. Plasma is formed only as micro-discharges in such mode carrying low current and surrounded by a neutral gas. The gas absorbs the dissipated plasma energy and transports the long-living plasma species (heat and mass transfer). The discharge gas can be provided in a flow through the DBD, by recirculation or by complete encapsulation. If the gas is ambient air, standalone application is possible without the need of technical fluid provision.

Table 1.1: Typical operation parameters of a DBD and of the SMD in this work.

Parameter	typical range [10, 30]	study range
Electric field strength *E* of breakdown	100 - 200 Td	*not defined*
Repetition frequency *f*	50 Hz - 10 kHz	0.5 - 6 kHz
Voltage *U*	3 - 20 kV_{pp}	8.5 - 10 kV_{pp}
Pressure *p*	1 - 3 bar	~ 1 bar
Gap distance *g*	<0.1 mm - several cm	0 - 10 mm (from electrode edges to dielectric surface)
Dielectric material	glass, ceramic, polymers, etc.	Teflon®
Thickness *d*	0.5 - 2 mm	0.5 mm
relative dielectric permittivity ε_r	5-10 (glass) - 7000 (ferroelectrics)	2.0 - 2.1

Other DBD configurations include annular discharge gaps between cylindrical electrodes or the waiver on a conventional discharge gap by using a mesh-like structured electrode (Figure 1.4). Whereas the usual DBD discharge generates volumetric plasma, the latter SMD configuration provides surface plasma with a filamentous discharge pattern. The mesh-like structure of an electrode enables the formation of little plasma channels along the edges of the mesh and the dielectric barrier surface. Unlike depicted in Figure 1.4, micro-discharges do not exceed the thickness of the mesh. Local ion or heat damage of sensitive targets can be excluded due to the remote treatment position. The target is positioned downstream and affected mainly by long-lived plasma species. The discharge surface can even be touched by bare skin without problems, because current flux is very low. Study parameters are indicated in Table 1.1.

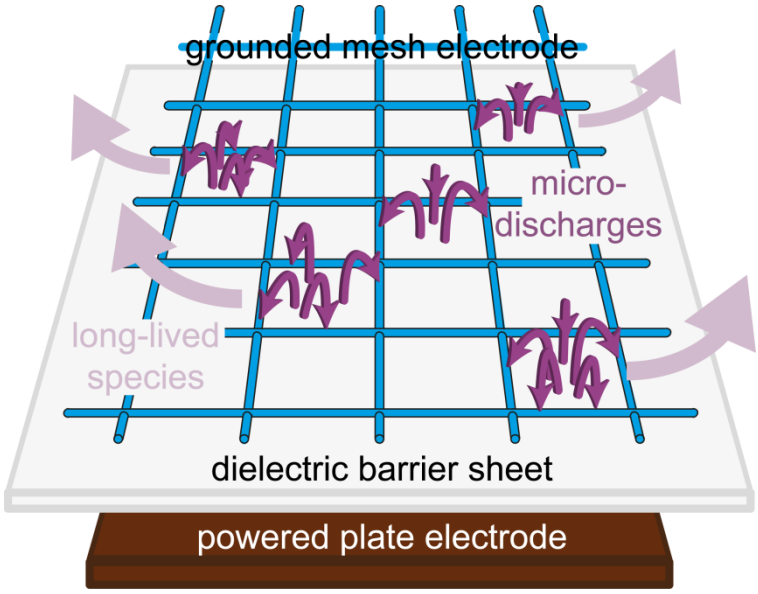

Figure 1.4: Schematic view of the SMD electrode system used in this study.

1.2.2.3 Entity of micro-discharge formation

The formation of filamentous micro-discharges is expected for gases that are forced into electrical breakdown in DBD settings at atmospheric pressure. Beside the filamentary mode though exists the mode of homogeneous diffuse glow discharges, which occur under certain conditions [32, 33]. Diffusive glow discharges are typically generated at lower pressures below 100 Pa (Figure 1.3) and have been applied in various fields, especially the semiconductor and medical device industry for the patterning by plasma etching or for the thin film formation by plasma deposition processes. However, short-lived plasma filaments predominately occur at elevated pressures and have distinct properties to vacuum plasma.

Each micro-discharge has a cylindrical-like plasma channel with about 100 µm radius, which is extended and flattened on the dielectric surface (Figure 1.5). The entity of a SMD can be described with a simple electric circuit (Figure 1.5). A high enough electric field applied externally can initiate a micro-discharge that equals the

condition of a circuit, when a switch is closed and current has to flow through a time-depended electric resistance.

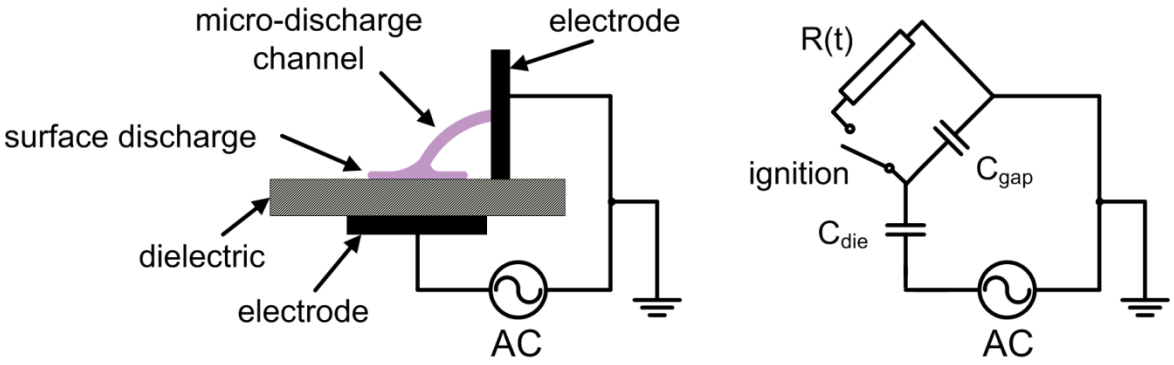

Figure 1.5: Surface micro-discharge and an equivalent electric circuit.

The real mechanism of filament formation correlates with the streamer breakdown theory [34-37], originally postulated for spark discharges. An initial free electron accelerated by the electric field produces secondary electrons by direct ionization of gas particles, leading to an electron avalanche and generation of its own electric field E_A. As a next step a streamer can develop, if the electric field of the space charge in an avalanche E_A equals the external field E_0 (following equations adapted from [38]):

$$E_A = \frac{e}{4\pi\varepsilon_0 r_A^2} exp\left[\alpha\left(\frac{E_0}{p}\right)d_A\right] \approx E_0 \qquad (1.1)$$

with
- α ionization coefficient
- e elementary charge
- ε_0 electric field constant
- d_A avalanche length
- p pressure
- r_A head radius of an avalanche

The requirement for the avalanche amplification parameter αd_A can be derived on the basis of the streamer development in the discharge gap under the assumption of an avalanche head radius of $r_A \approx 1/\alpha$:

$$\alpha\left(\frac{E_0}{p}\right) d_A = \ln\frac{4\pi\varepsilon_0 r_A^2}{e\alpha^2} \approx 20 \tag{1.2}$$

This equation is known as the Raether-Meek criterion of streamer formation $(\alpha d_A \geq 20)$. The total electron number N_e must reach the order of 10^8 to 10^9 for space charge effects to become relevant:

$$N_e = \exp(\alpha d_A) \approx 10^8 \text{ to } 10^9 \tag{1.3}$$

The fulfillment of this criterion causes the transition of avalanche to self-propagating ionized streamer at the anode. The streamer is reflected at the anode due to the high space charge at the streamers head and propagates towards the cathode [30, 39, 40]. By bridging the gap in a few nanoseconds the streamer forms a conductive ion channel (spatially-localized plasma filament) with maximum current flow. At this point, the micro-discharge appears visible through the photon emission of associated de-excitation processes. Charge accumulates at the dielectric surface observed as lateral filament spreading and reduces the electric field to such a degree that it collapses within nanoseconds. This principle mechanism is demonstrated for a DBD configuration in Figure 1.6, being the same to the used SMD setting in this work. As the current is terminated and the ionization process stops, the micro-discharge is extinguished. Despite of that, surface charges and ionic charges are present in this region after termination (cathode fall). The sustained charges allow the formation of a new micro-discharge at the same location when the polarity of the applied voltage is reverted [10]. This is the reason for the observation of single filaments with the naked

eye. The filaments likewise do not overlap, but repel each other. Higher power causes only the distribution of more micro-discharges over the dielectric surface that prevents sparking or arcing. In order to describe the situation with the SMD setting during my work, the proposed micro-discharge mechanism has found being valid for different DBD configurations [41]. Plasma filaments are also formed, when one electrode has no dielectric cover [38]. In this case, no surface charge can accumulate at this electrode and widening of the channel is prohibited (Figure 1.5 and 1.6).

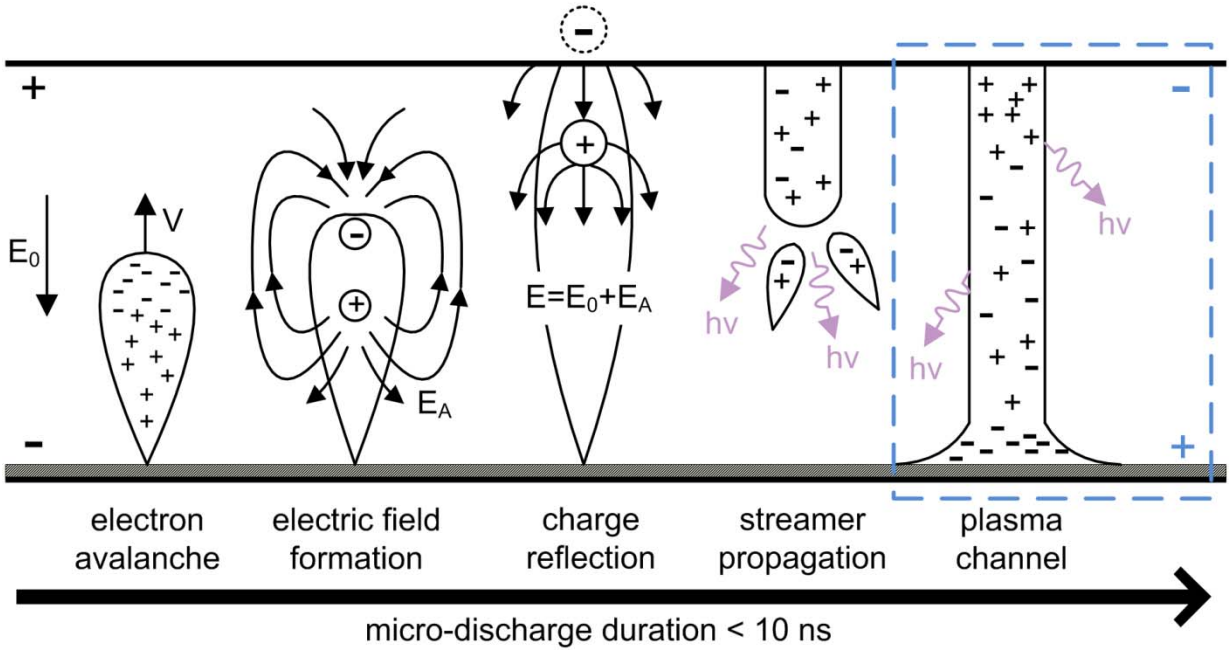

Figure 1.6: Principle streamer mechanism of micro-discharges in DBD.

Plasma filaments can be defined as transient glow discharges having a positive column and a developed cathode fall [10]. Electron and current densities of 10^{14} to 10^{15} cm^{-3} and 10^{2} to 10^{3} A cm^{-2} are obtained, respectively, and a single micro-discharge carries charges and energies of the order of 100 pC and µJ, respectively [30, 42]. The short current pulse produces only low local heating. The characteristics of a single micro-discharge channel are summarized in Table 1.2. In electronegative gases, the electron density is reduced by electron attachment processes which

create negative ions and cause filament radii being smaller than in other gases. Subsequently, diffuse discharges are feasible more easily with gases like helium with wide channels, where smoothening of the transverse field gradient can occur [10]. During my work, exclusively filamentous discharge occurred by using ambient air at atmospheric pressure.

Table 1.2: Characteristic properties of a single micro-discharge channel in air at atmospheric pressure [30].

Duration	few nanoseconds	Electron density	10^{14} - 10^{15} cm^{-3}
Filament radius	~ 100 µm	Mean energy of electrons	1 - 10 eV
Peak current	0.1 A	Total transferred charge	order of 10^{-10} C
Current density	10^{2} - 10^{3} A cm^{-2}	Gas temperature	close to room temperature

1.2.2.4 Humid Air Plasma Chemistry

Energetic electrons in plasma initiate upon collisions with other particles a cascade of dissociation, excitation and ionization processes being responsible for the generation of a unique variety of plasma-chemical species. Therefore, the electron energy distribution in non-thermal discharges is crucial for defining the plasma chemistry. Furthermore, there are two distinct regimens that have to be considered in chemical processes of plasma. The first is restricted to the micro-discharge region dominated by rather short-lived charged particle reactions. The second is located outside the micro-discharges and primarily characterized by the free-radical chemistry of neutral particles like excited atoms, distinct and fragmented molecules.

Typical plasma species involved in the SMD chemistry of humid air plasma (such as O_3, NO_x, OH, N_2^+, O_2*, H_2O_2, UV light) and the discharge pattern of the SMD electrode used in my work are shown in Figure 1.7. The reaction chemistry of humid air plasma is complex [43, 44] and therefore, difficult to be modeled in a quantitative

and adequate manner, far less of being experimentally determined at the moment. However, studies on air plasma chemistry in the last decades facilitated the generation of a profound database giving detailed insights to the reaction kinetics [12, 45, 46]. Notably, Sakiyama et al. simulated SMD air chemistry of micro-discharges with a big set of 50 species taking part in over 600 possible reactions [47] that yet reflects a big part of the real situation. It is important to understand the reaction kinetics of a given plasma system, in order to benefit from a subsequent adaption of its chemistry for a desired application.

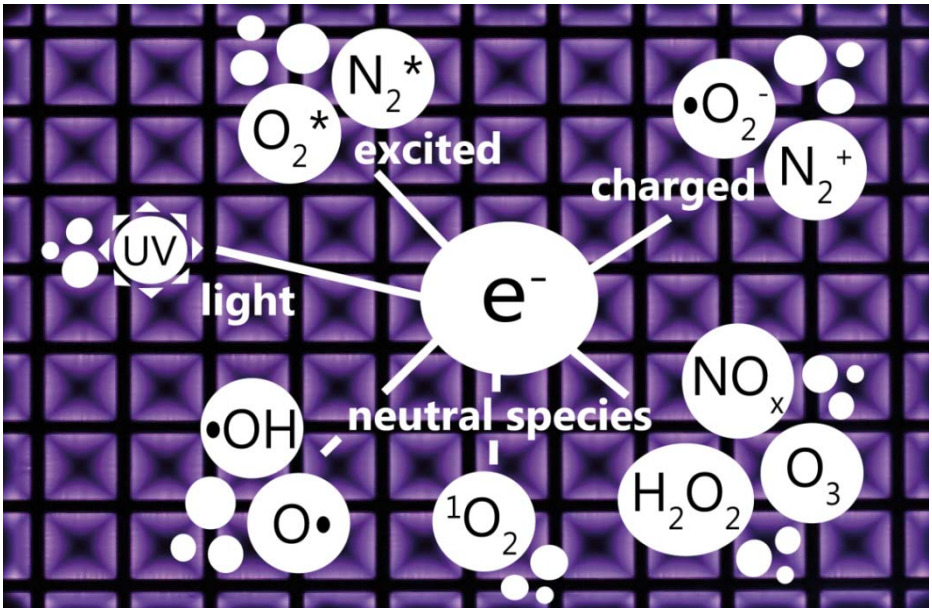

Figure 1.7: Discharge pattern of the SMD electrode and plasma-chemical species involved in humid SMD air plasma used in this work.

In general, DBDs have been investigated mainly to optimize the ozone generation using oxygen or air [30, 31, 39, 40, 42, 48, 49], especially for pollutant treatment in water [50]. The initial step includes the excitation of O_2 into two possible states (O_2*: $A^3\Sigma_u^+$, $B^3\Sigma_u^-$) that further dissociate according to following reactions [49, 51]:

$$O_2 + e^- \longrightarrow O_2^* + e^- \quad (1)$$

$$O_2^* \longrightarrow 2\,O \quad (2)$$

The resulting atomic O can be in the triplet state, $O(^3P)$, or in the singlet state, $O(^1D)$. Only $O(^3P)$ is able to react readily with O_2 (spin conservation rule) and a third collision partner M (O_2, O_3, O or in air also N_2) to form ozone:

$$O(^3P) + O_2 + M \longrightarrow O_3^* + M \longrightarrow O_3 + M \quad (3)$$

O_3^* is the transient excited state of ozone. Undesired side reactions compete with ozone formation, since they also consume atomic O [10]:

$$O + O + M \longrightarrow O_2 + M \quad (4)$$

$$O + O_3 + M \longrightarrow 2\ O_2 + M \quad (5)$$

$$O + O_3^* + M \longrightarrow 2\ O_2 + M \quad (6)$$

Using air, a great variety of nitrogen species also interferes in the reaction pathways of DBDs. In addition to ozone, many other oxidative species are generated [47, 52, 53]: NO_x (x = 1-3), N_2O_y (y = 1-5). In fact, nitrogen-based processes are responsible for ca. 50% of total ozone produced due to the contribution of additional atomic O [10]. However, NO_x species can reach a certain concentration level, for instance due to the application of excessive power, at which ozone formation is disfavored and breaks down completely (discharge poisoning). In this situation, O atoms are consumed more rapidly by NO_x reactions instead of the ozone reaction (3). Whereas NO, NO_2 and N_2O are accumulated, ozone is removed in an ozone destruction process catalyzed by NO and NO_2 [53]:

$$NO + O_3 \longrightarrow NO_2^* + O_2 \quad (7)$$

$$NO_2^* \longrightarrow NO_2 + hv \quad (8)$$

$$2\ NO + 3\ O_3 \longrightarrow N_2O_5 + 3\ O_2 \quad (9)$$

$$NO_2 + O_3 \longrightarrow NO_3 + O_2 \quad (10)$$

NO_2^* is an excited form of NO_2.

In combination with water, which can be present in ambient air (relative humidity or vapor) or as liquid, the complexity of the reaction system rises again. For instance, water and the singlet O atom, $O(^1D)$, are converted to H_2O_2 which has a high oxidative potential and is decomposed into reactive OH radicals [50]:

$$O(^1D) + H_2O \longrightarrow H_2O_2^* \longrightarrow 2\ OH \qquad (11)$$

In addition, OH radicals react with NO_x to nitrous and nitric acids that are corrosive. Reactions (1) to (11) present few examples, how reactive species are created and interact with each other in humid air plasma.

Thus, it is likely that long-lasting SMD plasma species such as reactive oxygen species (ROS: such as O_3, OH, O, O_2^-) and nitrogen species (RNS: such as NO, N, N_2^*, N_2O) determine the effects on targets outside the micro-discharge region.

1.3 Plasma Medicine

The emerging field of plasma medicine has drawn a lot of attention to the research society among physicists, biologist, engineers and physicians. Whereas thermal atmospheric plasma sources have been utilized for cauterization and blood coagulation for a long time, “cold” or tissue tolerable plasma has the advantage to circumvent the risk of burns and serious tissue damage [29]. Previously, the use of non-thermal plasma was restricted to vacuum applications with the sterilization of medical devices and the surface modification of biomaterials involving etching, cleaning, activation and thin film deposition. In 2002, Stoffels et al. have initiated the new era of plasma with the investigation of CAP interacting with living cells and tissues [54]. The development of non-thermal plasma sources at atmospheric pressure has triggered the investigation of a whole new possible application range of plasma in the medical field, which involves [55]:

- Prevention and treatment of diseases:

  Chronic wounds, skin and mucosal infectious diseases, localized tumors, keloid formation, promotion of angiogenesis, tissue ablation, hemostasis
- Inhibition of biofilm formation by active treatment and by material surface treatment
- Promotion of incorporation of implants into viable tissue by surface alterations (biocompatibility, wetting, plasma steered application of antimicrobial active layers with drug delivery function)
- Improved diffusion of topically applied drugs with therapeutic outcome (pharmacology)
- Improvement of sanitation of medical devices by surface modification

The reasons for such wide range of applications are implicated beside the low heat formation in the versatile technical realization and chemical properties of advancing atmospheric pressure plasmas. Plasma provides a “chemical cocktail” that can be tailored by alteration of the gas mixture, the power adjustments and the way of treatment (*direct* with or *indirect* without ionic species) and accesses in a fast and easy way confined spaces at the target site [56]. Hence, the mixture of reactive species can act synergistically for instance to inactivate infectious microbial pathogens and to promote cell/tissue healing processes at the same time. With CAP, free radical species (O_2^-, H_2O_2, OH^-, NO, $ONOO^-$) can be produced that are also employed by eukaryotic cells in the defense mechanism against invading bacteria [57]. In addition, many biochemical processes in cells rely on ROS and RNS that are part of CAP using air, which might enable the regulation of the respective cell signaling by plasma [58]. Therefore, scientists try to design CAP according to

desirable cellular responses, in order to induce for instance sub-lethal effects like cell detachment or apoptosis for healing, avoiding on the other hand lethal effects that cause inevitable necrosis with unwanted scar formation [59].

One of the major tasks for researchers is to determine the “therapeutic window” of a CAP source by tissue treatment. It is defined as the dosage range of plasma-derived reactive species that already causes antimicrobial or in general therapeutic beneficial effects but still is tolerated by healthy tissue without harming it. Such selectivity is based on the distinct defense mechanisms of eukaryotic and prokaryotic cells, when it comes to the interaction with reactive species. Eukaryotic cells possess greater possibilities to defend reactive species and to repair oxidative damage to the DNA or cell membrane than prokaryotic cells due to higher barriers (cytoskeleton, nucleus) as well as extensive enzymatic catalysis and repair mechanisms. Similar selectivity by CAP is proposed between healthy and cancer cells [60, 61]. Recently, SMD air plasma sensitized chemo-resistant brain tumor cells *in vitro* for temezolomide treatments [62] and induced senescence to melanoma cells [63]. Furthermore, CAP has already demonstrated its promising properties especially in the field of dermatology [64-66], by the first successful clinical trials *in vivo* on human chronic wound disinfection with a MW driven argon plasma torch [67-69].

A more detailed overview of the present knowledge and research subjects in plasma medicine is provided by recent publications [6, 70].

1.3.1 Nosocomial Infections

The European Center of Disease Control and Prevention (ECDC) reported that the prevalence of patients with nosocomial infections in European acute care hospitals reached 6% (3.2 million) in 2011-2012 [71] and solely 307,000 surgical site infections

were identified in European hospitals in 2008 [72]. In comparison, the American counterpart, the Center for Disease Control and Prevention (CDC), reported 1.7 million nosocomial infections with 99,000 associated deaths in the USA back in 2002 [73, 74]. From an economic point of view, nosocomial infections are associated with considerable costs for health care systems. They come along with an increased duration of hospitalization [75], a possible need for isolation and increased use of expensive alternative drugs for highly-resistant strains. It is estimated that infections by antimicrobial drug-resistant microorganisms (MO) in general increase morbidity, mortality and direct costs by approximately 30-100% [76, 77]. In the USA, the annual costs for the medical treatment of nosocomial infections are estimated around $40 billion [78]. Prevention of such infections would substantially improve clinical care quality for patients by decreasing morbidity, mortality and costs.

The concern about nosocomial infections is reflected by the substantial decline of the antimicrobial susceptibility of pathogens. This includes methicillin-resistant *Staphylococcus aureus* (MRSA), vancomycin-resistant Enterococcus (VRE), *Pseudomonas* spp., *Acinetobacter* spp., *Candida* spp., as well as extended-spectrum β-lactamase (ESBL) producing gram-negative bacteria such as invasive *Escherichia coli* or *Klebsiella* spp. [71, 72].

Notably, C*lostridium difficile* has emerged as a leading nosocomial pathogen [79, 80], which accounts for 48% of all healthcare-associated gastro-intestinal infections at the moment, with increasing prevalence in Germany [71]. The symptoms range from mild diarrhoea, fever to life-threatening pseudomembranous colitis. Use of antibiotics destroys the patient´s intestinal flora and promotes overgrowth of naturally resistant *C. difficile*, which used to be before a harmless concomitant inhabitant among many other bacteria species in the intestine. In addition, the evolution of hyper toxic genetic

variants of *C. difficile* such as ribotype 027 that produce aggressive toxins [81, 82] and a high recurrence rate of infections at about 20% worsen the situation [79]. *C. difficile* bacteria are anaerobic. Depending on the surrounding condition, they are able to change into a very endurable dormant form, called bacterial endospores. In general, spores exist in a “sleeping mode”, their metabolism is down-regulated, they are not motile and their structure is characterized by many dense physical barriers with low water content in the inner core, where the DNA is protected by small acid-soluble proteins (SASPs) [83]. In this fortress, spores are much more capable to withstand environmental stress such as heat or oxidative stress than their vegetative forms [84]. As soon as they reach conditions favorable for reproduction, spores germinate again into their vegetative states. Therefore, particular clinical attention is given to *C. difficile*. Its vegetative forms and spores are transmitted among patients through the faecal-oral route, for example from contaminated surfaces or personnel hands [85]. Many non-spore-forming nosocomial pathogens like VRE, MRSA or *Acinetobacter* spp. persist on dry inanimate surfaces for several days or even months [86]. Contamination by *C. difficile* endospores that are highly resistant against standard surface disinfectants worsens the situation [83, 87]. Moreover, insufficient sanitation per se or the use of inadequate cleaning agents is likely to lead to further sporulation and spread of *C. difficile* [88].

Therefore, proper decontamination including disinfection of environmental surfaces and hands of healthcare staff as well as sterilization of medical devices is important to minimize the risk of the transmission of nosocomial pathogens [89-91]. At the moment, no disinfection agent listed by the US Environmental Protection Agency is specific for the environmental control of *C. difficile* spores [92]. Hypochlorite based disinfectants are recommended [93], but their effectiveness and secure handling are

questionable [87]. In case of sterilizing agents, wet/dry heat, irradiation, chemical gas and H_2O_2 gas plasma are the conventional methods for the sterilization of devices in medicine or hygiene. However, all of these methods have several drawbacks that limit their application. The material properties of sensitive devices including polymeric biomaterials can be negatively altered such as in molecular weight, volume and morphology [94-97]. These alterations may influence the physical and biological performance of the medical device [96] and may be responsible for material failure [97]. Some sterilization methods require 120 °C operating temperature that can lead to the degradation of thermo-labile medical devices. Other limitations are the need of vacuum chambers in common plasma sterilization methods [98] or the use of toxic gases like formaldehyde or ethylene oxide [98-100]. As for any strong disinfectant with alkylating or oxidizing behavior, regular handling is a big issue due to its hazardous entity, unpleasant odor or material corrosive property. To circumvent this problem, alternative decontaminants complementary to manual cleaning are investigated [101].

1.3.2 CAP in microbial decontamination

CAP sources have originally been investigated due to their properties of variable plasma chemistry and geometry, of enabling low temperature application and of their great potential to inactivate bacteria and other resistant MO. In 1996, Laroussi introduced for the first time a CAP device specific for sterilization purposes [102]. Since then, many studies followed to demonstrate germicidal properties of different CAP sources, mainly corona discharges, DBDs, APPJs and more rarely thermal MW plasmas [103]. Each technology has its advantages and drawbacks: Corona

discharges are well suited to induce plasma species into liquids, APPJs are applied for the treatment of small localized areas and DBDs for treatments over a wide area.

Table 1.3 summarizes the recent studies conducted only with DBD plasma devices relevant for my work, using air at atmospheric pressure in direct treatment (with discharge contact) or indirect treatment (remote) mode. Direct treatment may damage sensitive materials due to the impact of charged particles, whereas it usually results in faster inactivation compared to remote mode. Notably, the majority of these studies were carried out after the conception and initiation of my project. Some parameters differed depending on the study goal: type of MO (vegetative bacteria, bacterial endospores, yeast, fungal spores, virus) and the treatment environment (dry, wet, biofilm, liquid, living tissue). Muranyi et al. showed that their cascaded DBD system could inactivate efficiently various MO with additional application of strong UV light from an excimer lamp [104]. Gadri et al. provide the most extensive study on both direct and indirect treatment with one atmosphere uniform glow discharge plasma (OAUGDP) in terms of the range of different exposed MO [105]. They have suggested the operation of such plasma devices not only in the medical/healthcare field, but also for food processing, other general industrial and commercial use as well as biological warfare defense. Moreover, equipment for space missions involves sensitive electronics/materials and conventional sterilization with dry heat would cause damages, therefore alternative DBD air decontamination became interesting for the planetary protection against terrestrial microorganisms [106, 107]. Ambient air is present everywhere, which makes it very attractive for plasma decontamination purposes.

For a decontamination study, it is crucial to utilize the right terminology (Table 1.4), in order to avoid misunderstanding. For instance, the term sterility describes a state of

being free of any viable MO, but is sometimes misused. Therefore, different tiers of sterility assurance levels (SAL) have been suggested for the validation of plasma sterilization [108]: pharmaceutical (SAL = 10^{-6}), high-level (10^{-4}) and low-level sterilization (10^{-3}). In addition, the decimal reduction value (D-value) is commonly determined to indicate the antimicrobial efficiency for comparison reasons. Furthermore, it is also important for a decontamination study to fulfill approved standards for testing the decontaminating behavior of an agent. This involves the use of appropriate biological indicators, often non-pathogenic bacterial endospores, which serve as surrogates and have shown a level of resistance against a given sterilization process (Table 1.5). However, validation standards for disinfection methods in human medicine frequently prefer vegetative bacteria and other MO relevant in clinical environments [91, 109]. Endospores of *C. difficile* have not been considered yet in standard testing despite their rising significance. Therefore and due to the fact that cultivation is sophisticated and long-lasting [110], *C. difficile* spores have been subject in only one CAP (APPJ) study until now [111].

Unlike other gaseous or airborne decontaminants, DBD/SMD air plasma consists of a mixture of reactive species such as O_3, H_2O_2, UV light and many others [47], which can act synergistically and be tailored for the possible prevention of infections [112]. Therefore, I investigated SMD air plasma as a promising candidate for the microbial control in public health and hospital care.

Table 1.3: Decontamination studies using atmospheric air DBD sources.

logarithmic reduction	time, s	microorganism (MO)	N_0, cfu	substrate environment	reference, year	DBD
direct treatment						
≥ 6	30	*S. aureus* [e]	10^7	PP, dry	[28], 1998	
≥ 5	24	*E. coli* [e]	10^7	PP, dry	[105], 2000	
7	10	human skin flora	10^7	agar, wet	[29], 2006	
≥ 4	70	*E. coli*	10^4	glass, dry	[113], 2006	
≤ 4	5	*A. niger* [FC, e]	10^6	PET, dry	[104], 2007	
≥ 6	1800	*D. radiodurans*	10^6	SSt, dry	[106], 2009	
5	340	*L. innocua* [e]	10^7	steel, dry	[114], 2010	
≤ 1	900	*B. atrophaeus* [S]	10^7	SS/PBS	[115], 2010	
≥ 5	120	MRSA [e]	10^7	glass, biofilm	[116], 2010	
6	30	*E. coli*	10^6	PBS, wet	[117], 2011	
≥ 6	1200	*G. stearothermophilus* [S, e]	10^6	PCB, n/a	[118], 2013	
indirect treatment						
≥ 4	25	*E. coli* [e]	10^7	PP, dry	[105], 2000	
≥ 3	25	*S. aureus* [e]	10^7	PP, dry	[119], 2000	
4	600	*B. subtilis* [S, e]	10^6	paper, dry	[120], 2007	
≥ 5	180	*G. stearothermophilus* [S]	10^6	SSt, dry	[121], 2008	
≥ 6	720	*G. stearothermophilus* [S]	10^6	SSt, dry	[122], 2008	
≥ 5	150	*B. atrophaeus* [S]	10^6	PE, dry	[123], 2010	
5.5	5400	MRSA [e]	10^9	glass, biofilm	[124], 2011	
≥ 6	240	adenovirus	10^6	PBS	[125], 2011	
≥ 5	60	*E. coli* [e]	10^7	agar, wet	[126], 2011	
≥ 6	360	*E. coli*	10^6	TBS	[127], 2012	
≥ 5	480	MRSA [e]	10^8	pig skin	[128], 2012	
≥ 6	120	*D. radiodurans* [e]	10^6	agar, wet	[129], 2012	
≥ 5	480	*C. albicans*	10^7	PE, biofilm	[130], 2012	
≥ 5	300	*G. stearothermophilus* [S, e]	10^6	SSt, dry	[131], 2012	
≤ 2	300	natural microbiota	10^5	seed surface	[132], 2013	
≥ 5	300	*E. coli*	10^7	various, dry	[133], 2013	
≥ 5	120	*E. coli*	10^5	SS/PBS	[134], 2013	
≥ 6	5400	*B. safensis* [S,e]	10^6	steel, dry	[107], 2013	

[S] bacterial endospores, [FC] fungal conidiospores, [e] example of tested MO; PP polypropylene, SSt stainless steel, SS physiological saline solution, PBS phosphate buffered saline solution, PET polyethylene terephthalate, PCB printed circuit board, PE polyethylene, TBS tris buffered saline; color-coding implies same DBD devices; – – studies below this line were published after start of my study.

Table 1.4: Definitions of commonly used terms associated with microbial control processes (adapted from [103]).

Term	Definition
microorganism	any microbiological entity, cellular or non-cellular, capable of replication or of transferring genetic material
biological decontamination	removal or neutralization of contaminating microbial substance
antimicrobial	tending to destroy microbes, prevent their development or inhibit their pathogenic action
inactivation	loss of ability of MO to grow and/or multiply
sterility	state of being free from viable MO
asepsis	activities that lead to a state of being free of living pathogenic MO
antisepsis	destruction of pathogenic organisms on living tissue to prevent infection
sterilization	validated process used to render a product free from viable MO
SAL	probability of a single viable MO occurring on an item after sterilization (= ineffective sterilization)
D-value	decimal reduction time required to reduce viable MO by 90%
disinfection	process that eliminates many or all pathogenic MO except bacterial spores on inanimate objects
cleaning	removal of contamination from an item to the extent necessary for further processing or for intended use

Table 1.5: Selection of microbial test indicators for sterilization (adapted from [103]).

agent	specification	MO	form
heat	dry	*G. stearothermophilus*	endospore
	wet	*B. atrophaeus*	"
radiation	UV	*B. pumilus*	"
	γ	*B. pumilus*	"
		D. radiodurans	vegetative
gas	C_2H_4O[a]	*B. atrophaeus*	endospore
	CH_2O[b]	*G. stearothermophilus*	"
	H_2O_2	*G. stearothermophilus*	"

[a] ethylene oxide
[b] formaldehyde

1.4 Aim and research objectives of my doctoral work

The project during my PhD involved four parts: First, I focused on developing a CAP device with an electrode system based on the SMD technology, which allowed homogenous filamentary discharge in ambient air at atmospheric pressure. Second, I aimed to characterize the discharge´s physical and chemical properties, using appropriate plasma diagnostic tools. Third, I validated the sterilizing and disinfecting action of the SMD air plasma according to European norm standard testing methods [135, 136]. This included the use and indirect treatment of biological indicators consisting of environmentally resistant vegetative bacteria (e.g. *E. faecium*) and bacterial endospores (e.g. nosocomial relevant *Clostridium difficile*) immobilized preferentially on dry inanimate carriers. Fourth, I assessed the surface conditions of the carriers and the microbial surface morphology by scanning electron microscopy (SEM) imaging, in order to identify factors influencing the efficiency of inactivation by plasma and to observe putative plasma effects on treated bacteria, respectively. Other influencing factors were subsequently identified and investigated.

The results give insights into the mechanism of bacterial inactivation by SMD air plasma and demonstrate its general potency as a prospective air-based decontaminant in clinical and other healthcare facilities compared to conventional methods. The vision of this study was to improve patients´ care and prevent the outbreak and spread of devastating nosocomial infections by a supportive CAP decontamination system in the future.

2 MATERIALS and METHODS

2.1 SMD plasma device development - FlatPlaSter 2.0

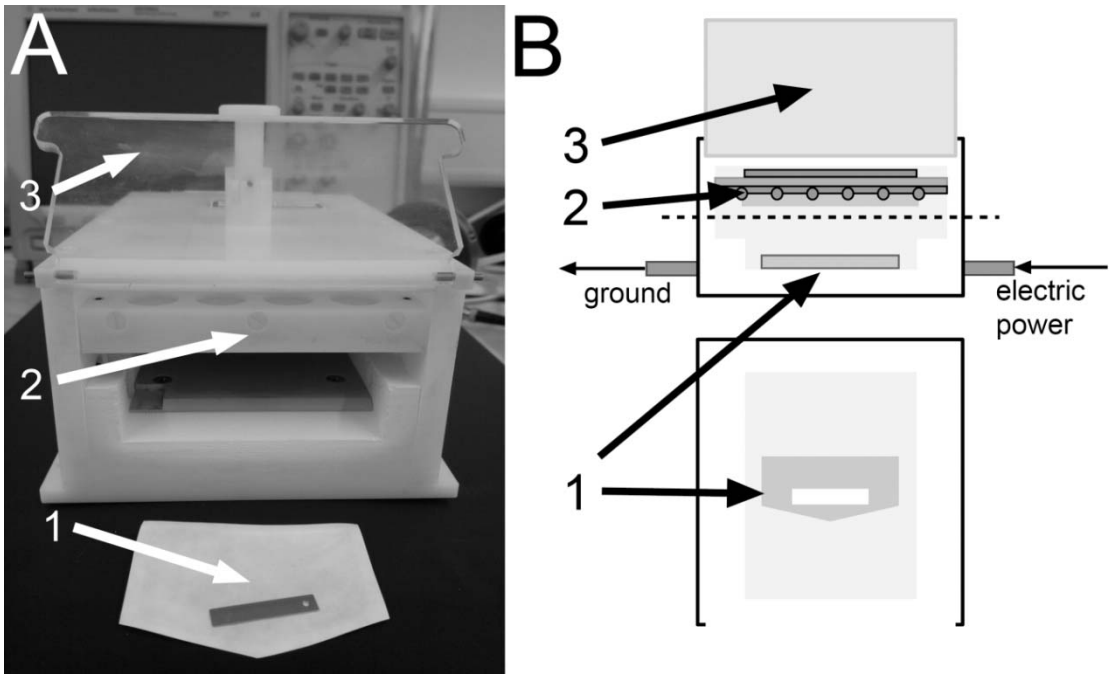

Figure 2.1: Photo image (A) and schematic view (B) of the SMD plasma device used for experiments: biological indicator (1), electrode system (2) and lid (3).

Initial situation

In the present study, the CAP discharge in ambient air is based on the SMD technology. The set-up of the plasma device, the FlatPlaSter 2.0 (FP2.0), is demonstrated in Figure 2.1. The housing is made of polyoxymethylene (POM) and has a front opening which can be closed by a transparent lid. The spatial dimensions of the interior are L 125 mm x W 90 mm x H 15-30 mm, which corresponds to min. 169 mL and max. 338 mL. This allows the insertion of biological test specimen such as an agar plate, 96-well plate or biological indicator sample (see Figure 2.1A). The electrode system is positioned in the upper part of the device and its distance to the bottom of the device can be adjusted from 1.5 cm to 3 cm. It generates filamentous air micro-discharges and enables the indirect treatment of samples placed below. The system consists of two plates, a powered solid plate and grounded mesh, both

separated by a dielectric layer. Application of electric power provided by an RF function generator (HM8150, HAMEG Instruments, Germany or 8202, Voltcraft, Germany) and an high voltage amplifier (PM 04015 or 10/10B-HS, TREK, USA) is sufficient to create micro-discharges between the dielectric surface and the grounded mesh. The general setting for plasma experiments is completed by an oscilloscope for monitoring the voltage and the current flux, by a current probe and by a filter pump system to remove extensive ozone (Figure 2.2). Sinusoidal wave frequency was employed throughout the whole study. The typical voltage and current measurement with an oscilloscope describes sinusoidal wave forms (Figure 2.3). From a certain high voltage micro-discharge formation is observable by the continuous creation and extinguishment cycle of a series of high current signals. The voltage is measured in kV_{pp} and the current in mA.

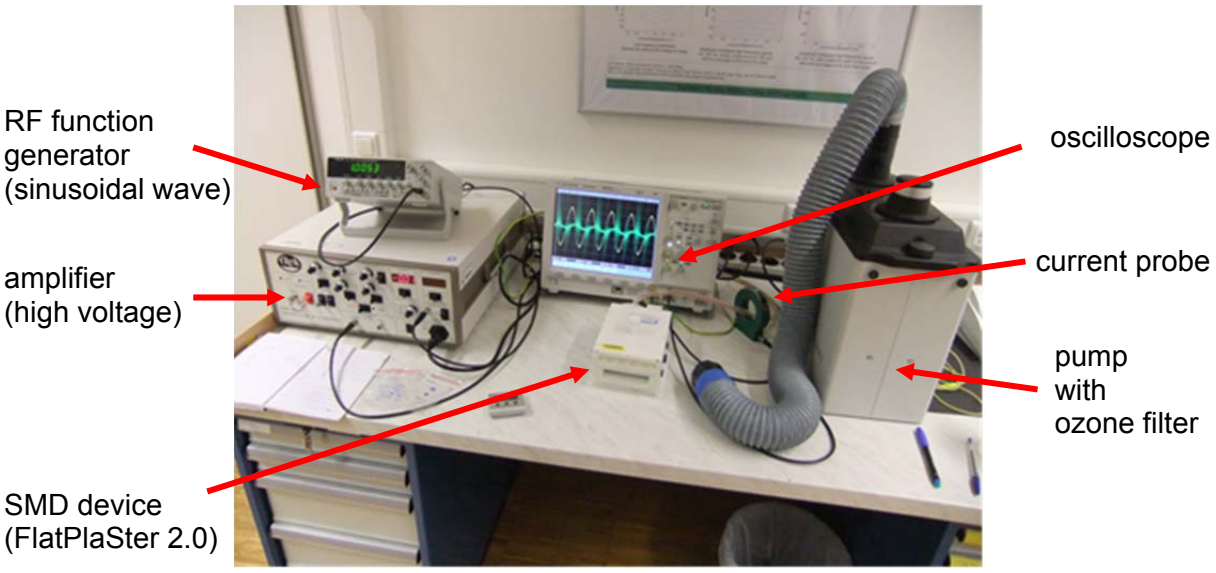

Figure 2.2: General setting for plasma experiments.

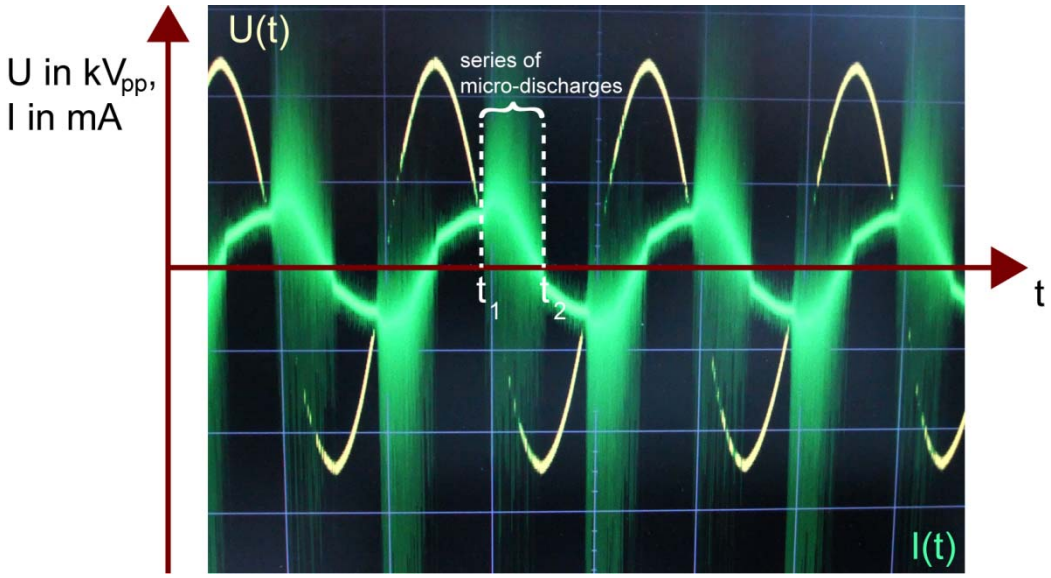

Figure 2.3: Typical measurement of the applied voltage U(t) and current I(t) shape of the filamentary discharge in air.

SMD electrode development procedure

At first, the electrode system had to be developed. This involved the selection of an appropriate grounded mesh electrode in regards of following criteria: assurance of homogenous discharge pattern over the whole surface, high bactericidal effect and robustness against corrosion. Initial tests with a flexible welding grid (stainless steel, 0.5 mm thick, 4.5 mm mesh size; from in-house workshop) demonstrated that its structure was too unstable for the area size that had to be spanned (145 × 109 mm^2), since the grid was locally not in touch with the dielectric layer and subsequently inhomogeneous discharge was obtained (Figure 2.4).

Figure 2.4: Inhomogeneous discharge pattern with welding grid.

Therefore, the metal material (steel, stainless steel, alumina, alumina anodized), mesh structure (square, round, hexagonal), mesh size and thickness were altered and tested (examples in Figure 2.5). For this experiment, a solid copper plate was chosen as the powered electrode with a smaller area size (L 126 mm x W 89 mm x T 3 mm) than the grounded electrode, in order to avoid sparking at the edges of the electrode system. Notably, the discharge area is defined by the size of the powered plate. It was placed in a frame (POM, 3 mm thick) to match with the dielectric (POM, 0.5 mm thick; from Goodfellow) and with the grounded electrode size. The frequency (2 kHz, 6 kHz) and the voltage (7 kV_{pp}, 9 kV_{pp} at 2 kHz; varying voltages at 6 kHz) were changed. The resulting discharge pattern was imaged with a Canon EOS 450D, Macro lens EF-S 60 mm.

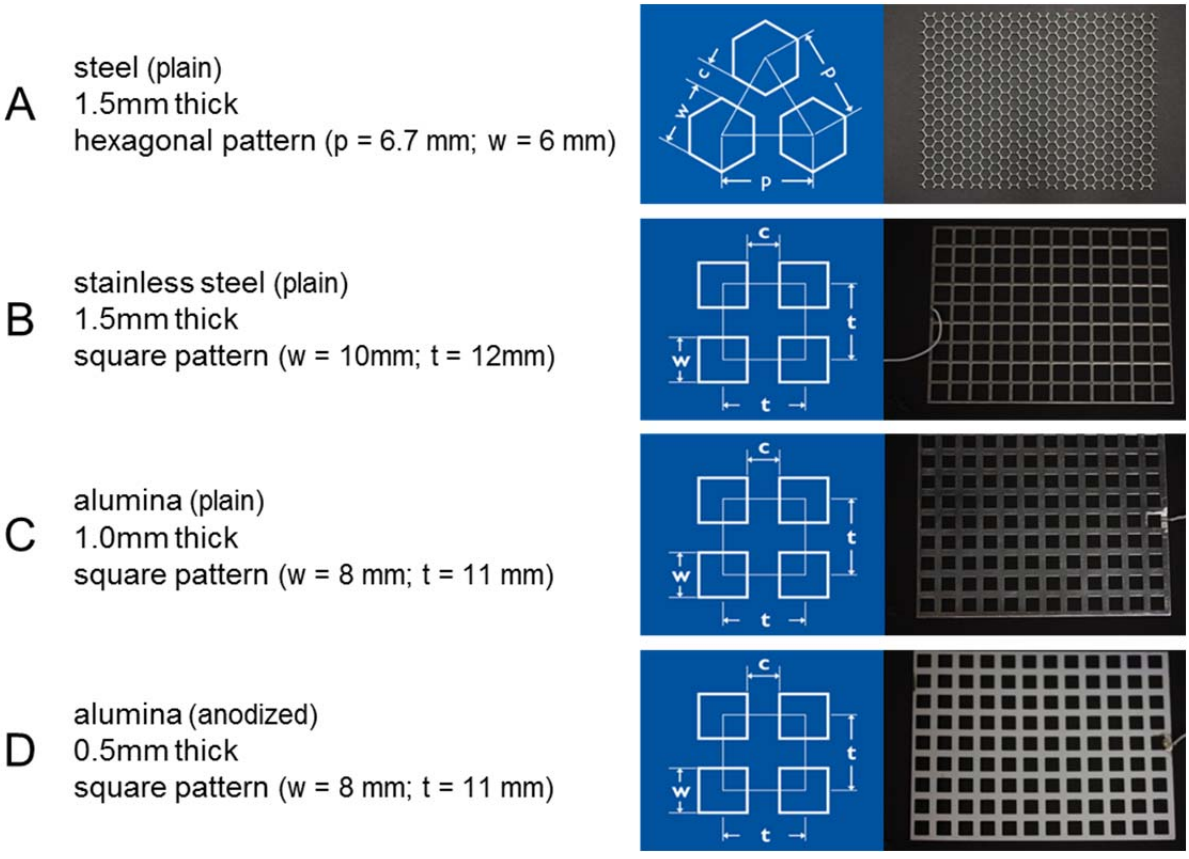

Figure 2.5: Examples of different mesh grids tested (purchased from Mevaco)

In order to evaluate the bactericidal efficacy, colonies from an overnight secondary culture of *E. coli* DSM 1116 (from German Collection of Microorganisms and Cell Cultures (DSMZ)) were suspended in 5 mL PBS and adjusted to a McFarland density of 0.5 (2×10^8 CFU/mL) followed by a dilution series (undiluted suspension, 10^{-2}, 10^{-4}, 10^{-5}) to determine negative controls. Müller-Hinton (MH) agar plates (Oxoid Deutschland GmbH) were inoculated with 100 µL of the undiluted suspension or the control dilutions (10^{-4}, 10^{-5}) and dried for 30 min at room temperature. Agar plate samples were placed one by one centered into the plasma device, the lid was closed and the sample was treated (t = 5 s, 10 s, 15 s or 30 s) at power settings mentioned before. The distance from the micro-discharges to the agar surface was 0.8 mm. After the treatment, the sample was removed and the device was evacuated from ozone and other long-living species with the filter pump for 30s prior to the next treatment, in order to create the same initial condition. The treated agar plates and negative controls were incubated at 35 °C ± 2 °C overnight. The resulting growth of *E. coli* colonies was imaged with the Canon camera and evaluated visually in a qualitative way.

Furthermore, each material of the electrode system was viewed for changes such as corrosive damage after treatments and documented with the Canon camera. The dielectric stability was proven against breakdown. The available power setting range was identified.

2.2 Plasma diagnostics

2.2.1 Optical emission spectroscopy

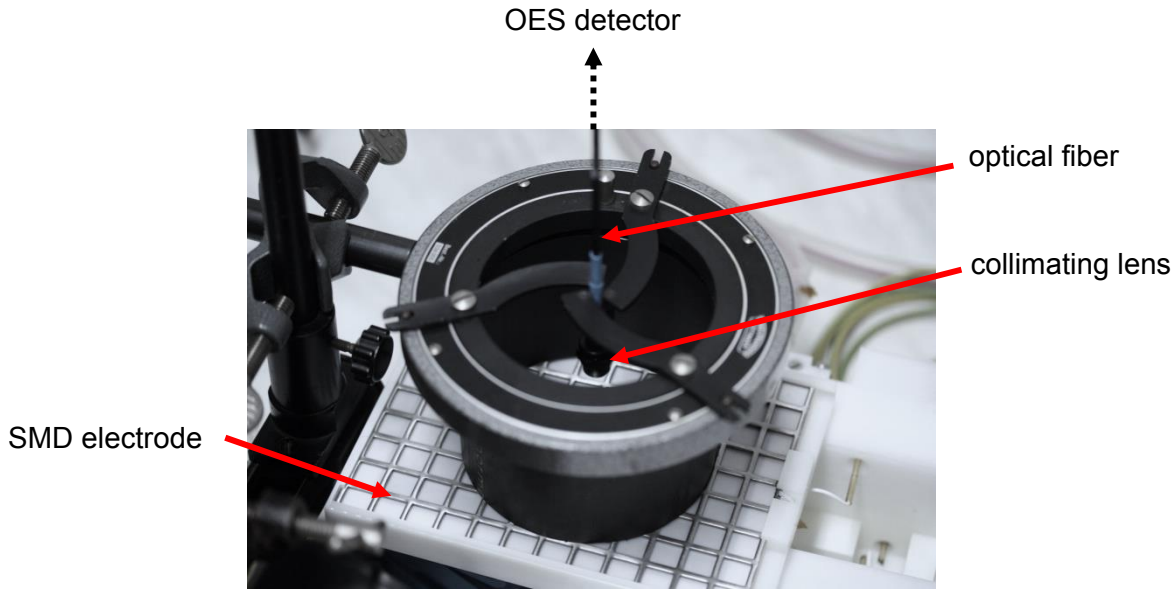

Figure 2.6: Experimental set-up for OES measurements.

In order to identify SMD air plasma species and also the character of emitted UV light, qualitative measurements were conducted by optical emission spectroscopy (OES). For this purpose, the electrode system was dismounted from the FP2.0 device and aligned accordingly for the measurement setting (Figure 2.6). The spectral emission lines were detected by a UV/VIS minispectrometer (C10082CA; Hamamatsu, Japan). Therefore, a collimating lens (74-UV, 200 - 2000 nm, Ocean Optics, USA) was placed orthogonally to the electrode surface in 2 cm distance. The photons emitted by the plasma were transmitted through fiber optics (UV/SR-VIS High OH content, 200 - 1100 nm, Ocean Optics, USA) to the spectrometer, separated into spectral elements and the spectra was detected by a CCD camera from 200 - 800 nm (Table 2.1). The measurement control was done with the software SOLIS (Andor, UK) in the scope mode. The integration time was set to 10 s, in order to achieve maximum 90 % of the maximum intensity scale at the highest electric

power measured. The spectra were saved which did not change significantly after a certain time (ca. 60 s). In addition, background spectra were measured without plasma discharge for basic intensity adjustment. All measurements were conducted in the dark. Resulting spectral resolution was 0.3 nm.

Spectra of SMD discharges were obtained varying the frequency (1 kHz, 6 kHz) and the voltage (8.5 kV_{pp}, 10 kV_{pp}). Measured spectral lines were identified with the use of a comprehensive library of molecular spectra [137].

Table 2.1: Wavelength range measured

notation	abbreviation	wavelength range, nm
visual range	VIS	800 - 400
ultraviolet A	UV-A	400 - 315
ultraviolet B	UV-B	315 - 280
ultraviolet C	UV-C	280 - 200

2.2.2 UV-C power emission

The fluence of the emitted light with special interest in the UV-C was measured with a digital UV power meter (C8026/H8025, Hamamatsu, Japan). The electrode system was installed outside the device as for the OES measurements. The sensor was positioned 2.5 cm away from the electrode with a Teflon cylinder and thin aluminum plate having both an inner diameter of 2 cm (Figure 2.7). This allowed a closed system around the sensor. In addition, measurements in 0.3 cm were conducted. Measurements were mainly carried out without filter which still allowed accurate measurements along the UV-C region (transmission window = 173 - 294 nm). For each experiment, measured values were documented in nJ/cm^2 after an integration time of 60 s during plasma discharge phase at 1 kHz and 10 kV_{pp} which is the plasma power setting mainly used in this study. The mean values of 10 independent

measurements was determined and reproduced. The results are expressed as power density in nW/cm^2.

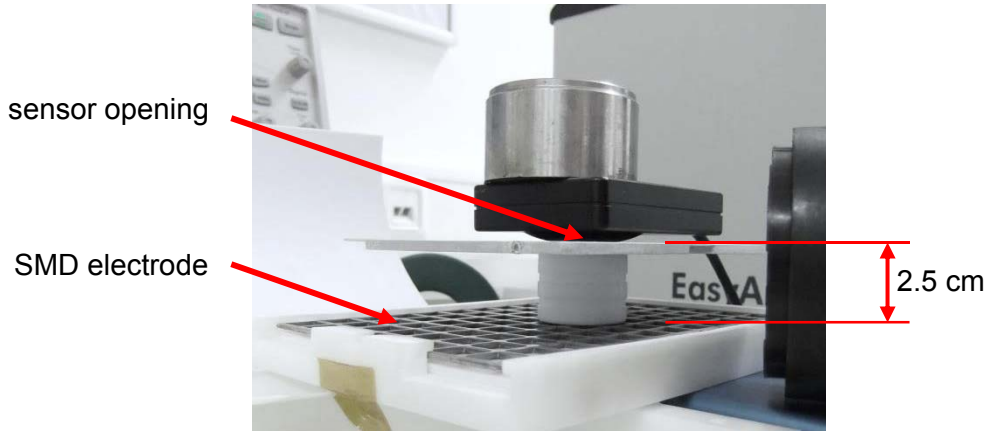

Figure 2.7: UV power measurement set-up.

2.2.3 Temperature profile

The air temperature inside the closed FP2.0 was measured with a digital multimeter (GTH 125, PeakTech, Germany). Therefore, one of the central holes at the sides of the housing was used. All holes were normally sealed by lamella rubber plugs made of ozone resistant rubber (ethylene propylene diene monomer, Smartplug, Gummivogt, Germany). The temperature sensor was inserted through a little hole drilled in one of the plugs that still assures a sealed condition. The temperature profile was measured three times á 5 min at 0.5 kHz, 3 kHz and 6 kHz during plasma discharge. At 1 kHz, 3 measurements were conducted á 10 min. The voltage was set constant at 10 kV_{pp}. The actual temperature value was documented with one decimal accuracy every 15 s. The air in the chamber was evacuated with a pump after each measurement, in order to return to the initial temperature (ca. 22 °C). The electrode system was positioned 1.5 cm away from the bottom plate. Average values and the standard error were calculated.

2.2.4 Dissipated plasma power via Lissajous figures

The dissipated power by micro-discharges was determined by the usage of Lissajous figures (Figure 2.8). The time-integrated current, the charge Q, was measured by placing a capacitance C_{exp} with 0.1 µF in series with the SMD experiment. The measurable voltage U_{exp} across this capacitor is proportional to the charge. The closed loop of the applied voltage versus charge usually describes a parallelogram and its area represents the electric energy E_{el} consumed per voltage cycle [24].

U_{exp} and $U(t)$ were measured during plasma discharges at 0.5 kHz, 1 kHz, 3 kHz and 6 kHz and constant 10 kV_{pp} with an oscilloscope. Five independent measurements were conducted at each condition.

The data was processed with Excel. The area of the loop A_{loop} was estimated from the experimental values using a visual basic macro formula written by a colleague, Tetsuji Shimizu. In principle, following equation is solved numerically to obtain E_{el} (adapted from [4]):

$$E_{\mathrm{el}} = \oint U(t)\, dQ = C_{\mathrm{exp}} \oint U(t)\, dU_{\mathrm{exp}} = \tag{2.1}$$

$$= 4C_{\mathrm{die}} \frac{1}{1 + C_{\mathrm{gap}}/C_{\mathrm{die}}}\, U_{\mathrm{min}}\left(\widehat{U} - U_{\mathrm{min}}\right) = \tag{2.2}$$

$$= 2\left(\widehat{U}Q_0 - \hat{Q}U_0\right) \equiv A_{\mathrm{loop}} \tag{2.3}$$

$\boldsymbol{U_{min}}$ is minimum external applied voltage at which the ignition occurs, $\widehat{\boldsymbol{U}}$ maximum voltage amplitude, $\widehat{\boldsymbol{Q}}$ maximal transferred charge, $\boldsymbol{U_0}$ maximum voltage without discharge, $\boldsymbol{Q_0}$ the maximum charge transferred before ignition, $\boldsymbol{C_{gap}}$ capacitance of the gap and $\boldsymbol{C_{die}}$ capacitance of the dielectric.

Solving (2.1) enables the calculation of the plasma power $\boldsymbol{P_{el}}$:

$$P_{\mathrm{el}} = f\, E_{\mathrm{el}} \tag{2.4}$$

where f is the frequency of the applied voltage.

Resulting values were averaged and standard errors were calculated. Beside the total consumed power in W, the power density was determined in mW/cm^2 across the discharge area (112 cm^2).

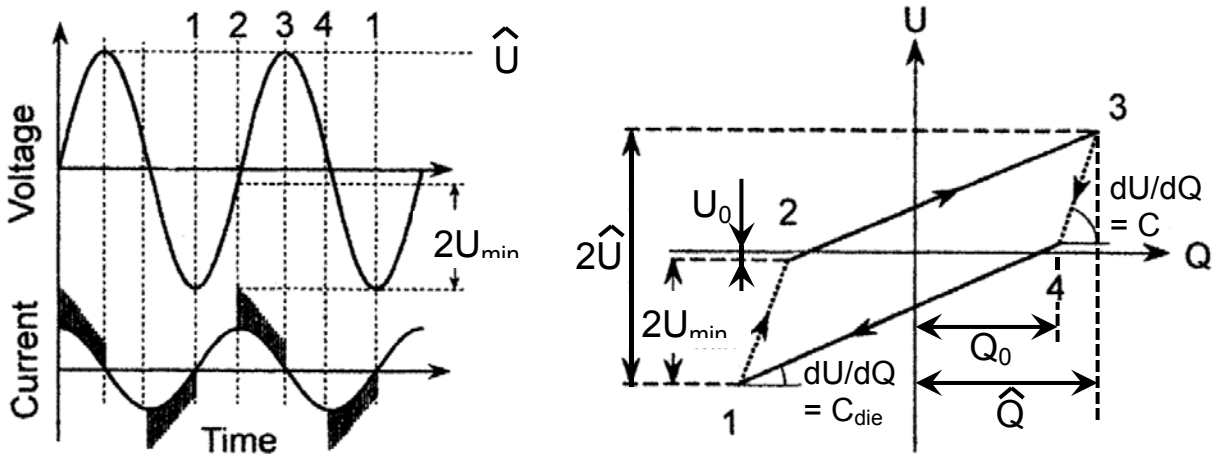

Figure 2.8: Symbolic presentation of micro-discharge activity and corresponding voltage/charge Lissajous figure (adapted from [10]).

2.2.5 Ozone concentration via absorption spectroscopy

The concentration of ozone produced during plasma discharge was measured inside the FP2.0 by absorption spectroscopy. The measurement is based on the Beer-Lambert law:

$$I_A = I_0 \mathrm{e}^{-\sigma_\lambda L c} \tag{2.5}$$

with
- I_A transmission intensity after ozone absorption
- I_0 incident transmission intensity without absorbance
- σ_λ absorption cross-section of ozone at specific wavelength λ
- L absorption path length
- c concentration

The concentration in ppm is derived from this equation by the involvement of Loschmidt´s number N_L(2.69 × 10^{19} cm^{-3}):

$$c_{O_3}[ppm] = ln\frac{I_0}{I} \cdot \frac{1}{\sigma_\lambda L} \cdot \frac{1}{N_L} \cdot 10^6 \quad (2.6)$$

A Hg lamp (Avalight-CAL, Avantes, Netherlands) provided the measurement wavelength 254 nm at which ozone shows highest absorption. Therefore, the absorption cross-section $\sigma_{O_3,254\,nm}$ was set to 115.9 × 10^{-19} cm^2/molecule [138]. The absorption path length was adjusted with adequate tubes to 1.35 cm, in order to avoid full absorption which was measured at lengths bigger than 2 cm. The experimental set up is given in Figure 2.9. The SMD electrode and the cover with the lid were mounted for closed conditions during measurements. The SMD electrode was positioned at the lowest height with a distance of ca. 0.5 cm from the grounded electrode to the light ray. Pinholes were used to confine the light. Quartz and MgF_2 windows being translucent for the 254 nm wavelength were used. The transmitted light was detected *in situ* via UV/VIS-spectrometer (AvaSpec, Avantes, Netherlands) and the data was recorded with Avantes software. The experiment was conducted in scope mode and the intensity of the transmitted light was obtained at 253.5 - 254.5 nm with an integration time of 250 ms. The starting intensity was around 25,000 or 50,000 counts. It was every time averaged from the values measured during the first 60 s prior to the start of the discharge and was corrected by the background signal noise of the measurement which refers to an averaged value during 10 s without incident light. The discharge lasted 5 min and the measurement was continued for 30 min afterwards, until absorption was not apparent anymore. Subsequently, the device was air-evacuated with the filter pump, before the next

measurement was started. This procedure was repeated three times at the same condition. The voltage was set constant to 10 kV_{pp} at varying frequencies of 0.5 kHz, 1 kHz, 3, kHz and 6 kHz. For additional measurements, the electrode system was positioned 1.5 cm higher at 1 kHz.

The ozone concentration was calculated for each measurement according to equation (2.6). Next, the measured data had to be averaged. Since the time intervals between measured data points were not constant, regression curves were fitted to the experimental data following polynomial equations of the 5th degree by Excel. Therefore the measurement curve had to be divided into three parts: discharge-on time (0 - 5 min) and two parts in the discharge-off time having the separation point at 10 min where the fitting result was sufficient for every measurement ($R^2 > 0.99$). Connecting data points between the parts were considered. Subsequently, data points of each resulting regression were derived in equal time intervals. Finally, the mean and the standard error of the data from three independent measurements could be calculated. In addition, the area under the curve was reckoned as the dose in ppm × min using the linear trapezoidal rule.

For comparison reasons, measurements were conducted at same conditions with a remote ozone gas analyzer (465M, Teledyne Advanced pollution instrumentation, USA) which had a possible measuring range from 0 - 10,000 ppm. The plasma gas was sucked in a Teflon tube (4 mm in diameter, 2 m long) which was inserted through a hole in a central plug and was transported to the absorption cell where it was analyzed *ex situ* according to (2.5). Digital values were documented every 10 s during the experiment. Every measurement was done three times. Averaged values and standard errors were determined.

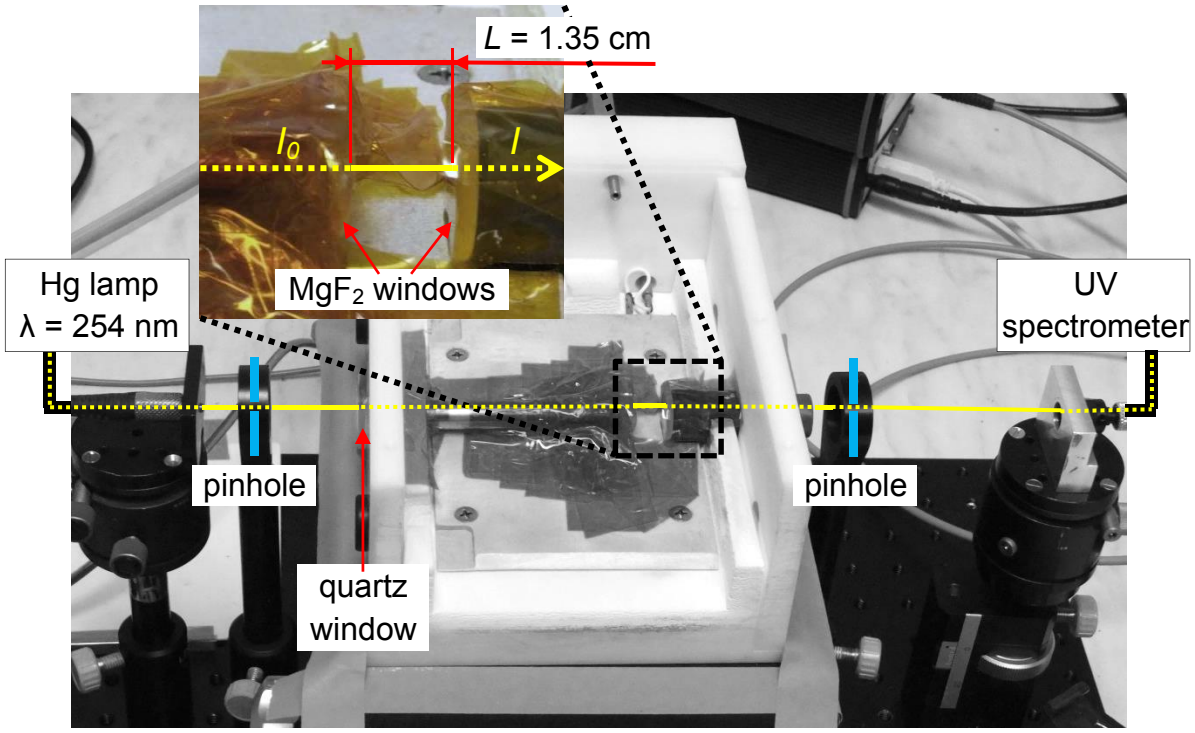

Figure 2.9: Experimental set-up for the determination of the ozone concentration via absorption spectroscopy.

2.3 Quantitative Methods assessing plasma decontamination

2.3.1 Testing the bactericidal effect using agar plates

This SMD plasma experiments were conducted with the vegetative bacteria *E. coli* ATCC 9637, *Enterococcus mundtii* ATCC 43186 and *Pseudomonas aeruginosa* ATCC 9027 on agar plates. Preparation of the inoculated agar plates, the treatment procedure and the incubation after plasma treatment follows the protocol described in section 2.1. Agar plates were treated for 15 s up to 5 min. Every treatment was performed three times at the same condition and the experiment was reproduced one time.

After incubation, the colony forming units (cfu) of surviving bacteria were counted. Results are shown as logarithmic cfu reduction curves in dependence of the treatment time. Log corresponds to $\log_{10}$. The log reduction was calculated from:

$$\log N_R = \log N_0 - \log N_S \tag{2.4}$$

N_R is the number of reduced bacteria, N_0 is the number of initial population and N_S is the number of surviving bacteria of a given strain in cfu after plasma treatment. If no colony growth was found, complete inactivation was achieved. The values were averaged and the standard errors were determined from both independent experiments.

2.3.2 Sterilization testing using dry inanimate carriers

The efficacy of SMD plasma against bacterial endospores which are commonly used as standard bioindicators for the validation of sterilization processes was investigated with different inanimate carrier materials (metal, glass and polymeric surfaces). Microbial carriers were wrapped in Tyvek® coupons (Figure 2.10). Tested bacterial endospores include spores of *G. stearothermophilus* and *Bacillus* spp.

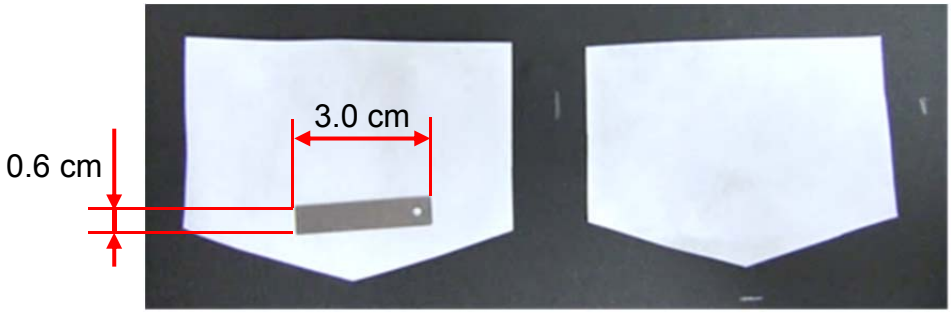

Figure 2.10: Biological indicator coupons: transparent impermeable PE cover on one side (left) and opaque gas permeable Tyvek® on the other side (right).

Experimental set-up

The bacterial endospores of *G. stearothermophilus* ATCC 7953, *B. subtilis* DSM 13019, *B. atrophaeus* ATCC 9372 and *B. pumilus* ATCC 27142 were used as biological indicators for the validation of atmospheric SMD air plasma as a sterilizing agent. The indicator samples were provided and analyzed quantitatively by Simicon

GmbH (Munich, Germany) according to DIN EN ISO 14937, which is the standard for the validation of sterilization processes of medical devices [135] and according to DIN EN ISO 11737-1 for the microbiological determination of surviving units on products [139]. Initially, 100 µL of spore suspension (2×10^7 cfu/mL deionized water) were placed on one side of the test specimen (2 cm^2) and dried under the laminar flow. The inoculated test specimen was wrapped according to medical packaging with Tyvek on the endospores facing side and with impermeable PE film on the backside. Other test specimens include Teflon (Goodfellow, USA), polyvinylchloride (PVC, Goodfellow, USA) and glass (Menzel, Germany). The spores were treated with CAP leaving the samples inside the Tyvek coupon, which has already been shown to be permeable for plasma [28, 122].

For experiments, the sample with the Tyvek side at top was placed in the center of the SMD device. The treatments lasted 1 min, 3 min and 5 min. Every spore treatment was conducted at least three times. Each sample was placed in a separate plastic bag after treatment and sent together with a transport control sample to Simicon GmbH (Germany) on the same day. There the spores were suspended in 10 mL H_2O medium (Ampuwa®, Fresenius Kabi, Germany) and treated for 10 min in the ultrasonic bath for spore detachment purposes. The recovery of viable spores followed a dilution series (10^{-1}, 10^{-3}, 10^{-5}). In case of 10^{-3} or 10^{-5} dilutions, 100 µL of the corresponding dilution were distributed on TSA. To analyze 10^{-1} dilutions, 1 mL from the suspension was poured together with liquid TSA into petri dishes. The agar plates inoculated with *Bacillus* spp. were incubated overnight at 35 ± 2 °C except *G. stearothermophilus* spores which were incubated for 48 h at 56 ± 2 °C. Viable counts of the colony forming units were performed. No detection of growing colonies implied

a minimum survival of ≤ 10 cfu. Results are shown as log reduction curves, D-values and SAL; log corresponds to $\log_{10}$

D-value and SAL calculation of spore reduction

The characteristic decimal reduction time was determined from the data of plasma-treated endospores by the equation:

$$t = D_{\mathrm{T}} \cdot \log N_R \tag{2.5}$$

t is the treatment time in minutes, D_{T} is the D-value in minutes for a single decimal reduction at the treatment temperature T. Here, T was room temperature (23 °C) at ambient pressure. Data points were selected assuming 1st order kinetics. Average values were used for calculation and interpolated except if detection limit was reached. Treatment times were determined as specific SAL that are equivalent to theoretical 6 and 12 log reduction [140]. An overkill with 12 log reduction means that a bacterial spore survives the plasma treatment with a predicted probability of 10^{-6}.

2.3.3 Disinfection testing

Two different standard approaches were chosen to investigate the disinfecting behavior of SMD plasma: The first one is dealing with bacteria on carriers for the disinfection of medical devices and the second one was modified from a proposed standard for testing surface disinfectants on PVC flooring.

2.3.3.1Treatment of bacteria on dry carriers (phase 2/step2)

In this study, the inactivation profile of SMD plasma was characterized against bacterial endospores from *C. difficile* ribotype 027. Endospores from *B. subtilis* and *G. stearothermophilus* served as surrogates. Gram-positive vegetative *Enterococcus*

faecium and *Staphylococcus aureus* were also examined. All germs were inoculated on carriers and optionally 0.03% BSA was added, simulating already pre-cleaned surfaces according to European testing standards for disinfection [136].

Preparation and analysis of microbial samples

Endospores and vegetative bacteria were prepared on conventional-sized dry stainless steel carriers (2 cm^2) to conduct phase 2/step 2 tests. The inoculated carriers were provided with or without low organic burden (= 0.03% BSA) by the Institute of Hygiene and Public Health (IHPH, University Bonn, Germany) or with distinct sample properties by Simicon GmbH (Munich, Germany) in gas permeable Tyvek coupons according to sterile medical packaging (Table 2.2). Spore-forming and non-spore-forming vegetative bacteria were preserved on the base of EN 12353 [141]. Plasma treatment results were assessed as logarithmic microbial reduction based on recoverable bacteria from negative controls and treated samples (average ± standard error); log corresponds to $\log_{10}$.

Table 2.2: Endospores and vegetative bacteria in this disinfection study

Microorganism	Strain(*)	Inoculum on carrier, cfu	grown on agar type(•)	Incubation for analysis			Standards
				Time	Temp.	aerobe	
Bacterial endospores							
C. difficile	NCTC 13366	10^6	GSBHI	72 h	37 ± 2 °C	- (o)	DIN EN 13704(a), CEN/TC 216 WG1(b)
B. subtilis	ATCC 6633	10^6	PC	48 h	37 ± 2 °C	+	DIN EN 13704(a)
G. stearothermophilus	ATCC 7953	10^6	TS	48 h	56 ± 2 °C	+	DIN EN 14937(c)
Vegetative bacteria							
E. faecium	ATCC 6057	10^6 (e), 10^8 (d, e)	PC	48 h	37 ± 2 °C	+	DIN EN 14561(d)
S. aureus	ATCC 6538	10^8	TS	48 h	37 ± 2 °C	+	DIN EN 14561(d)

(*) ATCC, American Type Culture Collection; NCTC, National Collection of Type Cultures
(•) GSBHI, glucose starch brain heart infusion with 0.1% taurocholic acid sodium salt hydrate; PC, plate count; TS, tryptic soy
(o) anaerobic condition: 1% O_2 level, 9 - 13% CO_2 level
(a) IHPH; adapted from standard suspension test for chemical disinfectants in the food, industrial, domestic and institutional area [142]
(b) IHPH; adapted from proposed standard suspension test with anaerobic spores for chemical disinfectants in human medicine [143]
(c) Simicon GmbH; standard carrier test for sterilising agents [135]
(d) IHPH; standard carrier test for chemical disinfectants [144]
(e) Simicon GmbH; sample preparations deviating from DIN EN 14561

Bacterial endospores

Enrichment of *C. difficile* endospores was conducted according to the work item of CEN TC 216 of WG1 [143] and of *B. subtilis* spores according to the SOP 112 in a self-made glass fermenter [145] (see enrichment protocols below). Prior to carrier inoculation, BSA in saline solution was optionally added to the aqueous test suspension, resulting in final 0.03% BSA. 50 µL were distributed onto carriers, dried and wrapped in Tyvek. The preparation of *G. stearothermophilus* spore samples was described in detail previously. For analysis, endospores were detached from carriers and suspended in H_2O by vortexing and in case of *G. stearothermophilus* also sonicating for 10 min. An appropriate dilution series was conducted, plated and incubated at conditions listed in Table 2.2. Viable counts were performed. If no

survival was observed, further qualitative analysis via the turbidity method was conducted with appropriate media and incubation for 7 days.

Vegetative bacteria

The preparation of working cultures, test suspensions and carrier inoculation was performed according to EN 14561 [144]. The number of cells in the saline suspension was adjusted to 2 - 5 × 10^9 cfu/mL with 8.5% tryptone-NaCl using McFarland standard. As for spores, BSA was optionally added to the saline test suspension and 50 µL were distributed onto carriers, dried and wrapped in Tyvek. Special *E. faecium* samples deviating from the EN standard (Simicon GmbH) were prepared under different conditions, in order to compare the bactericidal effect of plasma versus regular samples (IHPH). Therefore, the inoculation area (2 or 8 cm^2), microbial load (10^6 or 10^8 cfu), organic burden (± 0.03% BSA, heparinized sheep blood) and test suspension medium (saline solution or H_2O Ampuwa®) were altered. For analysis, each sample was vortexed in saline solution, diluted, plated and incubated at conditions described in Table 2.2. Viable counts were performed. As for bacterial endospores, the turbidity method was conducted, if no survival was observed via the plate count method.

Enrichment protocols for bacterial endospores at IHPH

C. difficile

First, working cultures were incubated from one bead of frozen stock cultures on columbia blood agar (CBA) under appropriate incubation conditions (Table 2.2). For enriching *C. difficile* spores, a single colony was added to pre-reduced tubes with meat medium covered with paraffin and incubated in an anaerobic chamber for at least 18 h. Pre-reduced CBA plates were inoculated with 100 µl of the inoculated

meat medium and incubated anaerobically for 7 days at 37 °C and subsequently for 14 days at room temperature in the absence of light. The spores were harvested by washing down with 2-3 mL sterile H_2O. The collected suspension was centrifuged (3000 G; 10 °C; 10 min) and washed three times with 50 mL sterile H_2O. The final suspension was adjusted to a density of 2×10^7 cfu/mL. To inactivate any vegetative cells, the spore suspension was heated at 80 °C for 10 min. Its purity was proved by phase contrast imaging and it was stored with sterile glass beads at 2 - 8 °C for six till eight weeks until use.

B. subtilis

First, the sporulation medium consisting of 900 mL of solution 1 (magnesium sulfate monohydrate, potassium chloride, nutrient broth, iron sulfate solution) and 100 mL of solution 2 (calcium nitrate and manganese chloride tetrahydrate) was filled into the 2 L fermenter. The exact composition of both solutions is described elsewhere [110]. The sporulation medium was inoculated with 5 to 6 colonies of the first working culture and incubated at 37 °C with magnetic stirring (120 rpm). After an incubation time of 5 h, clouding of the sporulation media occurs and aeration by activating a membrane pump was added. The incubation was continued with aeration for 72 h at 37 °C. Before harvesting the spores, a sonication step was carried out for 2 min at 10 °C. The spores were harvested by stepwise centrifugation (5000 G, 10 °C, 15 min) and washed three times with 25 mL sterile H_2O. The final spore suspension was adjusted to ~ 2×10^9 cfu/mL. To inactivate any vegetative cells, the spore suspension was heated at 80 °C for 10 min. The purity was proved by phase contrast imaging. Final suspension was stored with sterile glass beads at 2 - 8 °C for at least four weeks until use.

SMD plasma experiments

The SMD plasma was generated with an electrode system at ambient air conditions (23 °C). Individual microbial samples were treated within the Tyvek® coupon centred and 5 mm below the electrode system inside the closed FP2.0 for up to 10 min. Every treatment was carried out three times and experiments were reproduced with the same conditions. Plasma-treated samples were analyzed together with two negative controls, which were stored at the analyzing facilities, in order to determine the recoverable microbial load of each batch at the time of analysis for log reduction calculations; and with one neutral transport control, in order to detect possible inactivation during transportation from the plasma lab to the analysing facility.

2.3.3.2 The modified 4-field-test (phase2/step2)

The 4-field-test is a proposed EN standard test for evaluating the potency of surface disinfecting agents [146-148]. Briefly, it involves the mechanical distribution of a liquid disinfectant by a wipe for microbial inactivation. The wipe is guided over four fields with specific size (5 × 5 cm^2) only the first being contaminated on PVC flooring (DLW Vinyl Solid PUR, Armstrong, Germany) typically used in clinical facilities and the microbial distribution as well as the inactivation are assessed (Figure 2.11). For my study, this procedure was modified to the needs of gaseous plasma. Therefore, the mechanical wipe part and also the dynamic guidance over the four fields were omitted. Instead of inoculating only the first field, all fields were inoculated with the same bacterial load. The first three fields were treated one after another with SMD air plasma, the fourth field was used as control and microbial inactivation was assessed (Figure 2.12).

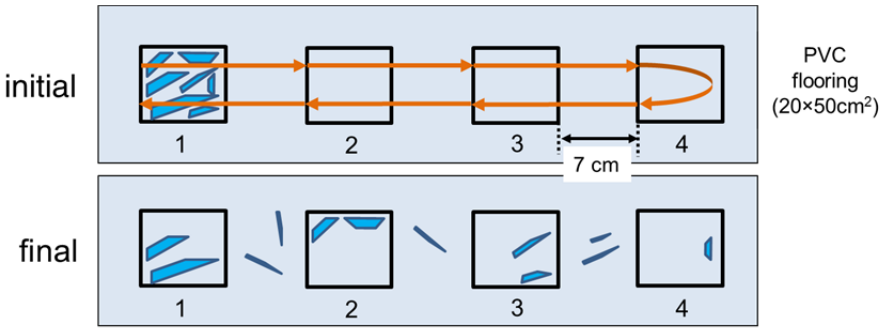

Figure 2.11: Schematic of the normal 4-field-test proposed as standard for surface disinfectants.

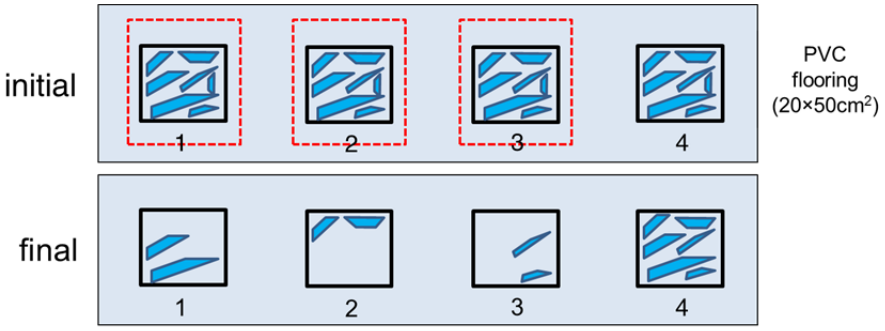

Figure 2.12: Schematic of the modified 4-field-test for the investigation of plasma in surface disinfection.

Modification of the plasma device

The set-up of the plasma device had to be changed for this experiment, in order to treat surface areas outside the FP2.0. Therefore, the electrode system was removed together with its frame from the housing. The assurance of the safety in use had the highest priority and for that reason critical parts (powered electrode, powered line) were isolated to minimize the risk of electric shock. A holder enables the guiding over the surface, while plasma is ignited. Teflon screws were installed as spacers at the corners of the electrode frame. This allows the treatment of the surface in constant 0.5 cm distance like in the carrier experiments. Two barrier layers (Teflon, 0.5 mm thick) were mounted at the edge of the frame, in order to avoid unwanted air turbulences like convection from outside which would influence the treatment and to

slow down diffusion of plasma species to the outside. The modified device is depicted in Figure 2.13.

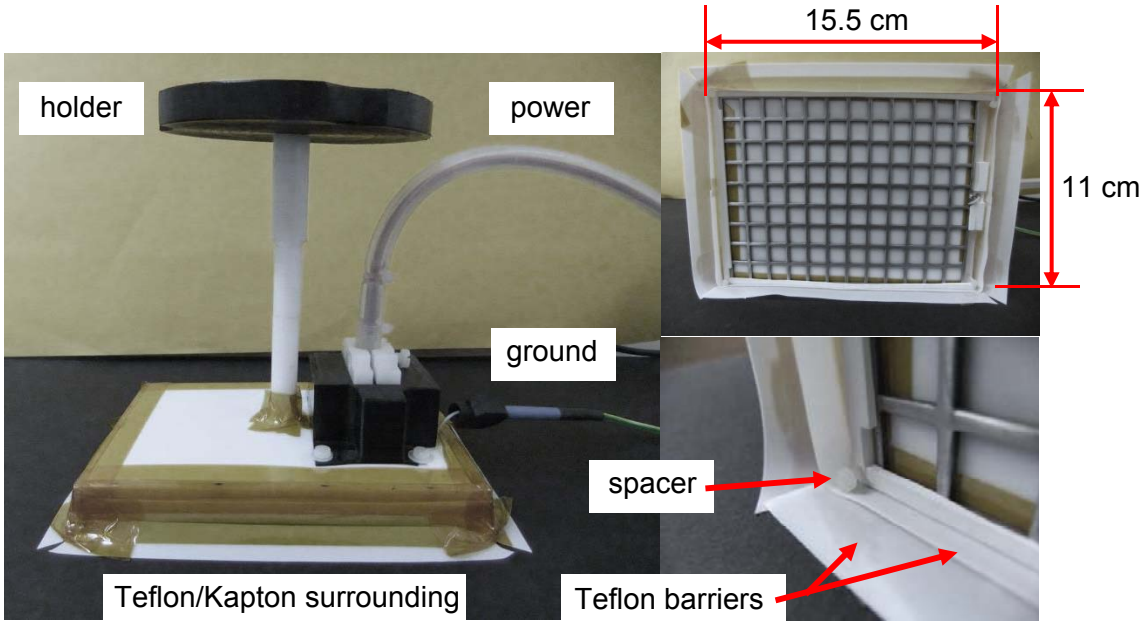

Figure 2.13: Set up of the modified SMD device.

Preparation, treatment and analysis of microbial samples at IHPH

Bacterial endospores of *C. difficile* and *B. subtilis* as well as vegetative bacteria *E. faecium* and *S. aureus* were used together with 0.03% BSA simulating pre-cleaned condition as previously described (Table 2.2). Instead of carriers, each field of the PVC flooring was inoculated with 50 µL of bacterial suspension with a glass spatula. Suspensions had a microbial density of around 10^7 cfu/mL for bacterial endospores and 10^8 or 10^9 cfu/mL for vegetative bacteria. At the same time, another field separated from the flooring with the four fields was also inoculated and served as the drying control D. It determined the initial reference load for log reduction calculations. After 30 min drying at ambient air, three of the four fields of the flooring were treated one by one with plasma inside a fume hood at ambient room conditions (23 °C). Therefore, the device was placed over the first field and treated for 1, 3, 5 or 10 min at constant 1 kHz and 10 kV_{pp}. Afterwards, the device was removed from the field

and the next treatment of an adjacent field was started after 2 min. Having finished the treatment of three fields, all treated fields of the flooring and the untreated fourth field, which served as control for side-diffusing plasma species, were analyzed via the standard swab method [149]. Briefly, bacteria were collected from the surface with two pre-wetted swabs per field, suspended in 5 mL medium and diluted appropriately. 100 µL were distributed onto agar surface and incubated (Table 2.2). Viable cell counts were performed. Log reduction and survival curves were determined. The experiment was reproduced one time. Results are given as averaged values and their standard errors from both experiments.

2.3.4 Testing the influence of Tyvek cover on microbial inactivation

The investigation of the real impact of the Tyvek cover on the microbial inactivation by SMD plasma was conducted with a series of treatments and subsequent analyses of *G. stearothermophilus* endospores on stainless steel substrates at MPE.

Preparation of samples

Biological indicator samples as used in previous experiments were purchased from Simicon GmbH (SIMICON-OX). In this experiment, all samples were from the same production batch no. 210413 having 2×10^6 cfu spores on their surface. Different sample configurations were prepared prior to treatments including either Tyvek cover or not. Optionally, substrates were placed in glass ($Ø_{inner}$ = 3.7 cm) or plastic vessels ($Ø_{inner}$ = 9 cm, PE petri dish) both with the same depth 0.7 cm but with different filling volume (7.5 cm^3 and 44.5 cm^3, respectively). Many of these were put in Tyvek coupon (Stericlin®, Simicon GmbH, Germany) and sealed by manual impulse hand sealer (hpl ISZ 200, Hawo GmbH, Germany). Occasional substrates were sealed in

impermeable PE coupons as controls for the exclusion of gaseous plasma species. Other samples were placed without cover on anodized alumina or thin Teflon plate.

SMD experiment

Individual samples were inserted in central position into the FP2.0. The preferred distance was 1.5 cm to the SMD electrode which was normally in the lowest position. Most samples were treated at 1 kHz and 10 kV_{pp} for 3 or 5 min at ambient conditions (23 °C) and inside the closed device. Frequency, distance or the height of the electrode system among others were altered in certain situations described in detail in the results section. After the treatment, the sample was removed, the carrier immediately placed into a tube with suspending medium, in order to avoid post-plasma effects. The device was air-evacuated with the ozone filter pump for 1 min, before the next treatment cycle could start. Six samples were treated at same experimental conditions and in the great majority of cases, each set of experiment was repeated one time.

Analysis of carriers

The quantitative analysis of *G. stearothermophilus* spores was carried out following the protocol of a standard that Simicon GmbH applies (see sterilization experiments) [139]. In detail, spores were suspended in 10 mL Ampuwa® water, vortexed for 1 min, placed for 15 min in the ultrasonic bath and vortexed again for 1 min. Afterwards a dilution series was conducted (always 1 mL in 9 mL). TSA plates were inoculated with 100 µL via the spread plate method and incubated at 56 ± 2 °C for 24 h. Counts of viable cells were performed with a manual colony count device (schuett count, schuett-biotec GmbH, Germany). Since the pour plate method was not applied as 10^{-1} dilution determinant (1 mL out of 10 mL of undiluted suspension

poured together with liquid agar), the detection sensitivity was lower compared to previous experiments with minimum 100 cfu or in other words, a maximum of 4.3 log reduction could be detected.

At the beginning, samples were analyzed at MPE and at Simicon GmbH for the validation of the analysis method.

Determination of the log reduction

In contrast to previous calculations, the median of the resulting cfu values from six individual samples was determined. The absolute deviations of each of the six values from the median were obtained and their own median, the so called median absolute deviation (MAD) determined. The analysis results of two times six untreated samples served as reference for the calculation of log reduction values. Results are expressed as the mean from the log reduction of normally two median values acquired from two independent series with six samples; log corresponds to $\log_{10}$

Determination of adherent spores to Tyvek cover

From an initial *G. stearothermophilus* suspension with 10^8 cfu/mL (SPW8206-8, Simicon GmbH) a dilution with 10^4 cfu/mL was prepared. 10 µL were distributed from this dilution over a piece of Tyvek cover (Stericlin®, Simicon GmbH) cut to the same size as the one covering biological indicators. The samples were dried for 30 min at ambient air. In order to detect the spore number that can be recovered from the inoculated Tyvek covers, samples were pressed directly on TSA surface, removed after short time and pressed again on another TSA plate. This was repeated until four agar plates were inoculated from one sample. The idea was to detect spores which were not detached from the Tyvek cover in the first press cycle. The backside of the

cover without the spores served as negative control and was pressed on TSA as well. Agar plates were incubated at adequate conditions. Cell count was performed.

Similarly, Tyvek covers from untreated biological indicator samples were pressed 20 times in series on different agar plates. Plates were incubated. If cell count was not possible, the number of colonies was estimated. The mean value and the standard error of three analyzed Tyvek covers were determined.

Tyvek covers from treated biological indicator samples were also analyzed. As for the carrier test, two times six Tyvek covers exposed to plasma (1 kHz, 10 kV_{pp}, 1.5 cm distance) were used.

2.4 Scanning Electron Microscopy of bacteria on carriers

The impact of microbial distribution and burden on the plasma decontamination was investigated by SEM imaging of carrier surfaces for the interpretation of inactivation results.

SEM imaging and energy-dispersed x-ray (EDX) analysis

Samples of *C. difficile* and *G. stearothermophilus* endospores and of *E. faecium* that were studied by SEM/EDX belonged to the same batch used in the SMD plasma experiments. At least two untreated and one treated samples were imaged per sample configuration. Four surface sites per selected sample were randomly imaged by SEM. The treatment time for SEM samples equals the maximum treatment time for samples used in the SMD plasma experiments (5 or 10 min).

Bacterial endospores

Scanning electron micrographs from samples of *C. difficile* or *G. stearothermophilus* endospores were taken using a SEM system from FEI (HELIOS Nanolab 600; Netherlands). Pre-coating of the sample was not required. The accelerating voltage

of electron beam was set constant to 5 kV and the working distance to WD > 4 mm. The system was operated in second electron detection mode at high vacuum (10^{-4} Pa). Vacuum drying and electron beam had no morphological effect on spores and supplements (data not shown). EDX analysis identified chemical structures found in SEM images by qualitative elemental mapping (Oxford Instruments, INCA PentaFET-x3 Si detector).

Vegetative bacteria

E. faecium samples from Simicon GmbH were imaged using a high resolution SEM from JEOL (JSM 7500F; Japan) with cold field emission electron source. The system allows the imaging with low electron beam power (accelerating voltage = 1 kV, beam current = 90 pA) and a long working distance (WD > 14 mm), in order to avoid bacterial damage by the beam. Dehydration cycles with ethanol and pre-coating were not necessary prior to the imaging process. The system was operated in second electron detection mode at high vacuum (10^{-5} Pa).

3 RESULTS

3.1 Developing the electrode system

To start with, I had to choose an appropriate electrode system for the following decontamination studies with the available developed SMD air plasma device. The housing of the FP2.0 as well as the frame for the SMD electrode was provided. I addressed this task by establishing certain criteria, which should be fulfilled by the prospective electrode system. This involved the supply of a homogenous discharge pattern along the dielectric surface, a far-reaching maintenance of the stability of electrode components used and an appropriate bactericidal effect of the generated SMD plasma.

For all the above reasons, the performance of various grounded electrodes with distinct materials and mesh structures was studied. The resulting discharge pattern and bactericidal effects are depicted in Figure 3.1. Homogeneity was present to a great extent for all grounded electrodes at 2 kHz, which was on the other hand more difficult to obtain at a higher frequency of 6 kHz, emphasized by the red arrows in discharge images. This phenomenon influenced clearly the bactericidal effect of the plasma. At areas where no discharge was observed, *E. coli* was more likely to survive the treatment and could grow to form dense layers (red arrows). This underlines the importance of acquiring a homogenously distributed discharge. The results from the 6 kHz treatments illustrate this adequately, although they cannot further indicate, due to the use of different voltage amplitudes, which electrode generated plasma with higher bactericidal effect. The limit of the power supply was reached at this frequency and the available voltage ranges were narrow and different. However, the bactericidal outcome is clarified at 2 kHz treatments, where plasma from electrodes D, C, B and A showed in that order increasing microbial inactivation.

In addition, the materials were visibly checked, if they underlay any alterations due to plasma exposure (Figure 3.2). The grounded electrode depicted in Figure 3.2 corresponds to A and exhibited strong features of corrosion due to its composition of plain steel. Less strong effect could be accomplished with plain and anodized alumina meshes C and D, respectively, whereas the stainless steel mesh B was not affected (data not shown).

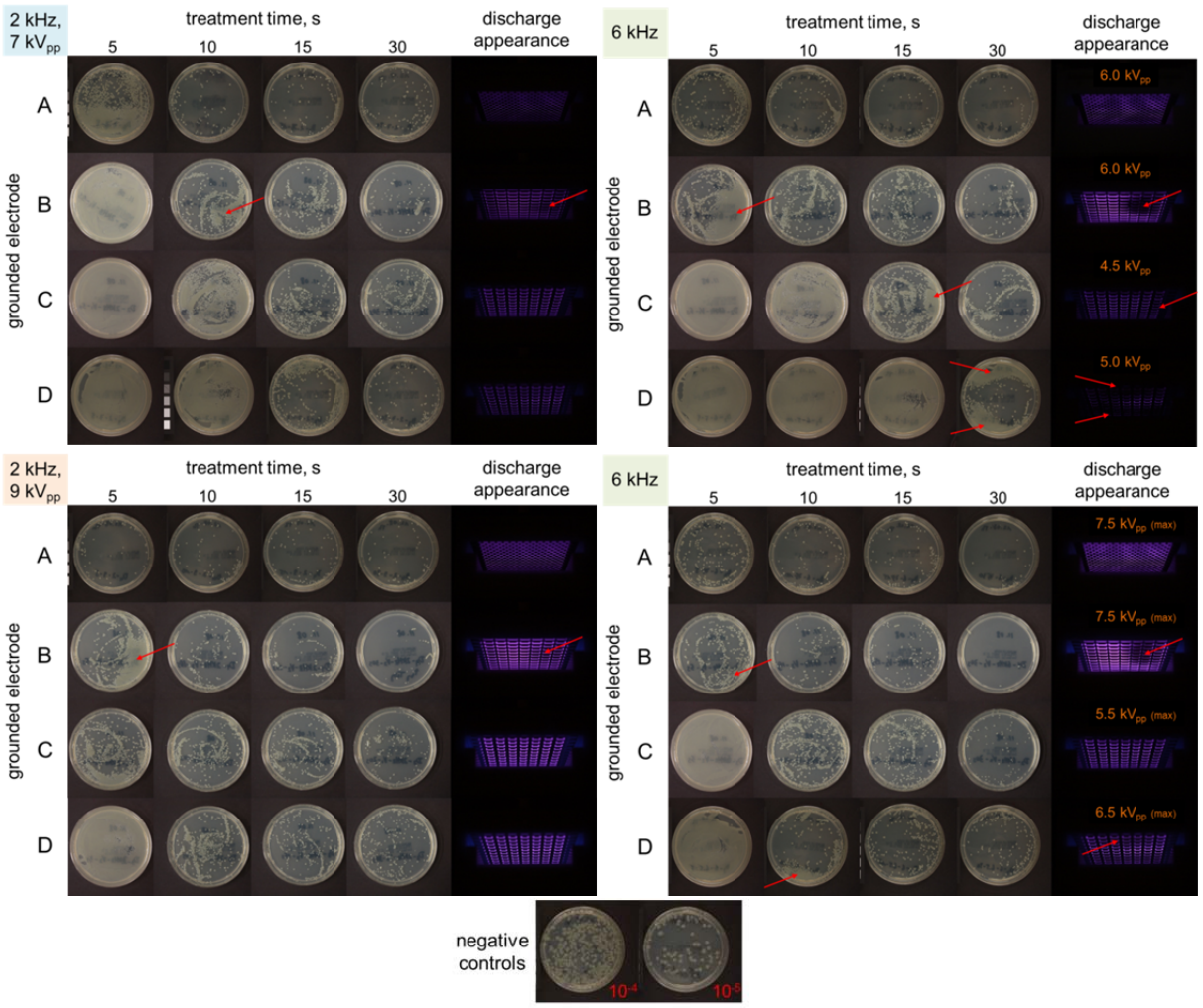

Figure 3.1: Photographic results of MH agar plates of *E. coli* treated with plasma derived from different grounded electrodes (A, B, C, D) at 2 kHz and 7 or 9 kV_{pp}, at 6 kHz and varying voltages and the corresponding discharge appearance.

Overall, the grounded electrode B was identified as the most suitable among tested objects and was installed permanently for further studies. The issue with the homogeneity of the discharge pattern was addressed by adjusting the fixation.

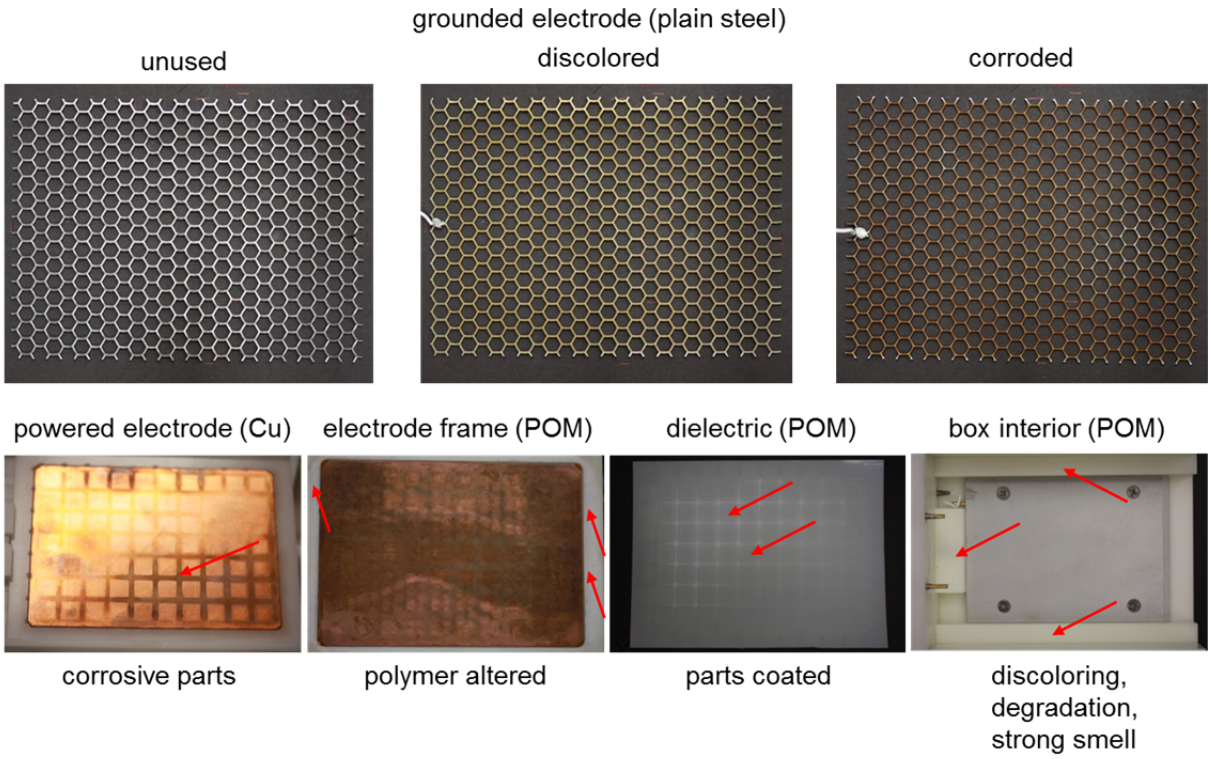

Figure 3.2: Effect of plasma exposure on diverse device components.

In addition, other device components were also examined for their stability against plasma Figure 3.2. Especially parts made of POM such as the dielectric and the housing were altered by plasma. The dielectric material POM tended as well to break down during treatments (lower minute range). Therefore, the dielectric material and the electrode frame were exchanged by chemically inert and more stable Teflon® film (0.5 mm thick, Goodfellow), however the POM housing was further used. Moreover, corrosion occurred on the powered electrode plate made of copper in form of tarnishing followed by patina formation at extensive use. For this reason, it was substituted by the composite brass that helps resist tarnishing.

The final configuration of the SMD electrode system consisted of a solid brass plate and a mesh grid made of stainless steel, both spaced by a dielectric Teflon film and its discharge appearance is demonstrated in Figure 3.3.

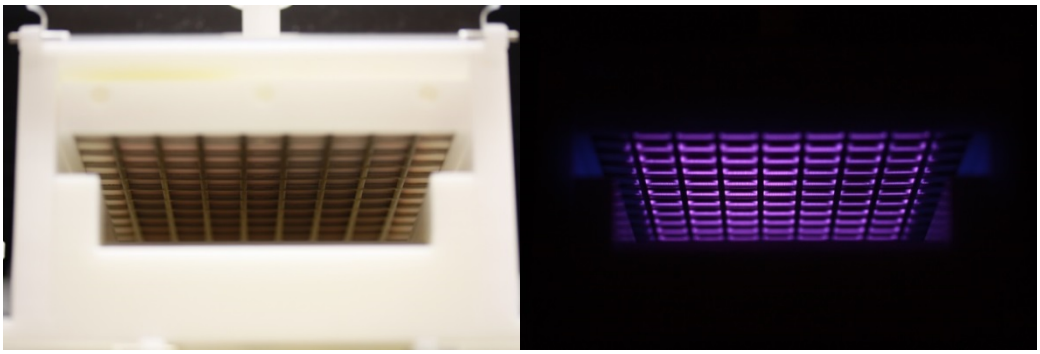

Figure 3.3: Final SMD electrode configuration.

Regarding to the development of the system, the dielectric material was found humid at the side of the powered plate after long time use. This was probably caused by discharge heating and subsequent water evaporation from the biological sample such as an agar plate. The humidity was assumed to accelerate dielectric breakdown and metal corrosion. In order to circumvent this issue, Kapton tape was wrapped around the electrode system except from the grounded mesh “sealing” the openings at its edges.

3.2 Plasma diagnostics

Following the setting up of the equipment, the physical and chemical entity of the SMD air plasma generated with the developed device was characterized, in order to elucidate its inactivating effect against bacteria in subsequent studies.

OES spectral analysis

The emitted photons of the SMD in ambient air are strongly dominated by excited N_2 molecules (Figure 3.4). The spectra exhibit almost no radiation in the most hazardous UV-C region below 280 nm. However, less harmful UV-A and UV-B are present. Moreover, higher external power due to higher frequency or voltage caused more prominent spectral peaks. Especially in the UV-C and the near infrared region weak spectral lines occur. These spectral lines refer mainly to excited N_2, yet peaks in the UV-C region could be related to photons from NO. A clear assignment to one of these molecules is not possible due to overlapping peaks. The peak at 685 nm could not be assigned to any molecule even with the aid of an extensive spectral library [137]. Due to its absence in other measured spectra, it might be an impurity. Indications of other chemical active molecules such as ozone or singlet oxygen are missing or questionable due to overlapping spectra (Table 3.1). Besides, ozone is in general hardly detectable by OES.

Table 3.1: Relevant plasma species and their wavelength appearance [137].

chemical species	expected wavelength range, nm
N_2 (2nd+)	280 - 497
N_2 (1st+)	640 - 780
N_2 (4th+)	220 - 280
NO (γ)	~ 247
OH	308
O_3	328
singlet O_2	762
atomic O	777

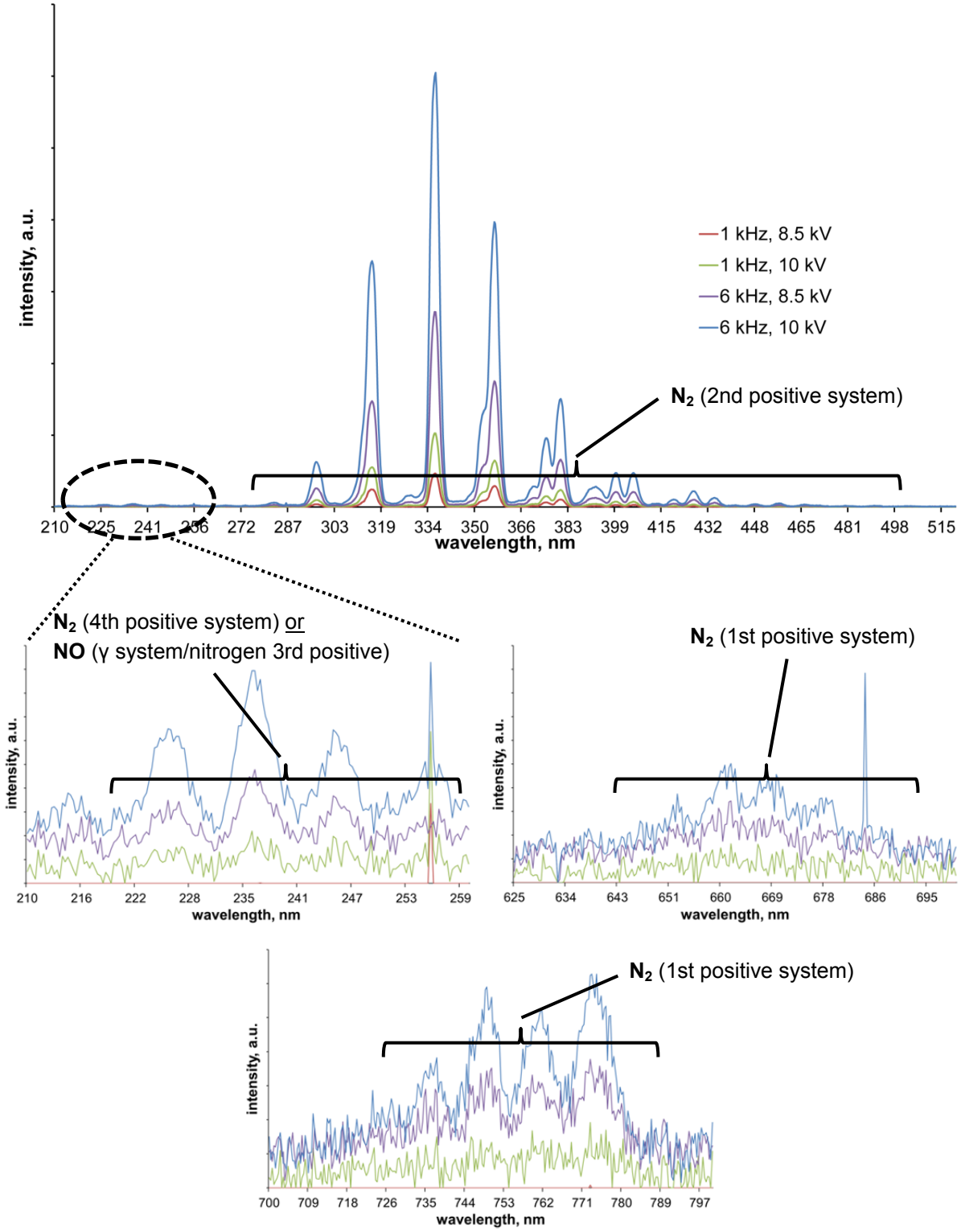

Figure 3.4: Dominating OES spectral lines of SMD air discharges (upper spectra) and magnified spectral regions with minor peak appearances (smaller spectra).

UV-C power density

The power density of the emitted UV-C photons was measured at 1 kHz, 10 kV_{pp} in the region below 280 nm which refers to the most harmful UV light at ambient air. The UV-C power density was very low with less than 40 nW/cm^2 detected in 2.5 cm distance from the discharge surface without the use of optical filters (210 - 294 nm). Measurements in 0.3 cm distance also did not exceed 110 nW/cm^2. According to the aforementioned OES results, it can be estimated that a six fold higher frequency would increase the emission or the power density by a factor of less than six (< 660 nW/cm^2).

Temperature profile

The heat that was created by the plasma discharge at constant 10 kV_{pp} elevated the temperature inside the closed FP2.0 (Figure 3.5). However, the rate of the increase was quite low with 0.1 °C, 0.3 °C, 1 °C and 3 °C per minute for 0.5 kHz, 1 kHz, 3 kHz and 6 kHz, respectively. Therefore, 40 °C, as a lower threshold for protein denaturation, would be reached in 180 min, 60 min, 18 min and 6 min of permanent plasma discharge for 0.5 kHz, 1 kHz, 3 kHz and 6 kHz, respectively. Exceeding 70 °C, which affects thermoplastic polymers such as Teflon from the dielectric, is theoretically reached earliest after 18 min at 6 kHz. However, the temperature of the metal electrodes is higher than the air temperature, which was solely measured. Since the metal electrodes are in direct contact with the dielectric, the critical 70 °C for the polymer are obtained in shorter time. Thus, it is recommended to choose the discharge duration up to maximum 10 min at 6 kHz and 10 kV_{pp}, in order to avoid damage of the electrode system.

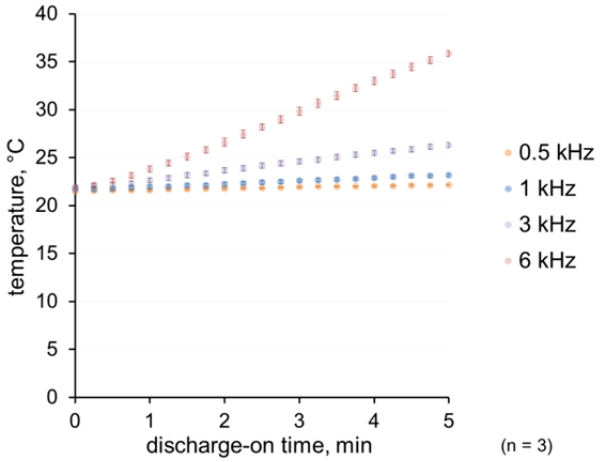

Figure 3.5: Temperature profile inside the closed FP2.0 at varying frequencies.

Dissipated plasma power

The actual power and the power density consumed by the plasma discharge at 10 kV_{pp} were determined (Table 3.2). As expected the plasma power correlates quite well with the applied frequency. For instance doubling of frequency resulted in nearly doubled dissipated power. The only exception is demonstrated at 6 kHz which showed a slightly lower power than the expected 24 W. A possible reason could be that the outmost limitation of the power supply was reached with 6 kHz and 10 kV_{pp}, being barely obtainable. This hypothesis is supported by the tendency of altering frequency shape from sinusoidal wave to irregular wave with pointy peaks at this power setting.

Table 3.2: Dissipated SMD plasma power at varying frequency.

frequency, kHz	plasma power, W	power density, mW/cm^2
0.5	2.2 ± 0.0	20.0 ± 0.1
1	3.9 ± 0.1	34.9 ± 0.6
3	11.8 ± 0.2	105.1 ± 1.5
6	22.4 ± 0.6	200.0 ± 5.5

Ozone concentration

As introduced, DBD plasma systems are known to generate ozone in ambient air. Here, the ozone concentrations of SMD plasma were obtained by *in situ* and *ex situ* measurements at 10 kV_{pp} and varying frequency (Figure 3.6).

Very high concentrations were measured *in situ* during discharge. Although the initial production rate of ozone increased with higher frequency, the concentration curves developed differently as this starting correlation. The absolute concentration grew at 0.5 kHz and 1 kHz steadily, but flattened over time and reached its climax with 13,500 ppm at 1 kHz after 5 min. At higher frequency of 3 kHz, the ozone concentration reached its maximum after 2 min with nearly 9,000 ppm and started to decline from that moment. This tendency was pronounced in the case of 6 kHz with a maximum of 7,900 ppm after 1.5 min and a higher descending rate which resulted in only 2,500 ppm after 5 min. Enhancing the distance by 1.5 cm, resulting in doubling the volume below the electrode system, led to a curve at 1 kHz driven plasma that almost equals the curve at 0.5 kHz.

Ozone exhibited a long retention time of up to 25 min after plasma discharge. The time was influenced by the original end concentration after 5 min discharge-on phase and by the underlying volume. A higher volume resulted in a longer retention time.

In *ex situ* measurements, concentration curves are remarkably distinct in comparison to *in situ* results. Whereas the initial production rate also increased with higher frequency, the maximum concentration was already reached in each case within 1 min and was much lower with highest values of 2,500 ppm at 6 kHz. The concentration level was hereby limited by the relatively high suction rate of the remote analyzer which prohibited further accumulation of ozone inside the FP2.0. In addition, the measured concentrations at 1 kHz for instance converge earlier than in

in situ experiments. However, the principal drop of the concentration level at 6 kHz is also recognizable.

Having extinguished the discharge, the suction rate was also responsible for the rapid drop of the concentration to zero level within two or three minutes.

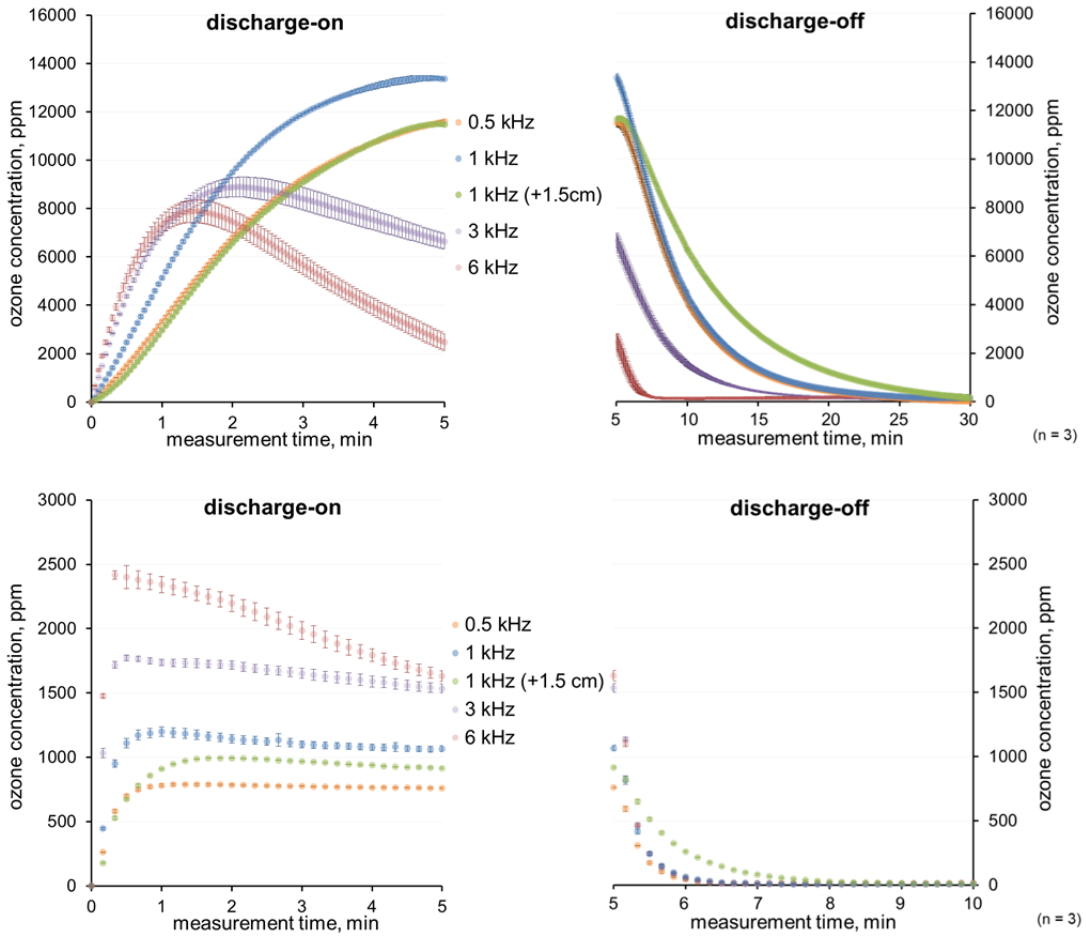

Figure 3.6: Ozone concentration profiles after *in situ* (top) and *ex situ* measurements (bottom) inside the closed FP2.0 during plasma discharge (left) and afterwards (right) at varying frequencies.

In regards of microbial inactivation, the ozone dose is an important measure and was calculated for *in situ* measurements (Figure 3.7). Interestingly, about the same doses with 36,000 ppm × min resulted from 1 kHz and 3 kHz operations after 5 min plasma discharge duration. Less was obtained from 6 kHz (27,000 ppm × min) and more from 1 kHz (47,000 ppm × min) operation. After plasma discharge was extinguished

also very high doses were reached due to the long retention time of ozone, even exceeding the doses derived during discharges at lower frequencies after 5 min.

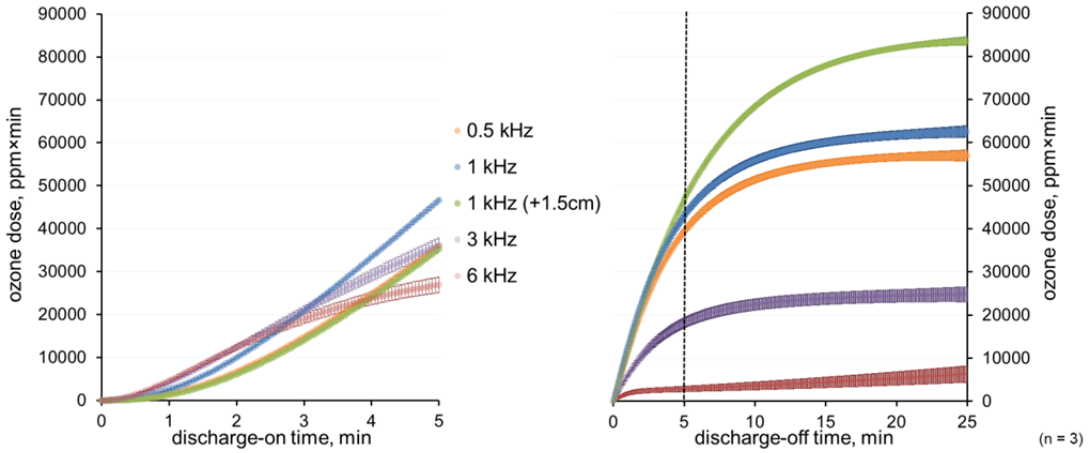

Figure 3.7: Ozone doses derived from *in situ* measurements.

3.3 Bactericidal effect of SMD plasma using agar plates

After becoming aware with the device (FP2.0) and its limitations, I moved on with determining the bactericidal effect of SMD air plasma. The general bactericidal effect of SMD air plasma (35 mW/cm^2, 0.7 cm distance) was assessed by treating various vegetative bacteria spread over agar plates (Figure 3.8). Reduction curves with characteristic two-slope kinetics were obtained for gram-negative *E. coli*, *P. aeruginosa* and gram-positive *E. mundtii* (Figure 3.8**A**). Rapid reduction was observed with more than 4.5 log after 30 s treatments followed by a retarded kinetic reduction resulting in 5.5 log up to complete inactivation after 5 min treatments. To approximate the possibility of having investigated bacteria with distinct resistance against plasma, first all values were normalized with the same initial load of 7.7 log which was the highest among tested species (Figure 3.8**B**). As a result, all species showed the same kinetic reduction up to 1 min treatments. Later the values started deviating from each other with a final difference of 1.4 log or 25 cfu between *P. aeruginosa* and *E. mundtii* after 5 min treatment. *P. aeruginosa* was the only species that could be completely inactivated by plasma within the treatment time range.

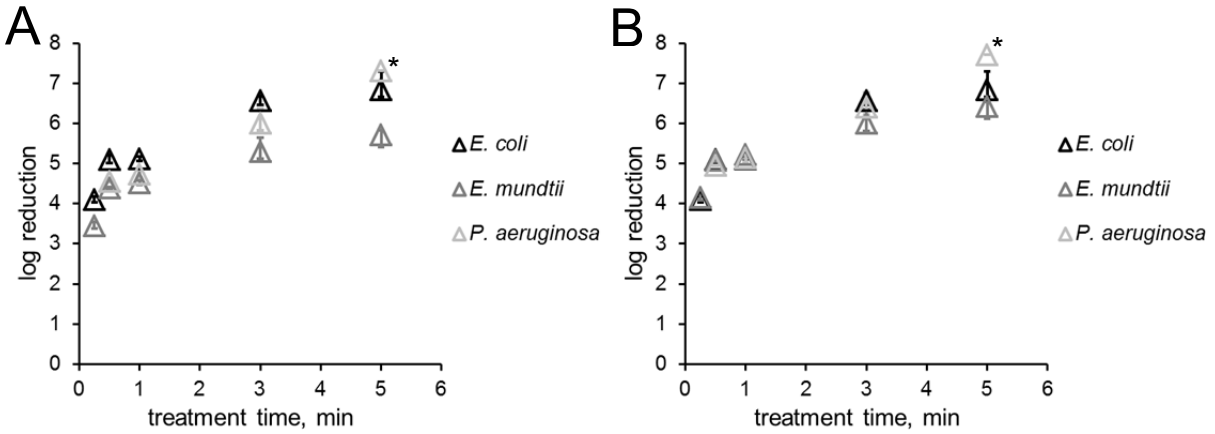

Figure 3.8: Reduction curves of plasma-treated vegetative bacteria on MH agar plates. Actual resulting values are shown in **A** and normalized values to the initial base of 7.7 log cfu in **B**; indicated are standard error (n = 3) and complete inactivation (*).

3.4 SMD plasma sterilization using carriers

The antimicrobial effect of SMD plasma (35 mW/cm^2, 1.5 cm distance) was further investigated with some of the most environmentally robust MO, namely bacterial endospores spread over dry carriers that are conventionally used as biological indicators to validate sterilization methods.

As for vegetative bacteria, plasma also strongly affected the ability of spores to survive (Figure 3.9). In contrast to previous agar experiments, the reduction curves strongly differ from strain to strain (Figure 3.9**A**). This is most obvious at 1 min treatments where *B. subtilis* spores were already reduced by nearly 4 log, whereas at the same time only 1 log inactivation of *G. stearothermophilus* spores occurred. The reduction values of *B. atrophaeus* and *B. pumilus* lie in between. Inactivation to the detection limit of 5.3 log (≤ 10 cfu) was obtained after plasma treatment of 3 min for *Bacillus* spp. spores except for *G. stearothermophilus* which required 5 min. Notably, *G. stearothermophilus* spores were among the tested strains the most resistant against plasma.

Therefore, further experiments were conducted with this spore type on model carriers equally sized and with varying materials also used in medical devices, in order to investigate their influence on the inactivation. In addition to stainless steel which is conventionally used in sterilization testing, spores were distributed for that purpose on glass, PVC and Teflon carriers (Figure 3.9**B**). Overall, the same reduction rate was achieved with plasma independent of the underlying carrier material.

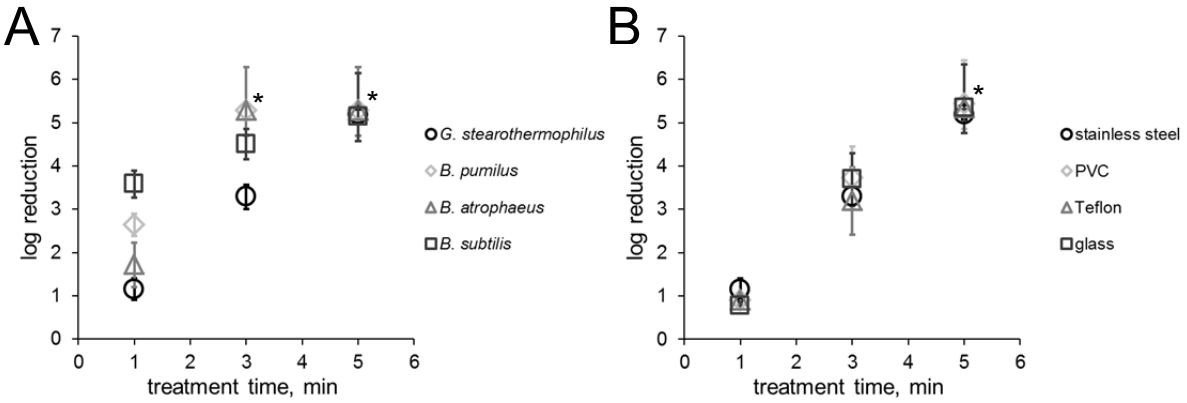

Figure 3.9: Reduction curves of plasma-treated bacterial endospores validating sterilization. Bacillus spp. were treated on stainless steel carriers in **A** and *G. stearothermophilus* on varying carrier substrates in **B**; indicated are standard error (n ≥ 3) and detection limit (* ≤ 10 cfu).

The characteristic D-values related to plasma inactivation were calculated and compared to reference values derived from conventional sterilization methods (Table 3.3). For instance, *B. subtilis* spores had a D-value of only 0.3 min, while endospores of *G. stearothermophilus* showed a D-value of 0.9 min, which is lower than the minimum standard D-value of dry heat or H_2O_2 sterilization. Furthermore, SAL values were determined for the plasma inactivation (Table 3.3).

Table 3.3: D-values and SAL of bacterial endospores treated by SMD air plasma and reference sterilization methods

Bioindicator	Strain	$D_{23°C}$-value, min	SAL, min		Reference method	D-value[a], min
			6 log	12 log		
G. stearothermophilus	ATCC 7953	0.9	5.7	11.4	H_2O_2	4.2 [b]
B. pumilus	ATCC 27142	0.5	3.2	6.5	γ-radiation	-
B. atrophaeus	ATCC 9372	0.6	3.4	6.8	ethylene oxide	3.0 [c,e]
B. subtilis	DSM 13019	0.3	1.7	3.3	dry heat	2.8 [d,e]

[a] D-values of reference sterilization methods provided by Simicon GmbH; dash (-) indicates: data not available

[b] $D_{60°C}$ of H_2O_2 (6.0 mg/L, saturated steam, 60°C);

[c] $D_{54°C}$ of ethylene oxide (600 mg/L, 54°C)

[d] $D_{160°C}$ of dry heat (160°C); [e] Devices used according to the standard regulations DIN EN ISO 18472 [150]

3.5 SMD plasma disinfection using carriers

Having studied the antimicrobial behavior against surrogate model organisms so far, the decontaminating effect of SMD air plasma (35 mW/cm^2, 0.5 cm distance) was examined this time in more detail with nosocomial bacteria such as *E. faecium* and *C. difficile* endospores. This involved the application of testing standards for disinfecting agents with low organic burden (0.03% BSA) in addition to bacteria on dry carriers which should aggravate the inactivation and simulate pre-cleaned conditions.

Table 3.4 exhibits all relevant control values that were measured in this study related to the following log reduction curves. In the case of endospores, the load of *B. subtilis* was distinct lower compared to others spore types. The inoculum of vegetative bacteria was in general higher at Simicon samples due to a lower recovery rate.

Table 3.4: Control values of tested bacterial batches

Microorganism	org. burden	preparation suspension	marker in diagram	prep./ analysis institute	inoculum on carrier, log	recovered from untreated controls (*), log	neutral transport controls, log
Bacterial endospores (ca. 10^6 cfu; Figure 3.10)							
C. difficile	-	water	◀	IHPH	5.9	6.6	6.3
	0.03%	water(+NaCl)	◁	"	5.9	5.9	5.8
B. subtilis	-	water	●	"	5.3	5.1	5.0
	0.03%	water(+NaCl)	○	"	5.3	5.3	5.1
G. stearothermophilus	-	water	◆	Simicon	N/A	6.6	6.4
Vegetative bacteria (ca. 10^8 cfu; Figure 3.11A)							
E. faecium	-	water	◀	Simicon	8.9	8.3	7.7
	-	water	◀	"	9.3	8.3	7.8
	-	NaCl	▶	IHPH	8.1	7.5	7.7
	0.03%	NaCl	▷	"	8.1	7.8	7.0
S. aureus	0.03%	NaCl	○	"	8.2	7.9	8.0
Vegetative bacteria (ca. 10^6 cfu; Figure 3.11B)							
E. faecium	-	water	◀	Simicon	7.5	6.6	6.5
	-	water	◀	"	7.1	6.5	6.0
	0.03%	water(+NaCl)	◁	"	7.6	6.5	6.4
	0.03%	NaCl	▷	"	8.0	6.5	6.3
	blood	NaCl	▲	"	N/A	6.5	5.9

(*) basic value for log reduction calculations

Initially, the results from the treatment of bacterial endospores are being introduced. Overall, the endospore reduction by 3 log in terms of sporicidal disinfection was achieved with all tested sample configurations, including with and without low organic burden, within the treatment time range (Figure 3.10). In more detail, *C. difficile* spores without organic burden were most susceptible to plasma. A 3 log reduction was accomplished after 1 min and the recovery of single spores failed after 5 min treatment. Approximately 3 min were necessary to reach the disinfection level for *C. difficile* and *B. subtilis* endospores with 0.03% BSA. Whereas the recovery of *B. subtilis* spores without organic burden failed after 4 min treatments, viable spores were found on samples with 0.03% BSA even after 10 min treatments. Despite the fact that the surrogate endospores of *G. stearothermophilus* were hardly affected within 2 min, the disinfection level was achieved after approximately 2.5 min.

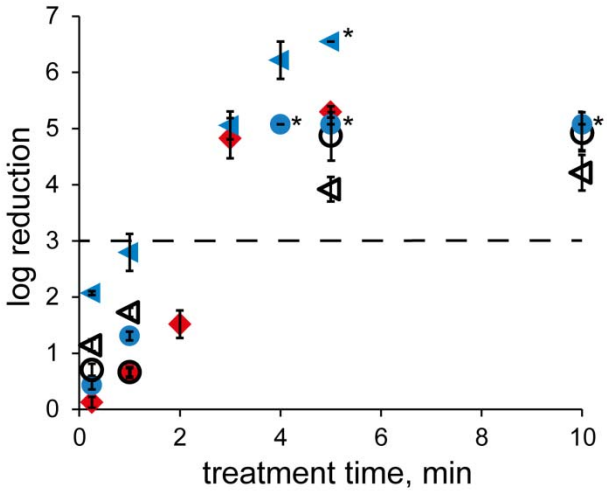

Figure 3.10: Reduction of bacterial endospores by plasma with 10^6 cfu on carriers for testing disinfection. Triangles stand for *C. difficile* spores without (◂) and with 0.03% BSA (pre-cleaned condition, ◁); circles for *B. subtilis* spores without (●) and with 0.03% BSA (○); diamonds for *G. stearothermophilus* spores without additional organic burden (◆). Endospores were prepared from H_2O suspension. Dashed line indicates required disinfection level (3 log), error bars the standard error (n = 3), stars complete inactivation (*).

In contrast to the endospores, the disinfection of *E. faecium* or *S. aureus* (10^8 cfu) on regular-sized carriers was insufficient (< 2 log in 10 min), but became sufficient, when the bacteria were inoculated on four time larger carriers (*E. faecium*, required 5 log in 5 min) (Figure 3.11**A**). As a consequence, a lower bacterial load (10^6 cfu) was applied on regular-sized carriers which indeed does not comply with the underlying disinfection standards, but coincided with the initial load of bacterial endospores. Under these conditions, it was possible to examine the influence of the load and additional substances on disinfection. However, this measure led rather to successful disinfection, perturbing gradually this effect with higher supplemental burden degree (Figure 3.11**B**). In detail, very similar kinetic behaviour was observed for *E. faecium* prepared in H_2O with or without 0.03% BSA (5 log in 3 min), but the preparation in saline solution with 0.03% BSA aggravated the reduction (4.3 log in 5 min). The disinfection level was even reached with heavy burden in form of sheep blood (5 log in 10 min). Notably, *E. faecium* was reduced most rapidly again using large carriers (5 log in 15 s).

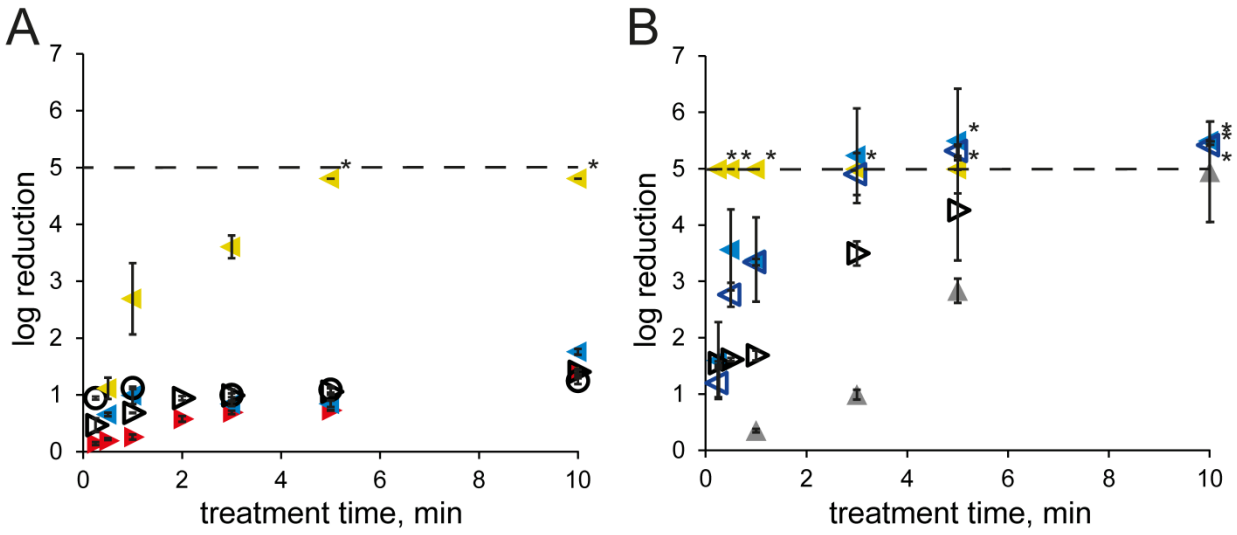

Figure 3.11: **Reduction of vegetative bacteria by plasma with 10^8 cfu (A) and 10^6 cfu (B) on carriers for testing disinfection**. Triangles stand for *E. faecium* without 0.03% BSA prepared either from WS (◀) or from SS (▶) and on large carriers (8 cm^2) from WS (◀); with 0.03% BSA from WS (◀) and from SS (pre-cleaned condition, ▶); with heparinized sheep blood (▲). Rings stand for *S. aureus* with 0.03% BSA from SS (pre-cleaned condition, O). Dashed line indicates required disinfection level (5 log), error bars the standard error (n = 3), stars (*) a possibly higher reduction (only analysed up to required 5 log reduction) in **A** or complete inactivation in **B**. WS = H_2O suspension, SS = saline suspension.

Next, the microbial distribution on test carriers was examined by SEM imaging, in order to interpret the different observed inactivation kinetics properly.

In the case of bacterial endospores (Figure 3.12), *C. difficile* without organic burden were found distributed in successive patterns over the surface and were usually not attached to each other, even in more dense regions (Figure 3.12**A**). In contrast with organic burden, they formed cluster regions with BSA covering them (Figure 3.12**B**) and were surrounded by NaCl crystals (Figure 3.13**A**). Remnants of vegetative *C. difficile* forms were found at both sample configurations (Figure 3.12**A/B**). *G. stearothermophilus* spores appeared on the surface in big agglomerations, surrounded by organic cell debris left from sporulation process (Figure 3.12**C**).

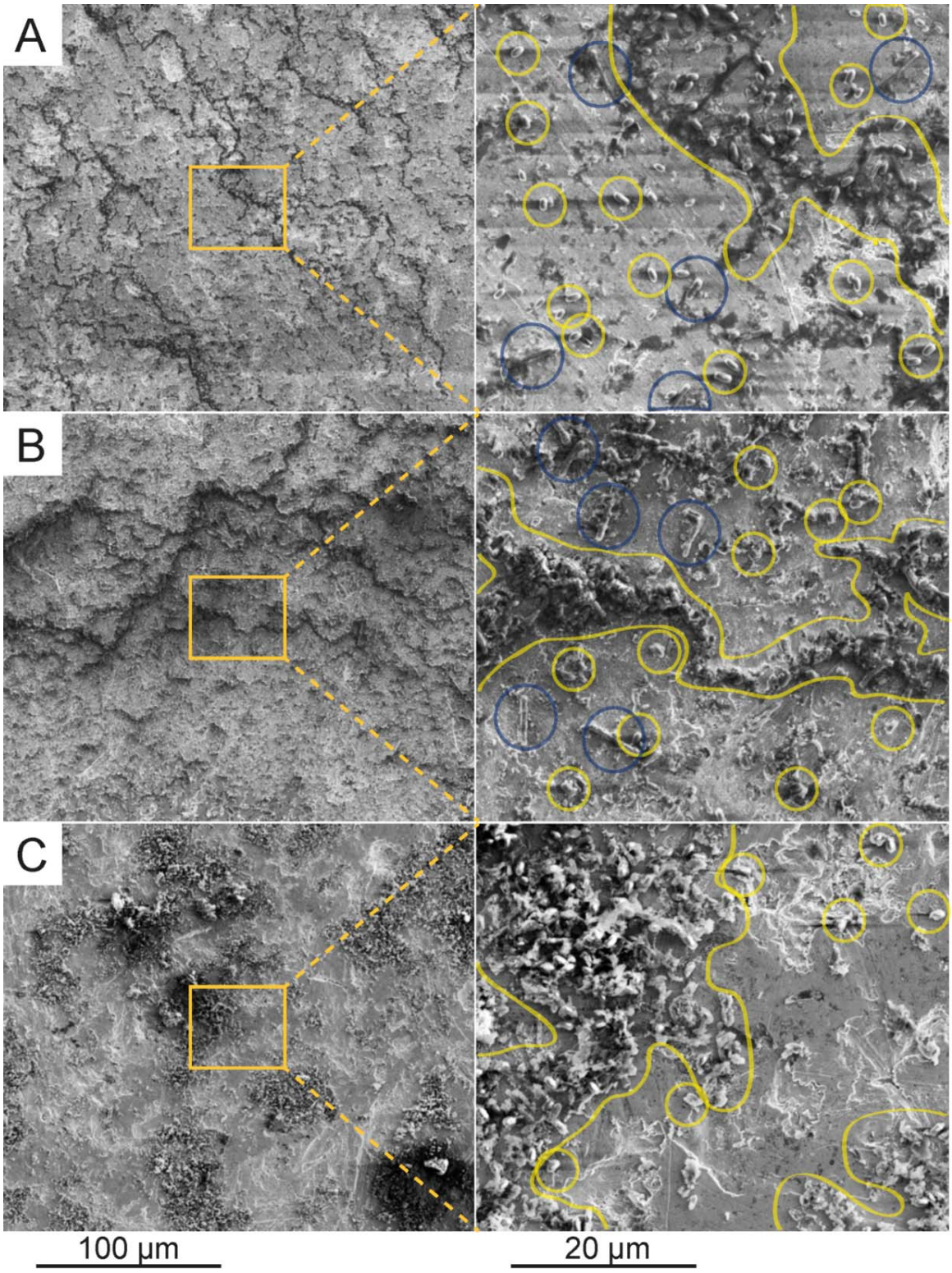

Figure 3.12: **SEM micrographs showing the distribution of untreated bacterial endospores.** *C. difficile* spores are depicted without and with 0.03% BSA including salt crystals in **A** and **B**, respectively and *G. stearothermophilus* with sporulation debris in **C**. Emphasized are representative single spores (yellow ellipses), single vegetative *C. difficile* cells (big blue ellipses) and dense spore regions (yellow outlined areas). Images on the right have 5x higher magnification.

Furthermore, the surface occupancy of *E. faecium* bacteria and varying burden was assessed by SEM imaging in respect of different loads (Figure 3.14). The rationale was based on the estimation of spore density in initial SEM images that multi-layering could occur on carriers with vegetative bacteria which aggravated the plasma inactivation. In detail, around 100 spores were counted on 50 × 50 μm^2 on average. This means that a load of 10^6 spores cover 100 μm^2 on 2500 μm^2 of the carrier, when one spore occupies 1 μm^2 and they are homogenously distributed. As a consequence, it can be estimated under the assumption of similarity that 10^8 bacteria would cover a 100 times larger area which exceeded the used carrier area by a factor of four. Thus, bacteria would need to from 4 layers to fit into 2500 μm^2 of the carrier. Examining this experimentally, SEM image results reveal that 10^6 cfu *E. faecium* were distributed mostly side-by-side in one layer (Figure 3.14A). Despite the fact that bacterial cells were not clearly apparent with sheep blood, shapes at the edge of blood matrix indicated their presence covered by matter (Figure 3.14B). On the contrary, 10^8 cfu completely occupied the carrier surface (Figure 3.14C) forming multi-layers of up to 10 layers (Figure 3.15). Morphological artefacts were present only at the macrostructure of the bacterial film: Already existing cracks in the dense film were widened slightly due to vacuum drying (Figure 3.16**A_1**, **A_2**).

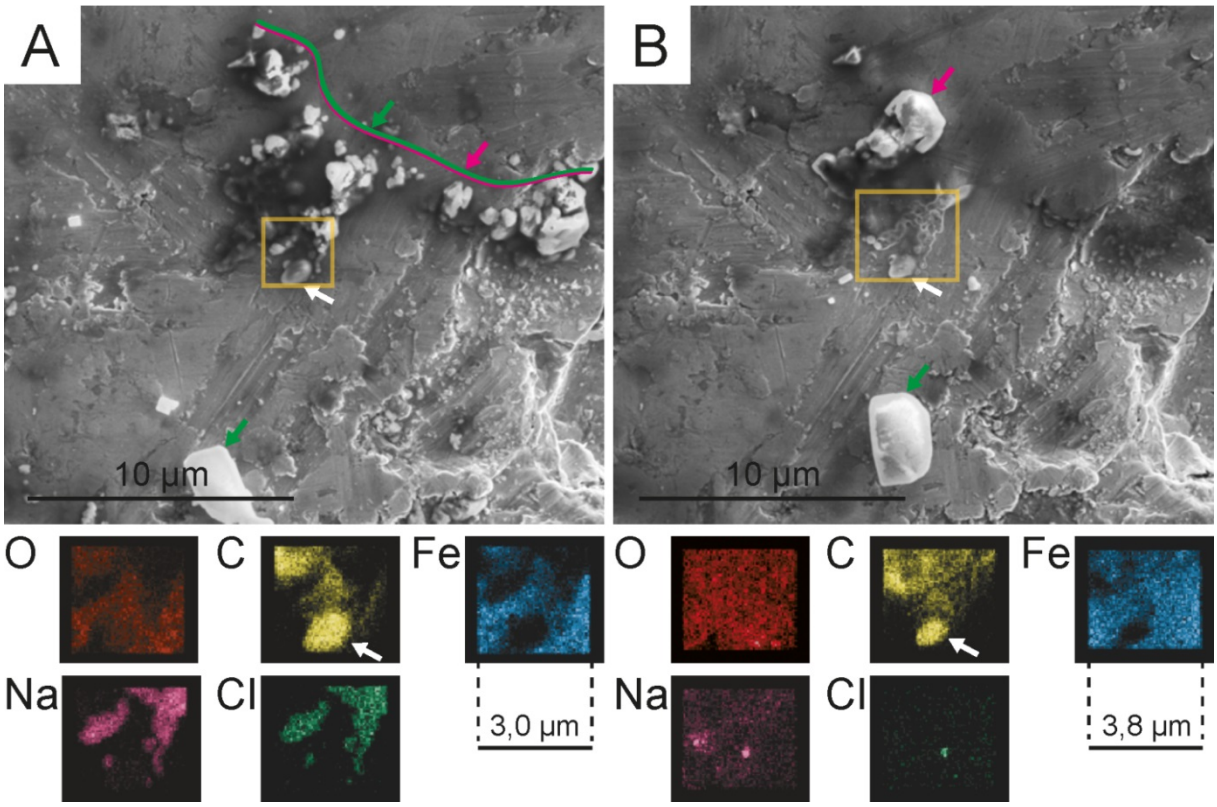

Figure 3.13: **EDX elemental mapping of the same untreated and treated *C. difficile* spore (pre-cleaned condition).** Sample with 0.03% BSA was untreated in **A** and plasma-treated for 10 min in **B**. Elemental mapping revealed organic matter (C), salt structures (Na, Cl) and oxidized stainless steel surface (Fe, O). The surface morphology of the spore remained unchanged (white arrows), but salt crystals were altered (other arrows) and the whole surface was oxidized after plasma treatment.

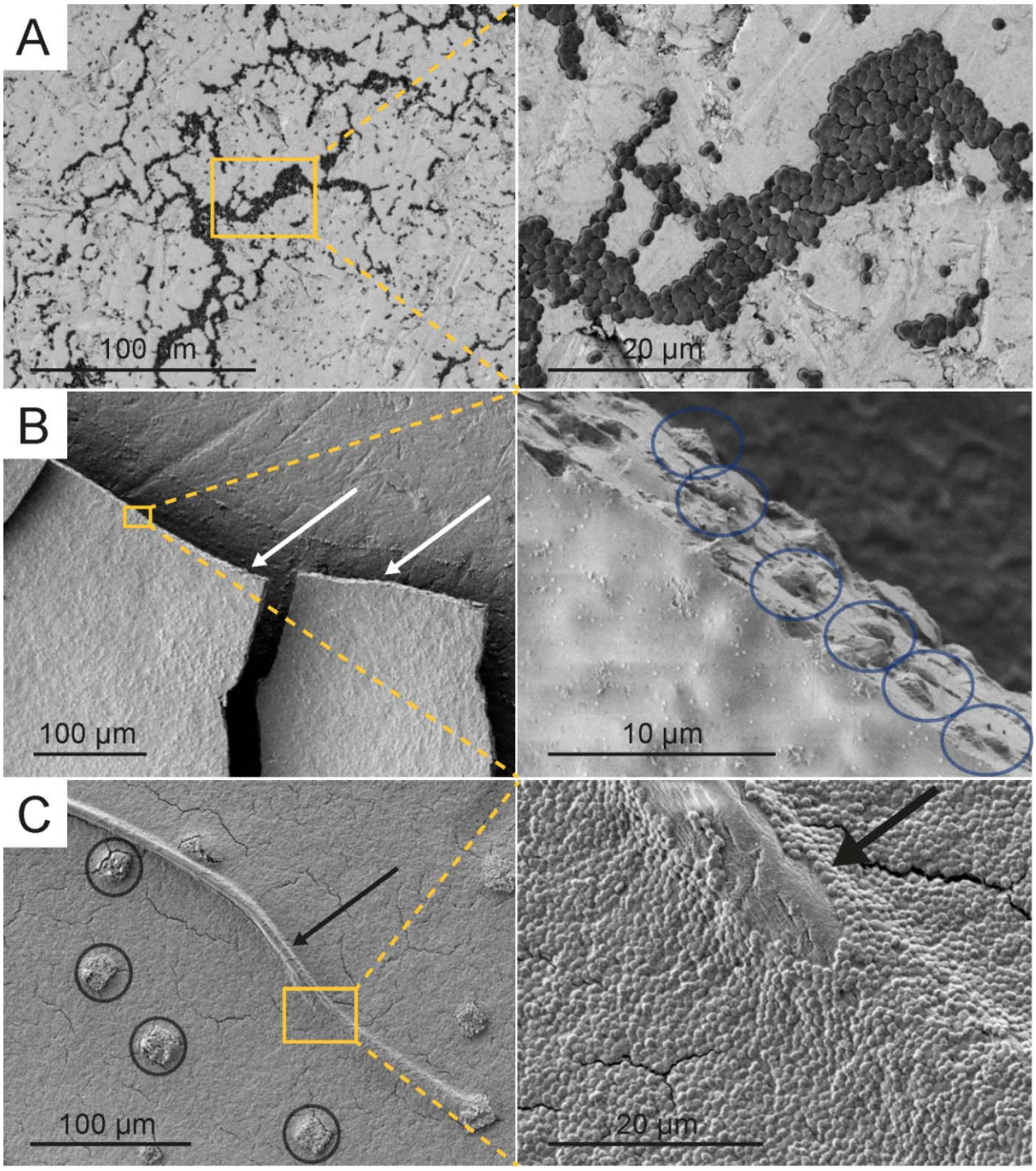

Figure 3.14: **SEM micrographs demonstrating the distribution of untreated *E. faecium* bacteria.** 10^6 cfu were prepared from H_2O suspension without organic burden in **A**, from saline suspension with heparinised sheep blood in **B** and 10^8 cfu with 0.03% BSA (pre-cleaned condition) in **C**. Bacterial cells form a single layer in **A**, are embedded in the matrix (blue ellipses) of blood flakes (white arrows) in **B** and form a dense carpet covering the carrier surface, a random single hair (black arrows) and salt crystals (black ellipses) in **C**. Images on the right have 5x, 20x and 7x higher magnification in **A**, **B** and **C**, respectively.

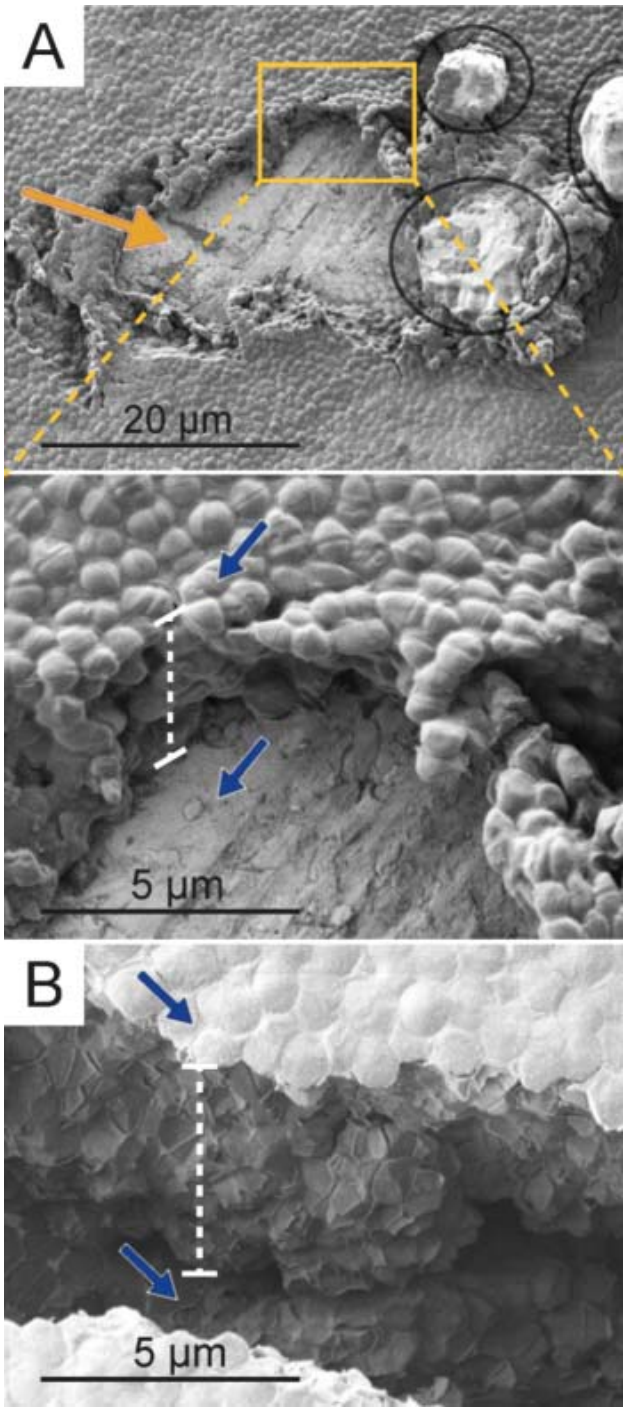

Figure 3.15: **SEM micrographs depicting multi-layers of untreated *E. faecium* bacteria (pre-cleaned condition).** 10^8 cfu with 0.03% BSA were prepared from saline suspension in **A** and from H_2O suspension in **B**. Scratches in the bacterial carpet revealed metal surface (orange arrow), bacterial multi-layers with 4-5 layers in **A** and up to 10 layers in **B**. Emphasized are NaCl crystals (black ellipses), bottom and top of bacterial layers (blue arrows) and thickness of the bacterial layers (white dashed line). Centre and bottom image have 4x higher magnification.

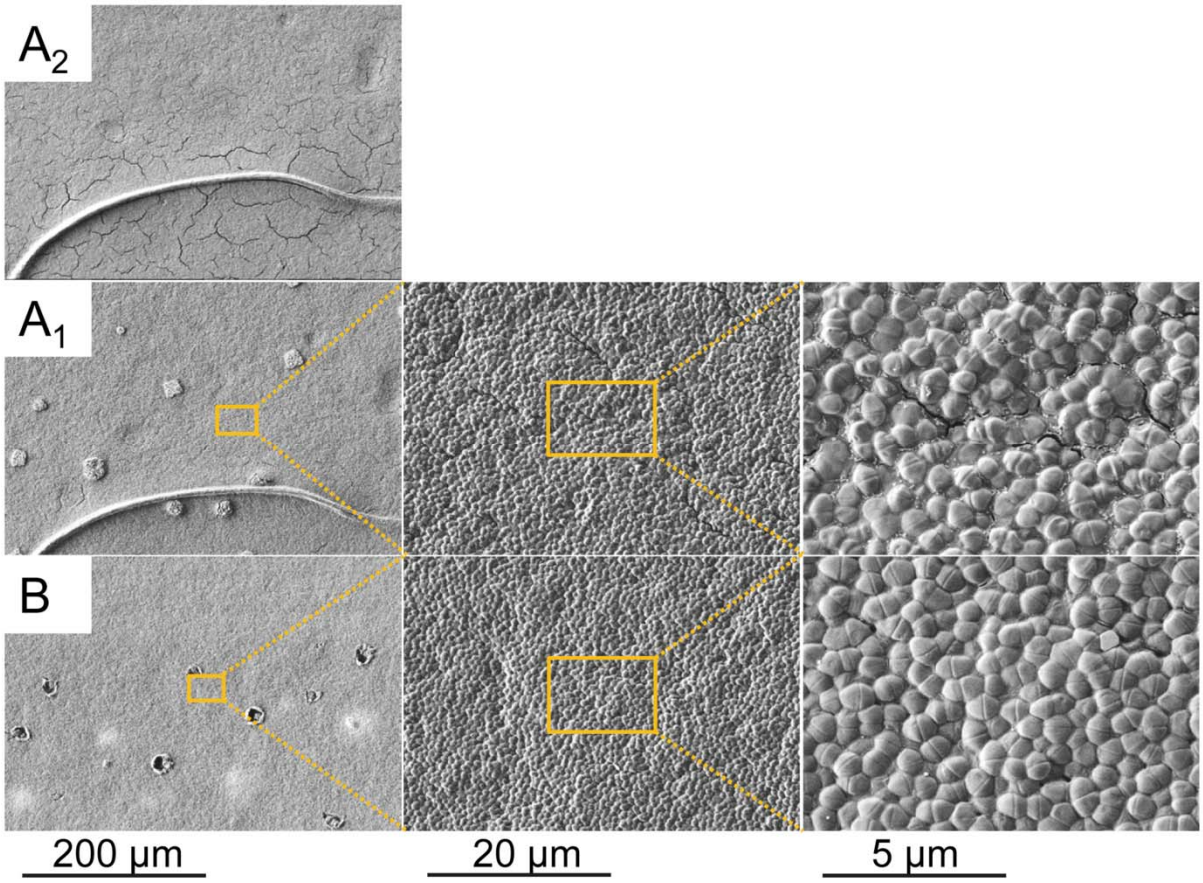

Figure 3.16: SEM micrographs demonstrating untreated and treated *E. faecium* bacteria (10^8 cfu; pre-cleaned condition). Samples were prepared with 0.03% BSA. The same untreated sample area (**A_1**) was imaged again after 7 days storage at 2 - 8 °C (**A_2**). Another sample was imaged after 10 min plasma treatment in **B**. Storage/vacuum drying caused an increase of already visible cracks and humidity change upon storage dissolved salt crystals at images on the left side in **A**. Missing salt structures can also be observed in **B** (holes). Plasma treatment itself did not affect the surface morphology of bacterial cells. Centered images have 10x and images on the right 40x higher magnification compared to images on the very left.

Finally, the impact of plasma treatment on the surface morphology of bacteria was investigated. No clear alterations were observed for *C. difficile* spores treated for 10 min (Figure 3.13), whereby salt crystals below 100 µm exhibited strong changes (Figure 3.13, 3.17 and 3.18). In general, varying structures of salt crystals covered bacteria or vice versa (Figure 3.19). Similarly, plasma caused no clear visible effects on other bacteria examined (Figure 3.21, 3.22, 3.23, 3.24 and 3.16). However, diverse organic matter such as BSA or sporulation debris from *G. stearothermophilus* samples was evidently eroded (Figure 3.22) and the surface of sheep blood matrix exhibited burst cell structures (Figure 3.24). In addition, EDX analyses revealed that all surfaces were oxidized after plasma treatment (Figure 3.13, 3.17 and 3.18).

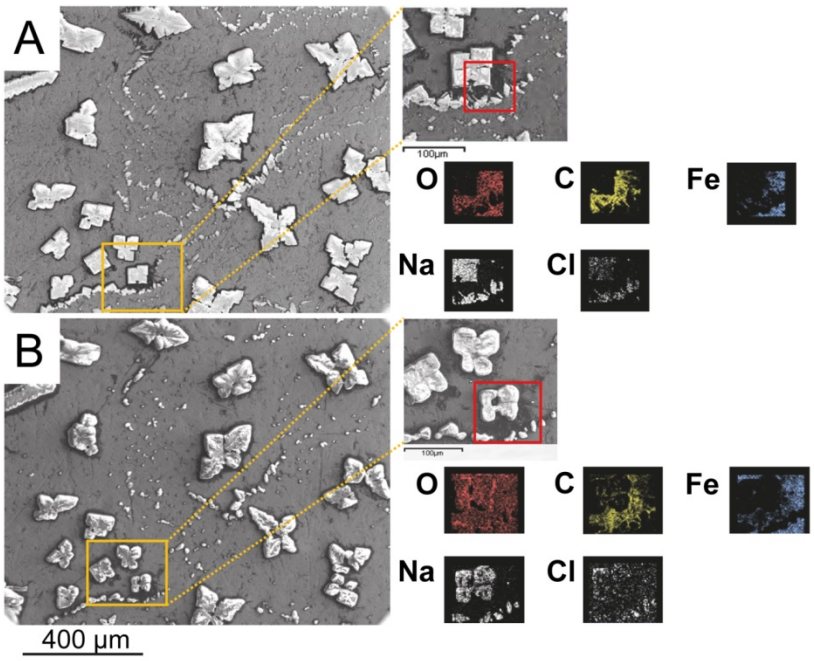

Figure 3.17: SEM micrographs showing the same untreated and treated salt macrostructures from carriers with 0.03% BSA. Sample was untreated in **A** and plasma-treated for 10 min in **B**. NaCl macrostructures were mainly not affected, but their edges were smoothed. Elemental mapping by EDX revealed oxidation of whole surface after treatment.

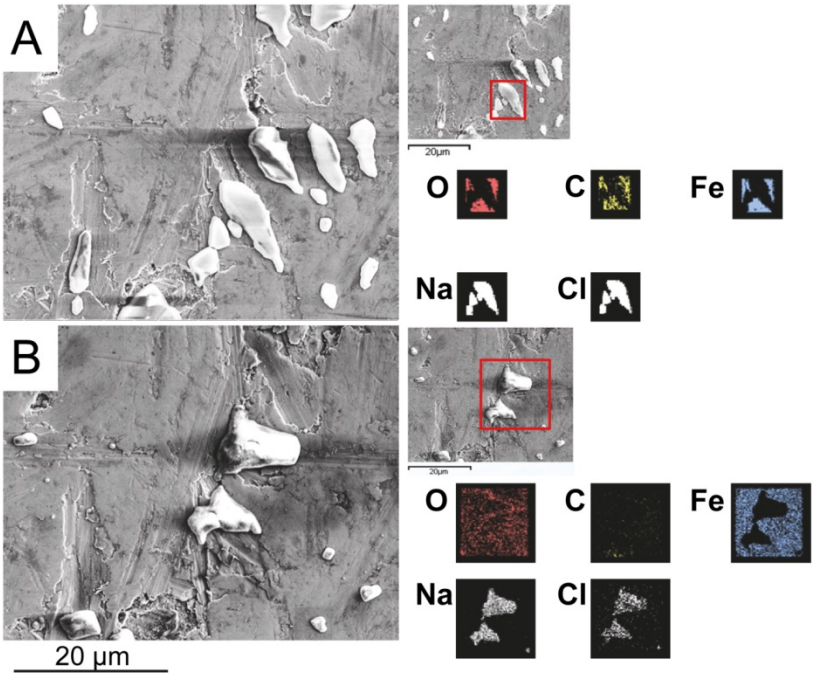

Figure 3.18: SEM micrographs demonstrating the same untreated and treated salt microstructures from carriers with 0.03% BSA. Sample was untreated in **A** and plasma-treated for 10 min in **B**. NaCl microstructures below 100 µm were strongly affected by plasma. Their crystal shapes were reformed. Elemental mapping by EDX revealed oxidation of whole surface after treatment.

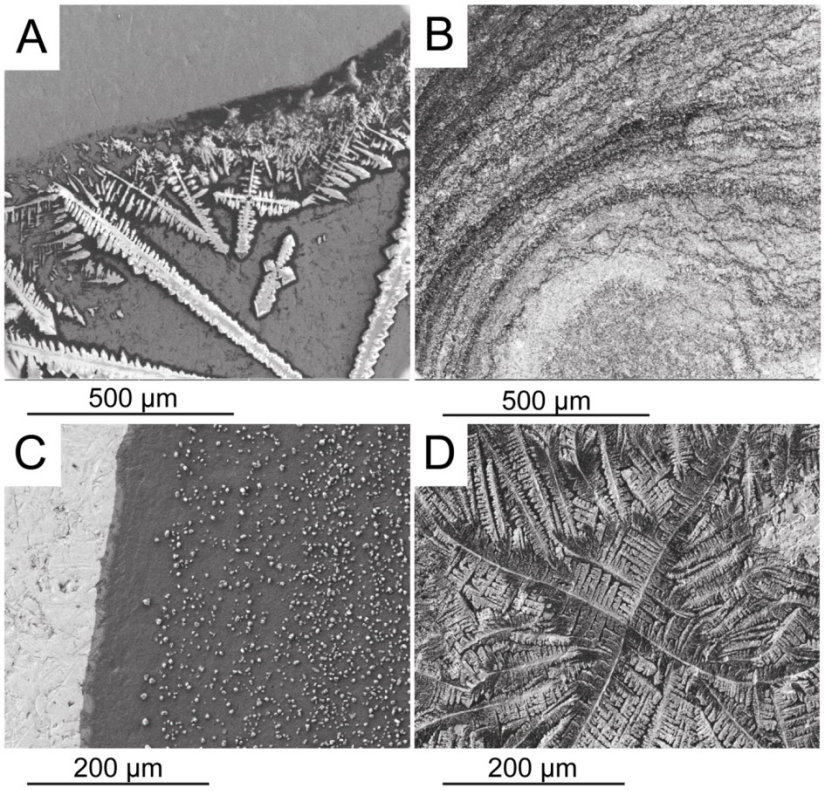

Figure 3.19: SEM micrographs from different samples exposing various salt structures after BSA addition. Bulky dendrites were observed in **A**, smaller structures distributed together with *C. difficile* spores in **B**, cubic crystals on an *E. faecium* carpet in **C** and a thin dentritic layer covering *E. faecium* bacteria in **D**.

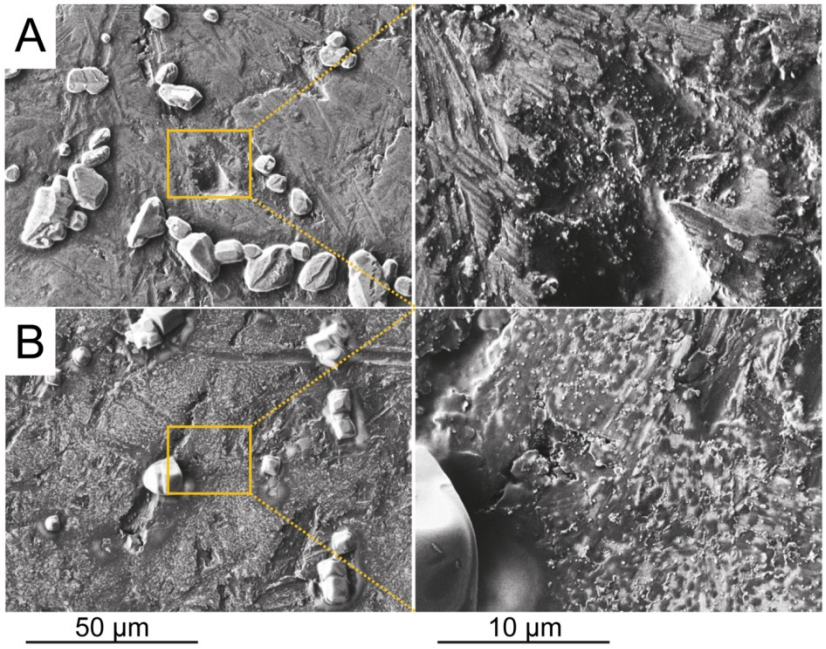

Figure 3.20: SEM micrographs depicting untreated and treated carriers with 0.03% BSA. The BSA film (dark spots) was disrupted by plasma and metal surface became apparent (bright spots). Images on the right have a 5x higher magnification.

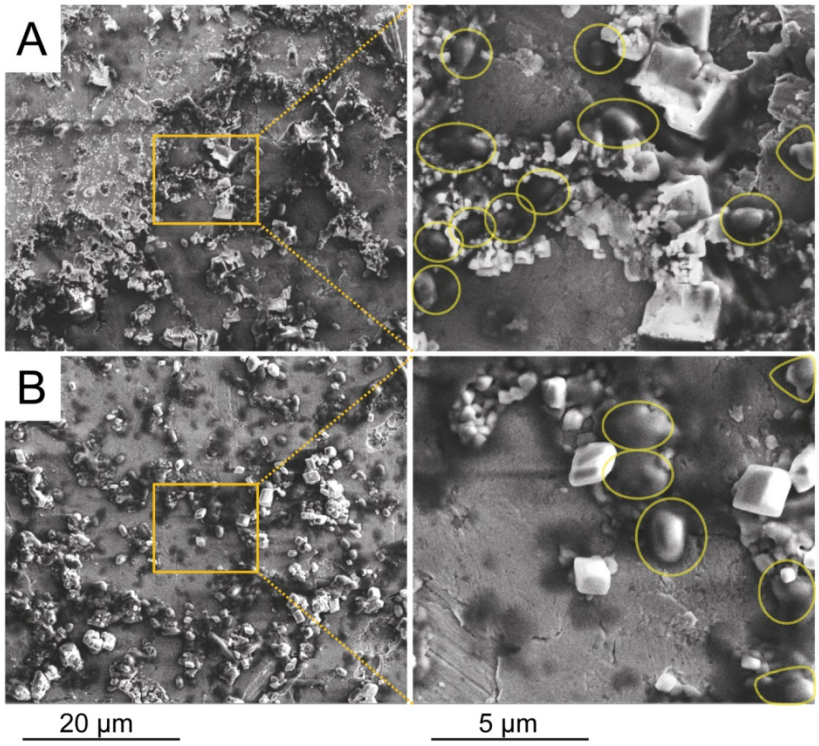

Figure 3.21: SEM micrographs showing untreated and treated *C. difficile* spores (pre-cleaned condition). Spores with 0.03% BSA were untreated in **A** and plasma-treated for 10 min in **B**. The morphology of *C. difficile* spores was not affected. Images on the right have a 4x higher magnification. Emphasized are single spores (yellow ellipses).

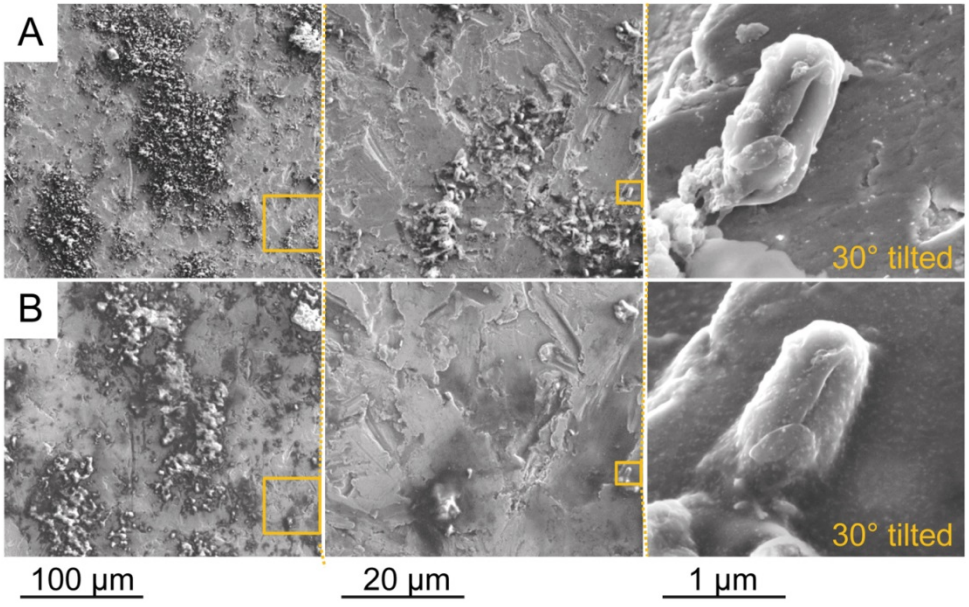

Figure 3.22: SEM micrographs demonstrating the same untreated and treated *G. stearothermophilus* spores. They were untreated in **A** and plasma-treated for 10 min in **B**. Cell debris was degraded and fused together after plasma treatment. Many spores vanished and present spores were covered by organic matter. Centered images have 5x and images on the right 100x higher magnification.

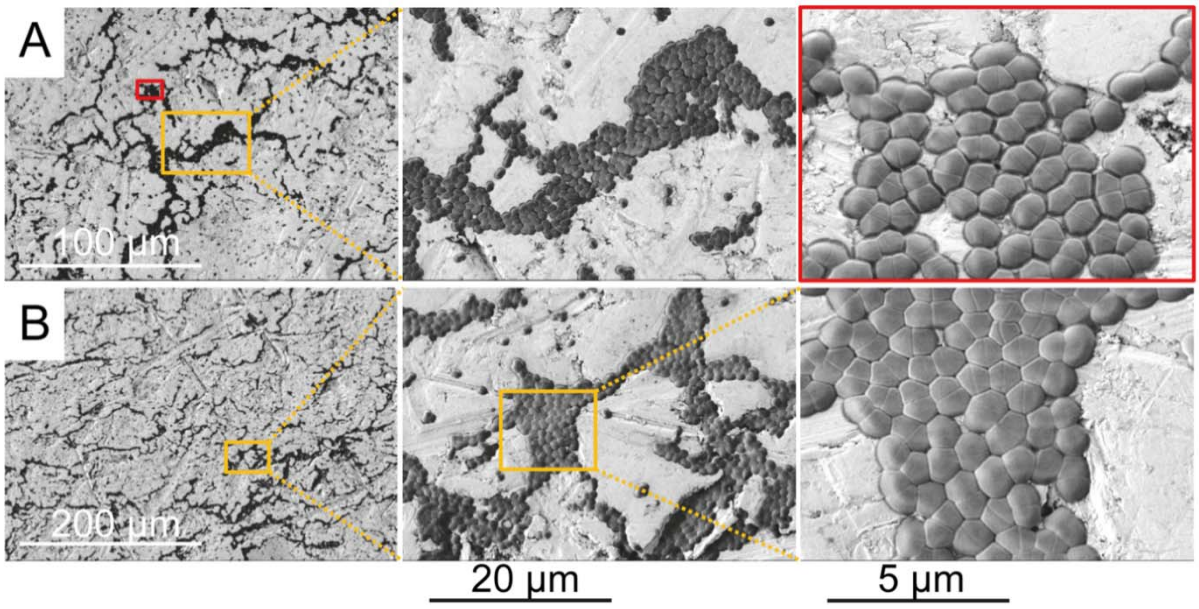

Figure 3.23: SEM micrographs depicting untreated and treated *E. faecium* bacteria (10^6 cfu) without organic burden. They were untreated in **A** and plasma-treated for 5 min in **B**. There were no morphological effects visible. Red squares indicate 20x and the orange square 5x magnified areas in **A**. Centered image has 10x and image on the right 40x higher magnification compared to the very left image in **B**.

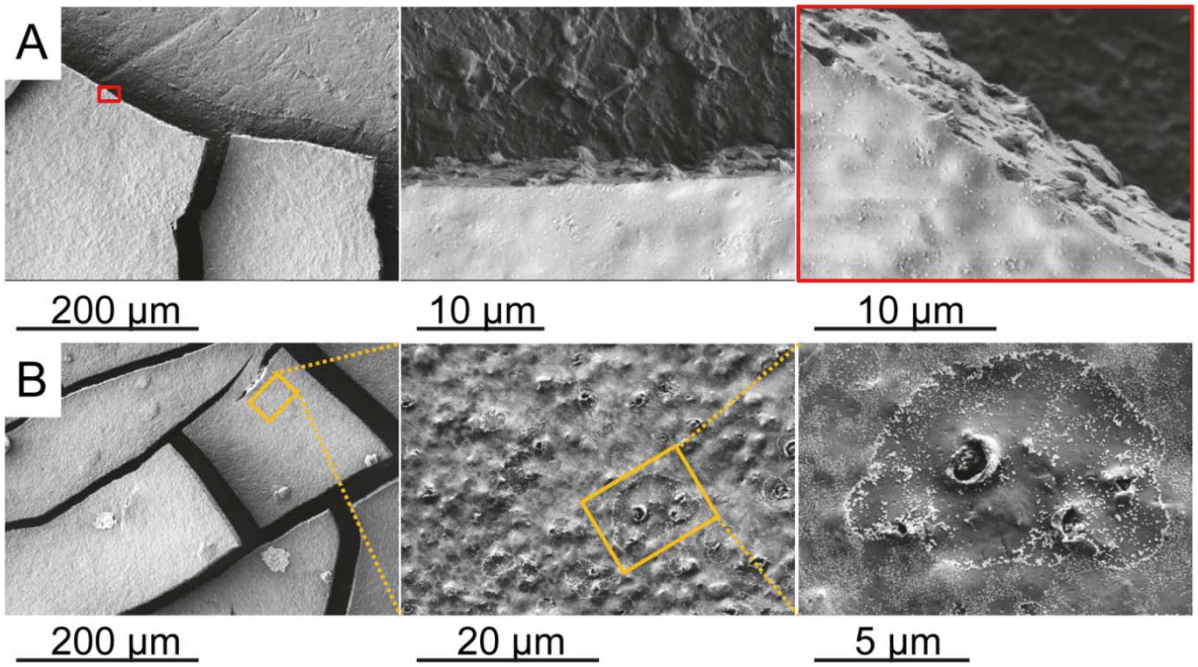

Figure 3.24: SEM micrographs showing untreated and treated *E. faecium* bacteria (10^6 cfu) within heparinized sheep blood. They were untreated in **A** and plasma-treated for 10 min in **B**. Macrostructures (blood flakes) were not influenced. Burst cellular components were evident on the blood matrix after plasma treatment. Red squares indicate 20x magnified area in **A**. Centered image has 10x and image on the right 40x higher magnification compared to the very left image in **B**.

3.6 SMD plasma surface disinfection (modified 4-field-test)

SMD air plasma has shown strong bactericidal effects against nosocomial bacteria on small model carriers inside the FP2.0 at closed conditions. The outcomes so far indicated some limitations of plasma inactivation especially that the bacterial density on carriers was a limiting factor. As a next step, the potential of plasma in disinfecting large-area surfaces such as floors in healthcare settings was studied. In the so-called modified 4-field-test, nosocomial bacteria were treated with plasma on 25 cm^2 fields marked on PVC flooring while simulating pre-cleaned conditions (with 0.03% BSA). Therefore, the SMD system was modified, in order to apply plasma at open conditions (35 mW/cm^2, 0.5 cm distance).

At the beginning, it was essential to specify the recovery of bacteria from drying control field D and from control field number 4, neighboring the plasma-treated fields, in order to elucidate the influence of side-diffusing plasma species (Figure 3.25**A**, **B**). The swab method allowed the recovery of ca. 50 % of initially loaded spores and ca. 15 % vegetative bacteria from the drying control. In the case of bacterial endospores, adjacent treatments caused a 30% and 20% loss of viable *C. difficile* and *B. subtilis* on the practically untreated field no. 4, independent from the treatment time, respectively (Figure 3.25**A**). In contrast, vegetative bacteria *E. faecium* and *S. aureus* did not show loss or a clear tendency towards loss through passive treatments (Figure 3.25**B**).

However, the static but this time active plasma treatment of bacteria on fields number 1, 2 and 3 missed required disinfection levels by far (Figure 3.25**C**). A maximum of 2 log reduction was achieved over the course of 10 min treatments among all tested bacteria. Bacterial endospores were more resistant with *B. subtilis* spores not significantly inactivated in 5 min, whereas *C. difficile* spores showed at least 1 log

and nearly 2 log reduction in 5 min and 10 min, respectively. Vegetative bacteria were more susceptible to plasma with *S. aureus* which was inactivated by 2 log in 5 min and *E. faecium* being less reduced in the same time but reached 2 log in 10 min. The actual survival of bacteria gives a better indication of the impact of active plasma treatments in microbial inactivation (Figure 3.25**D**). Thus, after normalization of the loss from passive treatments mentioned earlier, it can be concluded that *B. subtilis* spores experienced no reduction through active treatment, *C. difficile* only after 5 min in contrast to vegetative bacteria which were affected from the beginning.

The initial load of vegetative bacteria was decreased by a factor of ten to ascertain, if the microbial density had again an influence (Figure 3.25**E**). However, the proportion of recovered bacteria was for both loads the same after 5 min treatment, which was expected, since multi-layering on such large area can be excluded.

Overall, the results indicate that the concentration level of relevant plasma species and therefore the interaction strength with bacteria were not high enough in an “open” set-up due to side-diffusion.

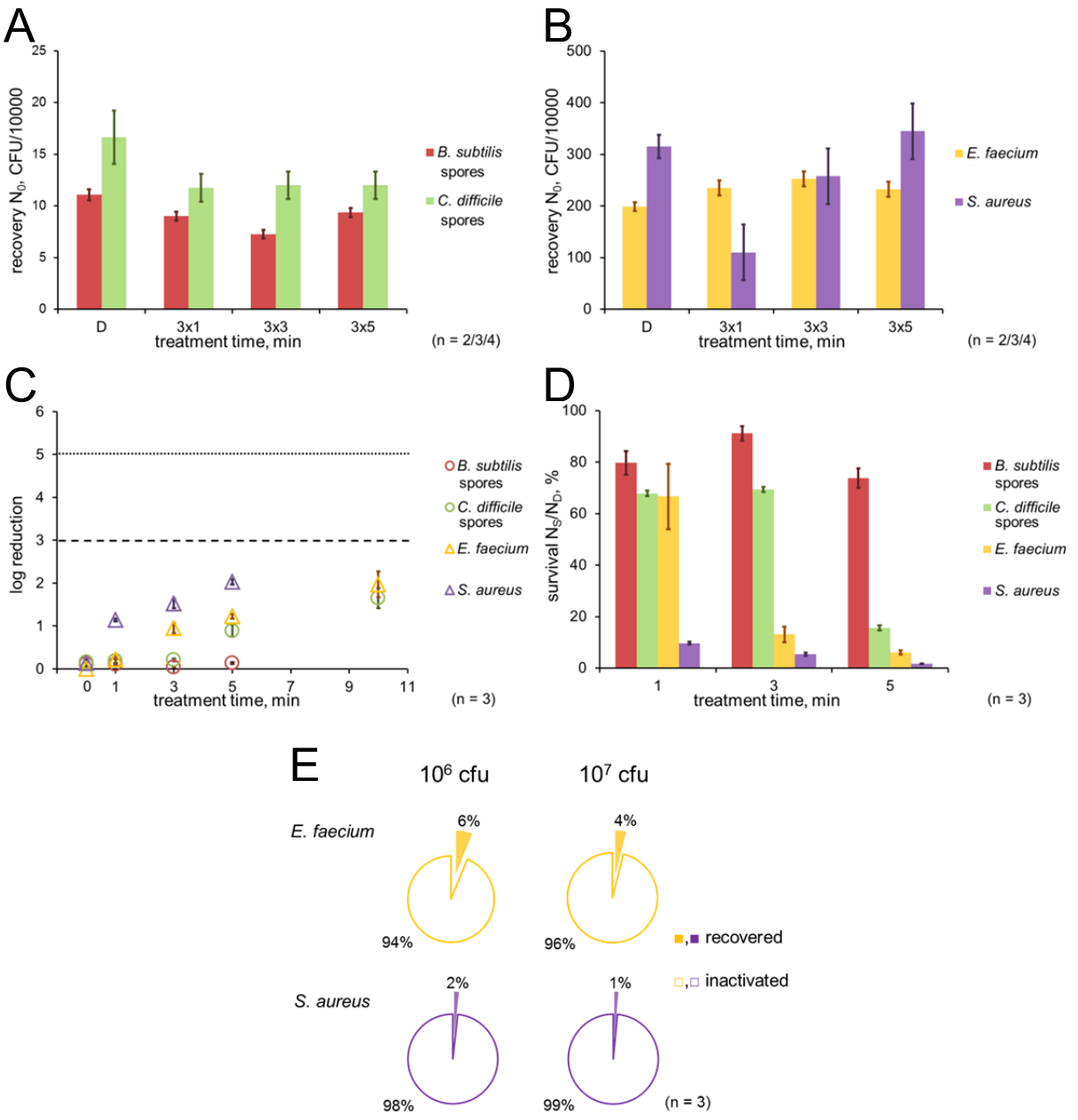

Figure 3.25: Results of the modified 4-field-test evaluating plasma surface disinfection. 20% to 30% less bacterial endospores were recovered from passively treated control fields in **A**, but no clear tendency of loss was found for vegetative bacteria in **B**. Low reduction (max. 2 log) were obtained for actively treated bacteria in **C**. Proportion of inactivation after active treatment were absent for *B. subtilis* and 60% for *C. difficile* only after 5 min in **D**. Decreasing the load of vegetative bacteria did not increase the inactivation rate after 5 min treatments in **E**. Emphasized are disinfection levels for vegetative bacteria (dotted line) and bacterial endospores (dashed line).

3.7 Influence of Tyvek cover on SMD plasma decontamination

In some of the previous experiments, bacterial species were treated with plasma, while they were distributed on dry carriers and wrapped in Tyvek coupon. In general, Tyvek is used for sterile packaging of medical devices. It consists of constricted high density PE fibers with porous structure (Figure 3.26), which allows permeability for gas/humidity and at the same time retains liquid substances. The permeability was proved for plasma in several studies including this one. Despite of that Tyvek is supposed to work as a physical barrier and inhibit the plasma inactivation. However, results of microbial carriers without Tyvek wrap were puzzling, since in contrast to what was expected, the plasma effect was significantly lower in comparison with the use of Tyvek (Figure 3.27**A**).

Therefore, a series of experiments were initiated with an increased load of *G. stearothermophilus* endospore samples per treatment/condition compared to previous treatments, in order to investigate this phenomenon. Plasma treatments were usually carried out at 35 mW/cm^2 and in 1.5 cm distance inside the closed FP2.0. Deviating conditions are described below.

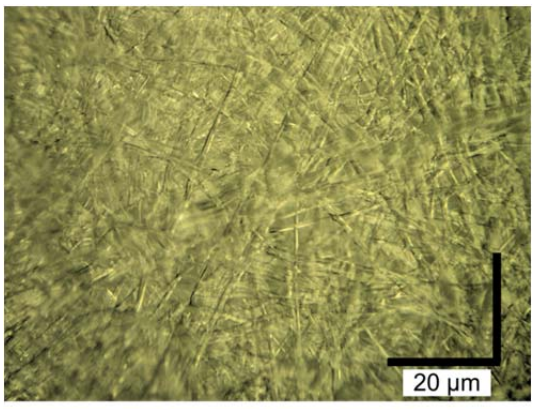

Figure 3.26: Microscopic structure of Tyvek (VHX-600 Digital Microscope, VH-Z500R, Keyence, Germany).

To begin with, the analysis method was validated by simultaneous analysis of microbial carriers at MPE and Simicon GmbH with subsequent comparison of the results of recovered spores (Figure 3.27**B**, **C**). In relation to certified 2 × 10^6 cfu by Simicon GmbH, 80% or 90% were recovered from untreated samples and 1% or 0.5% from treated samples at MPE or the company, respectively. These results were sufficient to move on with initial 1.6 × 10^6 cfu recovered from untreated samples at MPE which served as the basis for further determinations of log reduction after plasma treatment. Thereby, the fact of the large discrepancy in the log reduction of plasma-treated samples in or without Tyvek coupon was confirmed (Figure 3.27**D**).

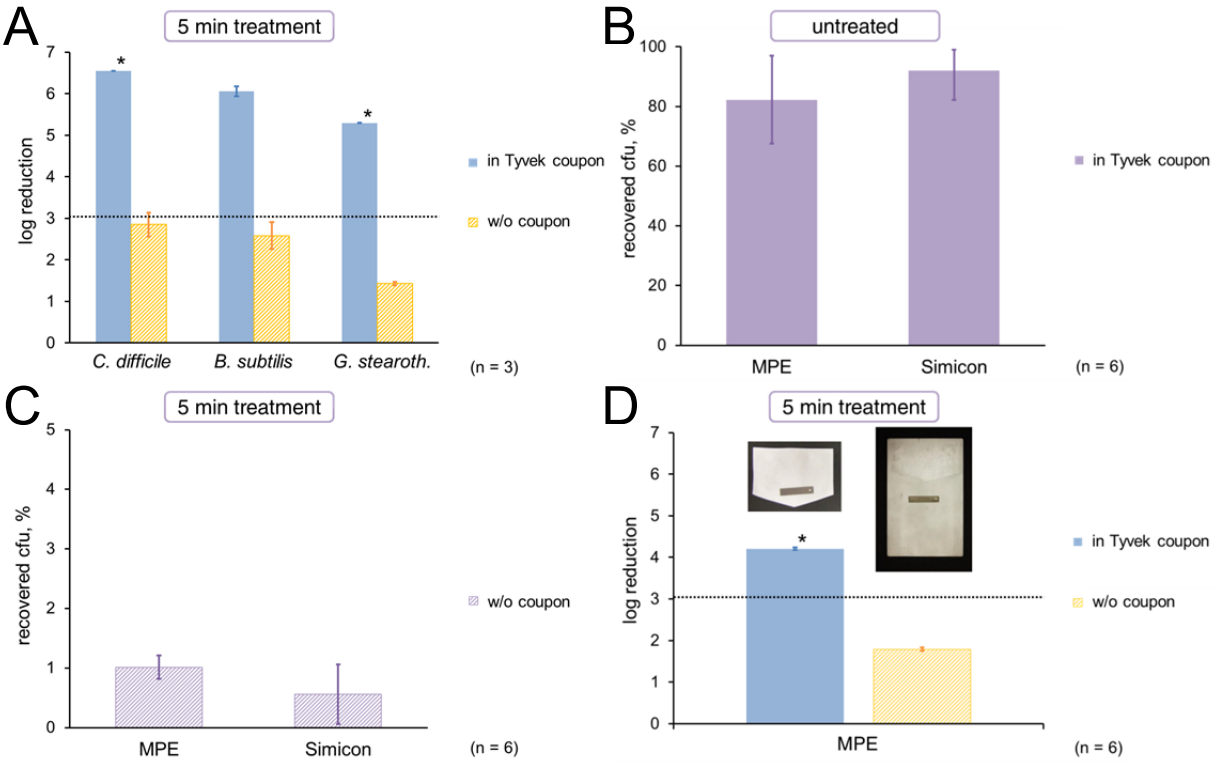

Figure 3.27: Quantification results of untreated and plasma-treated endospores recovered from dry carriers. Discrepancy in microbial reductions was observed with or without Tyvek use in **A**. Validation of analysis method of untreated and plasma-treated samples in **B** and **C**, respectively. Difference in inactivation was confirmed in **D**. Emphasized are disinfection level (dotted line), detection limit (*, *G. stearothermophilus*, Simicon GmbH/MPE) or complete inactivation (*, *C. difficile*, IHPH).

As a starting hypothesis, the Tyvek cover itself being in contact with the carrier surface could decrease the recovery of spores, because plasma is able to enhance adhesion to polymeric materials. Therefore, the recovery of untreated spores was evaluated from artificially inoculated Tyvek and from Tyvek wrapped around conventional biological indicator samples. The analysis of the first configuration proved that 100% of inoculated *G. stearothermophilus* were generally recoverable from Tyvek and analysis of the second configuration resulted in recovery of estimated 0.5 ± 0.1% from Tyvek surface being in contact with microbial carrier (certified 2×10^6 cfu load). Therefore, analysis of Tyvek covers from plasma-treated biological indicators is supposed to indicate clearly the degree of viable spores attached to Tyvek. However, 5 min treatment caused in concordance with the carrier results zero recovery which implied that all spores were inactivated independently from the adhesive behavior. In addition, the arrangement of spacing between Tyvek and the sample by placing the microbial carrier inside a vessel confirmed again that carrier contact to Tyvek per se did not influence microbial reduction (Figure 3.28**A**).

Surprisingly and most importantly, control tests without the Tyvek wrap disproved the described phenomenon and showed on the contrary same level of inactivation compared to tests with wrapped samples (Figure 3.28**A**). It was concluded from this finding that the Tyvek cover per se or related subjects such as the volume inside the coupon (Figure 3.28**C**) were responsible for the phenomenon. The Tyvek cover in fact hindered the inactivation as you would expect to happen (Figure 3.28**C**).

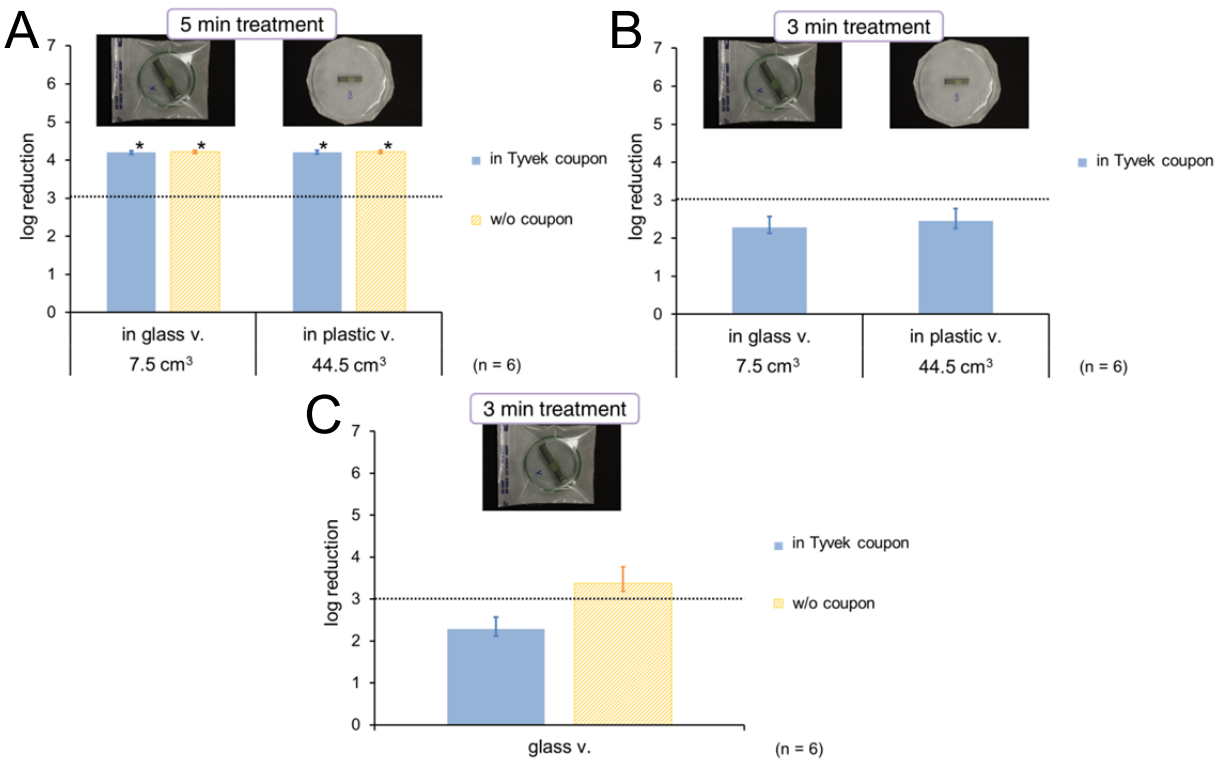

Figure 3.28: Results unraveling the role of Tyvek cover in microbial inactivation. No difference was observed for microbial carriers in vessels either wrapped or not in **A**. Volume inside Tyvek coupon had no influence in **B**. Tyvek cover prohibited higher reduction in reality in **C**. Emphasized are disinfection level (dotted line), detection limit (*).

Having unraveled the role of the Tyvek cover, it was further proposed that the separation of the microbial carrier from the grounded metal underground for instance through the PE film of the coupon or the glass vessel was in some way responsible. However, further investigations were not conclusive (Figure 3.29**A**). Despite of that it was demonstrated that the distance of the sample to the SMD electrode is important for the inactivation, which indicates again an influence of the electric field through charging (Figure 3.29**B**). Final experiments with varying plasma power densities support this assumption, since a higher power respectively a stronger electric field facilitated increased inactivation, while the ozone dose decreased (Figure 3.29**C**). These results show that plasma-generated ozone is not the only reason for the

inactivation of *G. stearothermophilus* spores. Further investigations on this topic are warranted.

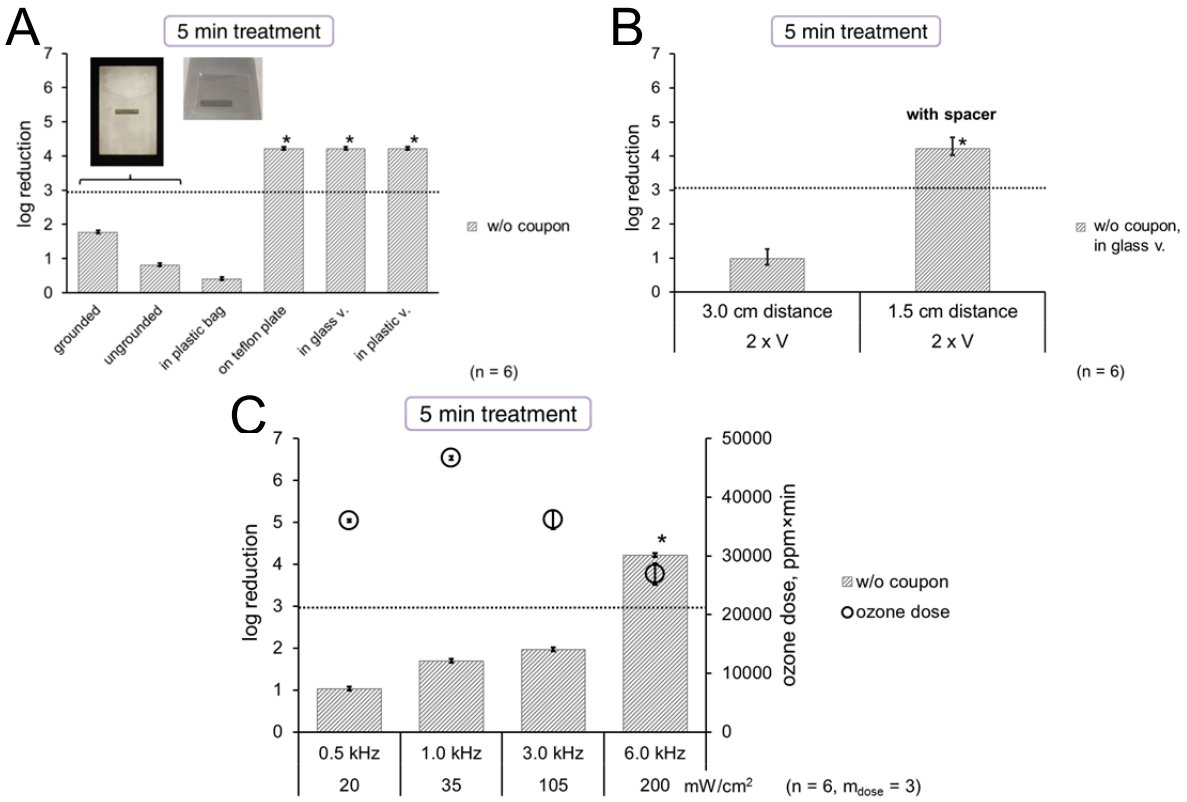

Figure 3.29: Experiments indicating influence of electric field on microbial inactivation. Emphasized are disinfection level (dotted line), detection limit (*).

4 DISCUSSION

4.1 Summary

During my doctoral work I developed a SMD electrode system, characterized the plasma generated at ambient air conditions, investigated its decontaminating behavior against bacterial species including nosocomial bacteria such as *C. difficile* endospores and revealed factors influencing the decontamination.

Certain requirements had to be fulfilled by every component of the electrode system. Essential was the chemical stability of used materials against oxidizing plasma species followed by homogenous discharge pattern and bactericidal efficacy which was assured by a stainless steel mesh grid as grounded electrode. A Teflon dielectric film showed best performance in regards of chemical and electric stability and a brass plate was favored as powered electrode. Finally, the electrode system was installed inside a box which served from then on as SMD device (FlatPlaSter 2.0).

Furthermore, with the help of plasma diagnostic tools I demonstrated that mainly excited N_2 and perhaps NO molecules emitted photons, the emitted UV-C power was below 660 nW/cm^2, temperature rise ranged from 0.1 to 3 °C per minute and the dissipated plasma power from 20 to 200 mW/cm^2. The ozone concentration was measured most appropriately *in situ* and reached maximum 13,500 ppm and higher power resulted in a change in the concentration curve with declining rate. Notably, the high ozone retention time led also to similar high doses, after the discharge was stopped.

Afterwards, I demonstrated in initial quantification experiments that SMD air plasma showed high bactericidal effects against different bacteria on agar plates with 5 log reduction in 30 s independent from the bacterial type and with a potential complete inactivation in 5 min.

Next, I studied the sporicidal action of plasma treating microbial carriers used as biological indicators according to standard sterilization testing. *G. stearothermophilus* demonstrated indeed the highest resistance among tested endospores, yet was inactivated to the detection limit within 5 min independent from the carrier material which was still faster compared to reference sterilization methods.

In the following, I addressed the plasma decontamination of carriers loaded with nosocomial bacteria using disinfection testing standards. The inactivation of *C. difficile* endospores surpassed the disinfection level even with 0.03% BSA burden within 5 min, which was not achieved with vegetative *E. faecium* or *S. aureus* at any time. Disinfection was thereby facilitated by reducing the bacterial density of *E. faecium* and thus avoiding multi-layering observed by SEM which prevented the access of gaseous plasma species to bacteria in lower layers. Other supplemental burden such as cell debris or salt crystals was identified by SEM that aggravated plasma disinfection. Nevertheless, disinfection was achieved even with heavy burden in form of sheep blood. Whereas surface morphologies of bacteria were not clearly altered by plasma, EDX elemental mapping revealed that treated surfaces were completely oxidized.

I adapted the SMD electrode in respect of secure handling for further antimicrobial tests with the same nosocomial bacteria outside the device. The 4-field-test was applied that was modified from a proposed standard test concerning the disinfection of large clinical surfaces. However, the disinfection level was neither reached for vegetative bacteria nor bacterial endospores on PVC flooring treated up to 10 min which was attributed to the side-diffusion of plasma species.

Finally, I investigated the role of plasma-permeable Tyvek cover which was used in carrier tests and had strongly facilitated the inactivation. This phenomenon was

disproved by treating and analyzing *G. stearothermophilus* endospore samples, where Tyvek rather functioned as a physical barrier and aggravated the plasma effect, as expected. Additionally, further results propose an influence of charging by the electric field applied during discharge. Finally, attributing the plasma effect solely to the ozone dose was excluded.

4.2 Considerations for developing a SMD device

Since this is a study based on a technology, some important technical aspects in the development of the SMD electrode system are briefly discussed. Overall, the underlying criteria for choosing the proper grounded electrode were adequate for material evaluation in my study. Inhomogeneous discharge patterns led to varying and insufficient inactivation results in agar plate tests. This was circumvented by the use of mechanical stable materials encompassing the electrode area and proper fixation. The bactericidal effect of the plasma gained significance in following experiments after the assurance that the given electrode material was chemically stable against plasma. Therefore, the chosen stainless steel mesh electrode fulfilled at best all criteria among tested electrodes.

However, there are aspects that have to be considered for future experiments. The dissipated plasma power was not measured, which would have been a more adequate parameter for comparing different electrode systems than the externally applied frequency and voltage. In the case of the chosen mesh, the dielectric surface was not optimally occupied by filaments. Hence, the density of generated micro-discharges each of them working as its own chemical reactor could be increased for a possible improved performance. This could be accomplished by a smaller mesh size and a hexagonal mesh pattern to utilize more space for micro-discharges.

However, processing to such shapes is complex in the case of stainless steel. In general, sole dimensioning does not make sense, rather a balancing of the geometrical and power parameters is required, as discharge filaments do not overlap with each other and can create discharge-free areas [38]. In addition, higher heat production and thus, a less stable dielectric might have to be considered.

The dielectric permittivity and thickness of a material define on the one hand the interaction strength between the electrodes and on the other hand the resistance against abrupt spark breakdown, which defines a disruptive discharge through insulation accompanied by a large increase in current. Because facilitated interaction allows rather a plasma discharge at lower electric power and at the same time has a higher chance of undesired sparking, careful choice of materials has to be made at a given power parameter range. In general, the dielectric material as any other materials in the device set-up should be resistant against corrosives generated in air plasma. Otherwise, frequent maintenance by exchanging parts have to take place or as well undesired interfering effects on the actual target such as coating can occur. Therefore, the substitution of the dielectric from POM to Teflon was correct, but also the housing parts made of POM, the polycarbonate lid as well as the powered electrode made of brass, which still exhibited strong features of tarnishing have to be substituted with chemically inert materials in the future. Especially POM has demonstrated bad performance: the device interior degraded or single parts even broke (sample removing pole, SMD electrode holding frame).

However, the lifetime of the Teflon dielectric varied and its removal became necessary every time accidental spark breakdown occurred. Notably, I experienced that the exclusion of humidity, which preferably condensed between the powered electrode and the dielectric, by sealing the free electrode parts enhanced the

dielectric lifetime remarkably. Therefore, it is suggested to seal the combined parts of the electrode system or to use one-piece systems, like printed circuit boards (attention: non-resistant metals normally used) or like electrodes sticking together with hardening ceramic dielectric as applied by Li et al. [151]. However, separate electrode parts have the advantage that only the dielectric has to be exchanged upon failure.

If the application of the SMD device is considered for the prospective treatment of living tissue such as for hand sanitizing purposes [56, 64, 112, 131, 152], a great safety issue has to be circumvented. Is it possible to avoid fatal spark breakdown through dielectric failure at any time of use? Beside the concerns about acquiring the proper hand disinfection results and about unknown long-term effects of plasma on human skin, the avoidance of life-threatening sparking cannot be assured upon frequent usage of the SMD electrode of my work. This disqualifies it for the treatment of human tissue, even if it is possible to touch the actual micro-discharges. However, the situation could be improved by the use of micro- or nanosecond pulses instead of sinusoidal wave frequency as described for a floating-electrode DBD in direct contact with tissue or sensitive materials [70, 153]. Pulses would allow a random spread of micro-discharges over the dielectric surface and avoid the continuous filament formation in the same spots. It would result in higher discharge uniformity and less stress to the dielectric material, especially polymers, since local temperature rise. Thus temperature can be elevated in filament channels and local electrostatic charges can be limited. However, there are examples of DBD devices that seem to be electrically safe [29, 154]. In addition, remote treatments with the hands far from the DBD source would be quite safe.

Finally, up-scaling the SMD device prototype (FP2.0), which might be required for commercial use, is technically not a problem, as it has been demonstrated for other industrial DBD reactors [10]. However, the prototype was not totally sealed. Therefore, it might be appropriate to provide air-tight closures such as at the lid opening, in order to prohibit putative diffusion of gaseous plasma species to the outside first of all to protect the user and further to avoid losing potential species for the decontamination goal.

4.3 Ozone and other traits about SMD air plasma

The characterization of the SMD air plasma revealed physical and chemical specifications of the discharge. Ozone was measured in enormous concentrations, whereas UV radiation and temperature are physical measures with minor importance, while maximum 23 W are consumed by the discharge.

For the majority of the microbial experiments, the power was set low to 4 W, which corresponds for instance to the power consumed by a modern current-saving LED lamp for households. In addition to the measurement of the air temperature inside the FP2.0, I recommend to monitor the material temperatures at the electrode system, in order to control dielectric breakdown in a better way. The generated UV-C power is far below the critical power density of 50 $\mu W/cm^2$, which are known to start affecting bacterial viability [155]. This is not surprising due to the production of considerable quantities of ozone that absorb UV-C. However, OES analysis showed that UV-A and UV-B radiation occur in higher quantities and thus, could participate as well in photodissociation processes. OES spectral analysis was not able to identify in a clear manner excited plasma molecules other than N_2. Since NO emissions are assumed to be present in the spectra and ozone was quenched at higher plasma power

probably by NO_x reactions, spectral change is supposed to occur in the OES at such power setting after certain discharge duration. Therefore, this experiment would have to be conducted at closed device condition, e.g. through a window, which is already present in the bottom plate. Despite of using this window, OES measurements with a more sophisticated spectrometer (iHr550, Horiba Jobin Yvon) with greatly enhanced spectral resolution revealed many additional peaks, but not conclusively the appearance of other excited molecules (data not shown). However, the aim was not to identify spectral changes depending on the discharge duration which could be saved for prospective investigations.

Ozone is a powerful oxidant which is reactive to biomolecules and is used as a disinfectant that can inactivate viruses and bacteria [50, 101, 156]. In aqueous solution or in connection with water vapor it decomposes to reactive hydrogen peroxide, superoxide and hydroxyl radicals and thus, can initiate further microbial damage [50]. However, it is also known for its mutagenic potential [157] and toxicity for humans [158]. Therefore, regulations permit a maximum ozone concentration of only 0.1 ppm at working place over the period of 8 h [159, 160]. Ozone levels of 5 ppm or higher are considered immediately dangerous to health or life [160]. For these reasons, very careful handling of the plasma device has to be considered with the generated exorbitant high concentrations of ozone. This includes the demand for a completely sealed device and an implemented suction system that removes ozone automatically after the treatment. A manual opening of the device and subsequent evacuation of ozone will be prohibited for commercial use due to safety issues.

In my study, the ozone concentration profile was altered upon changing plasma power. Shimizu et al. revealed this tunable feature of ozone concentration with SMD air plasma previously and pointed out that ozone is inhibited by side reactions

favoring NO_x formation [161]. This is an important feature that allows tailoring the plasma chemistry for the specific application, e.g. the dose of ozone for microbial decontamination. Furthermore, I showed that the way of measuring ozone is essential for the characterization of microbial treatment conditions. In any case, a similar high ozone dose was reached after extinguishing the discharge. This could cause considerable damage to bacteria and its effect has to be clarified in further investigations in the future.

In general, the number of potential reactive species in humid SMD air plasma which can interact with matter is large. Sakiyama et al. highlight other major ROS/RNS (N_2O, NO_2, N_2O_5, HNO_3) in SMD air plasma measured *in situ* by Fourier transform infrared spectroscopic imaging [47, 134]. Other studies investigated the influence of humidity on the inactivation of bacterial species with DBD air plasma achieving contradictory conclusions [123, 126, 162]. Altogether, it can be assumed that humidity alters the plasma chemistry and subsequently also the microbicidal effect. However, the underlying huge reaction system is not easy to control. New sophisticated tools in plasma diagnostics, especially in the *in situ* determination of electron, atom, excited species and free radical concentrations are available. Spectroscopic methods such as electron spin resonance (ESR) spectroscopy [47, 163-167] and laser methods [167-169] will contribute together with advances in modeling to the deeper understanding of physical and chemical processes of filamentous barrier discharges.

4.4 Bactericidal effect of SMD plasma

After developing and characterizing the SMD device, I continued to examine the general ability of the generated plasma to prohibit bacterial growth. For that reason, I

treated indirectly with plasma various bacteria inoculated onto agar and assessed quantitatively, how many bacteria were able to grow after treatment.

My kinetic study showed that 30 s treatments were sufficient to reduce the initial bacterial load by 4 to 5 log. Longer treatments caused in all cases a progressive, but retarded reduction curve with the potential of complete inactivation after 5 min (> 7 log). My findings coincide with the observations made by Gadri et al., who treated similarly with a remote air DBD system *E. coli* on agar plates, which resulted also in a 7 log reduction after 5 min treatment [105]. In another study from my group, we could demonstrate that 30 s plasma treatment inacivated 15 different bacterial species, which were partially isolates from clinical patients (e.g. MRSA, VRE, *C. difficile*) or nosocomial relevant type strains (e.g. Group A *Streptococcus pyogenes*, *Corynebacterium jeikeium*), in the same log range as I achieved in my work [131].

In our studies, no clear difference in the inactivation between gram-negative (here: *E. coli* or *P. aeruginosa)* and gram-positive (here: *E. mundtii*) was observed. Results of both studies herein suggest that there is no selectivity or protection to CAP based on the bacterial cell wall structure. In my work, the spread of the reduction level among different bacterial strains can be assigned to the deviation of initial loads, which is normal in microbiological testing and was circumvented by normalizing. For that reason, the spread cannot be referred to specific characteristics of a MO that result in higher resistance against chemical stress (such as antibiotic agents in the case of MRSA [131]) or physical environmental stress (such as desiccation, heat or irradiation in the case of *B. pumilus* [131]). In addition, the effect of SMD air plasma was not influenced by mechanisms of microbial resistance against antibiotics (innate or acquired) [131, 170]. This is reasonable, since plasma consists of a mixture of

various reactive species (UV photons, electric field, neutral reactive species etc.) that contribute to the inactivation process. At atmospheric pressure conditions, the most harmful UV components such as vacuum UV or UV-C (λ < 280 nm), which could cause intrinsic photo-desorption or DNA damage, are missing or are only generated to a low extent, respectively. The UV light of SMD air plasma is mainly emitted from N_2 molecules (N_2 second positive system) with power densities below 50 µW/cm^2, which are not expected to affect directly the inactivation [155]. However, UV-A and UV-B can still play a role by influencing the plasma chemistry. Plasma discharges create charged particles and an electrical field. It is suggested that electrical forces at the cell membrane might cause electrostatic disruption or at least permeabilization for a short time [171]. As a consequence, plasma-generated ROS/RNS (such as NO, OH, superoxide, H_2O_2, O_3) might penetrate into the microorganism and cause oxidative damage to cellular components such as proteins or microbial DNA. For instance, ROS/RNS can violate the integrity of the microbial cell structure by lipid peroxidation, resulting in membrane damage [172], which been also suggested for plasma-derived ROS/RNS [173]. Pompl et al. pointed out that the bactericidal effect of CAP can occur, before morphological changes indicated cell wall disruption [173]. Overall, this suggests that a more complex inactivation mechanism takes place, where different plasma species create a synergistic effect by altering in-cell processes being responsible for the antimicrobial effect. Although the inactivation rate of SMD air plasma was high, results of the agar model are not really feasible, because conventional decontaminating agents are tested with different models in accordance to EN standards.

4.5 Plasma sterilization

The application of the agar model indicated primary the inactivation of bacteria by plasma, but it is not suitable for modelling the treatment of medical devices or dry inanimate surfaces. Therefore, dry carriers were utilized as substrates for the treatment of environmentally more resistant bacterial endospores according to standard sterilization methods.

Bacterial endospores possess robust physical barriers and no metabolic activity, which could be influenced by chemical reactive species. Endospores are highly resistant to environmental stress including heat, UV- and γ-irradiation, desiccation, mechanical disruption and toxic chemicals such as strong oxidizers or pH changing agents [174, 175]. Their remarkable resistance has made them proper biological indicators for the validation of disinfecting and sterilizing agents.

The results show that SMD air plasma inactivated spores less efficient than vegetative bacteria on agar, but still quite rapidly by reaching the detection limit within 5 min treatment. In detail, Bacillus spp. were reduced in 3 min by 5 log. Kelly-Wintenberg et al. reported that their DBD reduced *B. subtilis* spores with the same sample configuration in less than 5 min treatments in direct mode [28]. In my study, the D-values stayed below the values of standard reference methods. Furthermore, my results suggest that maximum 6 min or 12 min are sufficient to reduce theoretically the microbial load of all tested strains by 6 or 12 log, respectively. Endospores of *G. stearothermophilus*, which are commonly used as biological indicators for H_2O_2 sterilization, were more resistant against SMD air plasma than spores of Bacillus spp. This coincides with the results of Kelly-Wintenberg et al., who reduced *G. stearothermophilus* only by 3 log after 7 min treatment [28]. In my study, the resulting D-value with $D_{23°C} = 0.9$ min calculated for the reduction of

G. stearothermophilus is four-fold lower than the standard $D_{60°C}$ = 4.2 min for H_2O_2 sterilization. Although this implies a strongly improved treatment efficacy, it is advisable not to overrate these results due to the fact that a plasma prototype was used. The validation has to be repeated with an up-scaled SMD device suitable for the sterilization of medical instruments.

In addition, the influence of different non-metal test carriers on the inactivation of *G. stearothermophilus* was investigated and the same inactivation rate was observed with all tested materials. Mahfoudh et al. found that polymeric materials treated with ozone, a major component in SMD air plasma, could affect indirectly spores of *B. atrophaeus* [176, 177]. They exposed the polymeric materials to ozone concentrations of 4000 ppm, which was lower than in my study. However, their actual dose was much higher due to the treatment over hours and afterwards they spread spores over the surfaces, which were sporicidal by the treatment except the chemically inert Teflon [176]. The selection of the carrier material did not cause any distinct plasma inactivation in my study. However, I used only carrier materials with quite smooth surfaces that face the plasma generating electrode. A greater challenge would be the involvement of surfaces with higher roughness or more complex structures, which aggravate the access of plasma species such as plasma averted surfaces, edge transitions or lumen. Screws were used in a recent low-pressure plasma study regarding space component sterilization with *B. pumilus* and *B. subtilis* spores [178] and thus, could be a more suitable model. In addition, a DBD study showed similar inactivation of *G. stearothermophilus* spores on carriers either facing or being averted from the plasma-permeable Tyvek cover [121]. This gives hope in the activity of SMD air plasma with more complicated sample configurations.

Although this study was entitled to obtain plasma sterilization, I have to admit that sterility per se, thus the total absence of microbial life on carriers, was not assessed. The applied quantitative methods ensured the determination of the reduction to a certain degree (≤ 10 cfu). The qualitative validation of sterility is usually determined by using a turbidity method, which should be respected in prospective studies. Therefore, not the sterilizing effect of plasma was studied, but rather its decontaminating effect suggested as the appropriate term by Woedtke et al [108]. In my study, kinetic curves were determined with only a few treatment times and a quite small sample size. Application of more treatment times (at least five) and a larger sample size are recommended for more precise results. This would also allow the appropriate examination of the log-linear kinetic model, which I have initially applied.

Considering the inactivation mechanism by plasma, Eto et al. supposed that ozone and other neutral reactive species such as OH are important for the sporicidal activity of SMD plasma in humidified air [121]. Gaseous ozone has been found sporicidal in diverse studies [179, 180]. Yardimci and Setlow investigated the sporicidal effect of UV in plasmas and observed that plasma inactivation occurred even in the absence of UV [181], which coincides with Eto´s finding. This correlate also well with the data of my experiment, where the opaque Tyvek cover blocked UV from the plasma discharge and inactivation occurred at the same time. In addition, microbial macromolecules can be damaged functionally by reactive plasma species including enzymes and membranes, which diffuse into the spore and inactivate the spore. Thus, Cortezzo et al. suggested that the treatment of *B. subtilis* spores with oxidizing agents lead to the damage of spore proteins, specifically proteins of the inner membrane whose integrity is essential for spore viability [182]. ROS in atmospheric SMD air plasma might have a similar effect.

Overall, there is still a substantial lack of knowledge about the way plasma inactivates bacterial endospores, because highly diverse plasma species are not easy to measure appropriately. Despite of that, it is assumed that the synergy effect of various SMD air plasma species is responsible for the inactivation of vegetative planktonic bacteria, as well as for endospores. The development of tools, which can identify and quantify relevant plasma species, is obligatory in combination with biochemical studies for the investigation of the inactivation mechanism of MO evoked by SMD air plasma. Therefore, physiological studies are supportive that combine different methods for the provision of multimodal information e.g. on a single bacterial spore *in situ* [183], as described for studying the dynamics of wet-heat sterilization [184]. Especially studies on MO mutants, which lack of specific resistance-giving proteins, can help to gain understanding.

It can be concluded that my SMD device operating in ambient air has demonstrated its ability to remove microbial contamination from dry inanimate surfaces by efficient reduction of viable bacterial endospores. Moreover, inactivation was achieved with this SMD prototype more rapidly compared to reference sterilization methods. This gives confidence in the possible contribution of SMD plasma in an improved hygienic care in hospitals by efficient and safe sterilization of sensitive medical devices in future. Prospective studies with devices tailored for clinical application and with more complicated sample configurations will give better information on the suitability of the SMD plasma technology in hygienic practice.

4.6 Plasma disinfection

4.6.1 Using dry inanimate carriers

This is the first experimental study of kinetic inactivation by CAP treatment against spore- and non-spore-forming nosocomial pathogens including *C. difficile* spores on dry carriers and in fulfilment of disinfection standards which means the inclusion of additional organic burden. Furthermore, the surface condition of used microbial carriers was determined by SEM imaging and EDX analysis in detail.

Disinfection with bacterial endospores was successful within 10 min treatment, but failed with vegetative bacteria due to the high bacterial density that caused the formation of multi-layers on regular-sized carriers. However, the disinfection level was achieved at lower bacterial density. Salt crystals or cell debris on the carrier influenced the inactivation by SMD air plasma. Moreover, plasma oxidized all treated surfaces, yet did not affect the surface morphology of endospores or vegetative bacteria, but degraded BSA and cell debris.

Previously, inactivation of *Bacilli* and *Clostridia* endospores was demonstrated in H_2O suspension using CAP by Tseng et al. [111]. Furthermore, I utilized dry carriers and treated *Bacilli* endospores on them using SMD air plasma in respect of sterilization standards as described in my former experiment [131]. In contrast to both studies, the crucial influence of organic burden on plasma inactivation was also examined here. Overall, conditions observed on carrier surfaces were related to the inactivation kinetics: rapid log-linear for *C. difficile* without organic burden, from slow to rapid after the degradation of sporulation debris for *G. stearothermophilus* and slowed down for *C. difficile* with 0.03% BSA, which restrained the access to highly covered spores. Notably, endospores of *C. difficile* and *B. subtilis* without organic burden were inactivated more rapidly than *G. stearothermophilus* spores. In contrast to *C. difficile*,

G. stearothermophilus spores were mostly surrounded by sporulation debris forming agglomerated regions that served as additional organic burden and hindered the accessibility for gaseous CAP species. Furthermore, lower initial load of *B. subtilis* was applied compared to other spore types. Thus, the general notion that *C. difficile* spores are less robust against biocides than other endospores is questionable, when the same sample conditions cannot be assured.

Notably, Mahfoud et al. demonstrated that dry gaseous ozone that inactivated bacterial endospores did not affect the integrity of spore coat, which correlates with my SEM imaging results [185]. However, they observed strong erosions of spore structures, when humidity was present [185], and this is discrepant to my results, since humidity was never excluded in my experiments and still clear morphological effects were absent.

In comparison to other studies with liquid disinfectants, Block et al. reported that Perasafe®, a product with 0.2 % peracetic acid, reduced *C. difficile* and *B. atrophaeus* spores on stainless steel discs after 10 min exposure by about 6 log [186]. They found that chlorine-releasing sodium dichloroisocyanurate (NaDCC), which was commonly used at that time for environmental decontamination in Israeli hospitals, was strongly inferior (< 2 log) [186]. However, they did not include any additional organic burden such as BSA in their study. Barbut et al. compared an innovative hydrogen peroxide dry-mist disinfection system with the common disinfectant sodium hypochlorite (NaOCl) by treating hypervirulent *C. difficile* spores on laminate and PVC carriers (2 cm^2) [187]. They found that both methods reduced spores equally more than 4 log after 10 min treatment or after one cycle in the case of hydrogen peroxide *in vitro*, but could show with an *in situ* randomized field study that the innovative system was superior in decontaminating *C. difficile* from surfaces

in a single room [187]. Perez et al. demonstrated that acidified bleach was able to achieve a 6 log reduction of *C. difficile* spores, which were distributed with high level soiling on stainless steel discs, in only 3 min [188]. Maillard summarized studies about the sporicidal activity of alkylating agents such as glutaraldehyde and oxidizing agents such as peracetic acid, chlorine dioxide and chlorine-releasing agents including surface tests and pointed out the possible failure of decontamination due to several factors [189]: biocide concentration, contact time, level of soiling, type of surface, temperature and relative humidity.

In the case of vegetative bacteria *S. aureus* and *E. faecium*, up to 99% of all bacteria could be inactivated in my experiments, although standard compliant *E. faecium* samples showed bacterial multi-layering, which blocked reactive plasma species. Furthermore, larger carriers or lower microbial loads enabled inactivation up to the disinfection level with increasingly significant additional burden. Disinfection was achieved, even if *E. faecium* was embedded in blood matrix that prevented the access of plasma. To my point of view the high electric field being necessary for plasma generation contributes to the inactivation or that it is difficult to recover bacteria from the blood bulk of plasma-treated samples. In favor for the latter, atmospheric plasma can enhance the adhesion of organic surfaces by oxidation [190]. This suggests that bacterial cells might be stuck together in organic clusters on the carrier, unable to be separated by vortexing with subsequent false negative viable counts.

Compared to the treatments on agar plates, SMD plasma was less effective in carrier tests. This can be attributed to the higher bacterial density on carriers and to the wet agar system per se. As demonstrated here, lowering the microbial density on carriers caused similar inactivation kinetics. Furthermore, Boxhammer et al. have shown that

the inactivation of *E. coli* in small quantities of liquid (20 µL) can be correlated to the formation of H_2O_2 and NO, which in combination lead to nitrosative and oxidative stress [127]. This could further explain an accelerated reduction on wet agar compared to dry carriers.

In comparison to another SMD study, Pavlovich et al. treated *E. coli* (10^7 cfu) on various surfaces with SMD air plasma in direct and indirect mode [133]. They observed a similar kinetic reduction in both modes with 1 to 2 log after 60 s and 4 to 5 log after treating *E. coli* for 5 min on stainless steel discs, which is a slower effect than in my study (see kinetics without BSA). I believe that the relation factor between the total volume that microfilaments occupy (= reaction volume) and the chamber volume was higher in my study and thus, could be one possible explanation of the difference. However, a clear explanation is difficult, since distinct plasma power densities were applied in both studies with a lower density here. Furthermore, Pavlovich revealed similar inactivation for rubber and silicon carriers, but much lower inactivation for pig skin as well as the inferiority of plasma to increasing concentrations of chlorhexidine (2%) [133].

In comparison to liquid disinfectants, Block et al. showed in their study with vegetative bacteria that chlorhexidine reduced *S. aureus* and *E. faecalis* on stainless steel discs (10^8 cfu) by 4 and 6 log after 10 min exposures, respectively [191]. Povidone iodine was even more efficient with 6 log reductions after 2.5 min [191]. Therefore, liquid disinfectants seem to be much more efficient in the inactivation of vegetative bacteria. Pottage et al. revealed that hydrogen peroxide vapour was able to reduce *G. stearothermophilus* spores by 5 log after 30 min, yet achieved only 2.5 log for MRSA with the same initial load of 10^6 cfu and after the same treatment time [192]. They assumed that the effect of catalase in MRSA detoxifies H_2O_2

molecules. In my study, vegetative bacteria were not necessarily more resistant than bacterial endospores. The similar kinetic behaviour can rather be explained by the higher initial loading that was required in the case of vegetative bacteria, in order to recover 10^6 cfu in the negative control samples. In addition, my results show that catalase-negative *E faecium* was not more susceptible to plasma than catalase-positive *S. aureus* on carriers with 10^8 cfu. For that reason, this suggests again that synergy of active plasma species takes place.

SMD air plasma serves as a source of ROS/RNS and here, it degraded BSA protein film and sporulation debris. Similarly, Finnegan et al. demonstrated that oxidizing agents degrade proteins like BSA and other macromolecules present in microbial cells [193]. However, spore coats provide physical barriers to large molecules and detoxify ROS, before they can penetrate into the inner spore [83]. In my study, CAP had no obvious effect on the surface morphology of endospores or *E. faecium* cells. This implies again that oxidizing agents can damage key proteins in the inner membrane of spores that leads to membrane integrity and viability loss upon further stress [182]. In contrast, the outer spore coats were shown to get degraded by oxidizing agents solved in aqueous solution, which exposes the essential compartments in the core [194]. Despite of that, liquid-phase H_2O_2 is not as strong oxidizer as vaporized H_2O_2 [193], a constituent in humidified air plasma. In addition, the contribution of other plasma components (electric field, UV) to microbial cell inactivation is probable and was discussed in the sterilization section.

My study and others indicate that the choice of suspending medium is important [195, 196]. Standard compliant, bacterial endospores are prepared in H_2O and vegetative bacteria as well as BSA in saline medium. The latter medium causes salt crystals on the surface upon drying, whose macrostructures cover bacteria and

potentially shield biocides. Considering that salt is present on contaminated hospital surfaces from body fluids, justifies its use in standard biocide testing. Moreover, tests with nosocomial pathogens that model the real procedure of cleaning and disinfecting surfaces such as the proposed “4-field-test” are still missing as standards, but are close to be approved [147]. In general, a unique standard does not exist for testing disinfectants with bacterial endospores not to mention *C. difficile* endospores or specifically testing of gas-borne surface disinfectants in the human medicine area due to anachronistic regulations [197]. Instead, valid standards are applied considered for the food and domestic area [142], which cannot be considered reliable methods in human medicine. Therefore, many products claim to be sporicidal against *C. difficile* spores, but fail at more practical conditions with high burden and short contact times [87].

Considering application, biofilm disruption and microbial density reduction by mechanical cleaning are inevitable to enhance the disinfecting action of SMD air plasma. Like other disinfecting agents, SMD air plasma has some disadvantages: O_3 and other oxidative species are potentially harmful to living beings and corrosive to materials; CAP devices are electrically driven and require maintenance; high voltage demands careful handling; the target surface has to be close to the electrode generating SMD plasma; side diffusion of gaseous plasma species must be avoided for best performance results. However, the versatile nature of SMD air plasma systems allow for instance the adjustment of O_3 concentrations [161] and recent studies have already proven that SMD devices do not harm human tissue cells while being operated at bactericidal dosages [154, 198, 199].

In conclusion, the outcome of this study and the adaptable properties of CAP are compelling evidence for a prospective contribution of SMD air plasma for the

environmental control of *C. difficile* spores and other nosocomial pathogens, especially in instrumental disinfection. Therefore, SMD plasma could serve as an alternative to conventional liquid disinfectants among other promising air-borne decontamination systems including gaseous hydrogen peroxide, chlorine dioxide, ozone, air/filter decontamination technologies and UV disinfection [101]. However, further investigations have to prove its antimicrobial action and safety in field studies. A prerequisite is the use of well-defined microbial samples as well as reformations in the regulation of decontaminant testing.

4.6.2 Clinical surface disinfection

In general, environmental surfaces are regarded as a reservoir for persistent nosocomial pathogens available to be transmitted via personnel hands to susceptible patients. Therefore, I assessed the applicability of SMD plasma at the disinfection of clinical surfaces with an adjusted practical testing method, which is proposed to become a European standard [146, 147, 200]. Results have shown that plasma was not able to remove enough microbial contamination - neither bacterial endospores nor vegetative bacteria - for fulfilling disinfection criteria within long 10 min treatments.

In contrast to previous treatments with in part higher inactivation results in the same time range, the treatments were carried out in an open volume and with microbes on larger areas. Therefore, I regard the side diffusion of plasma species as the main reason for the low reduction. To this end, provisionally fixed Teflon barriers were not able to sustain a sufficient high plasma concentration under the electrode that would stress more the bacteria. The side diffusion could also lead to passive inactivation in the proximity of the actual treated surface, since surviving in control fields of the

experiment was diminished in the case of bacterial endospores. However, a loss in control fields was not observed with vegetative bacteria. Thus, to limit side diffusion, adequate precautions like barriers that confine properly the treatment volume are of great importance.

As mentioned, the test was modified in respect of plasma. The original test combines practical cleaning and disinfection by mechanical distribution of liquid disinfectant and microbes with a wipe over four fields. On the one hand, mechanical force on bacterial contaminations such as with a brush would probably also enhance the plasma action, since the bacterial density is decreased, agglomerations are disrupted and hence, the available surface of single bacteria is potentially enlarged. Furthermore, only one field is contaminated in the original approach with bacteria and then distributed to other fields, in order to determine their spread, instead of loading all fields and applying static one by one treatment. On the other hand, I demonstrated that reduction of bacterial load did not lead to improved log reductions of vegetative bacteria as it did in carrier tests. Therefore, the limitation of multi-layering or agglomerating was missing. This observation pinpoints once again that side-diffusion was the limiting factor. In addition, moving the device over the surface would supposedly further decrease the local concentration and contact time of plasma species with microbes. However, surface disinfection usually implies mobile treatment, which should be also implemented for future plasma testing. This could be achieved by installing small wheels and guidance could be ensured by the already installed holder.

The chance for a successful surface disinfection with SMD plasma is low in this study, because applying the treatment for minutes at the same position is not practical and most of the times also not realistic in the everyday practice. However,

conventional liquid disinfectants have the same problem. They are mainly validated by standard suspension tests with treatment times of more than 10 min up to several hours, recently including *C. difficile* endospores [87, 201, 202]. Buettgen et al. have shown with this method that the same hypervirulent *C. difficile* spores were more susceptible to disinfectants (e.g. chlorine releasing agents, glutaraldehyde) than *B. subtilis* spores [201], which I also demonstrated with my 4-field-test results, but not with my carrier tests. Their conclusion that the required disinfectant concentration might be reduced for nosocomial relevant *C. difficile* is based on my results doubtful. Moreover, the suspension test might make sense for instrumental disinfection, but not for surface disinfection, since inactivation of microbial contamination on dry surfaces is more difficult [191]. In surface disinfection, liquid disinfectants are applied in quantities that are maybe sufficient for wetting the whole surface, but allow only short exposure times due to early evaporation [203] which is addressed with the 4-field-test. In combination with wipes that remove per se a lot of the contamination by uptake, disinfectants which passed the suspension test have shown good reduction performance in the 4-field test in only 2 s cleaning procedures and after certain exposure times, but some disinfectants promoted also inadequate high spread of microbes [204]. In a very similar approach including wiping, Ali et al. treated 25 cm^2 big laminated surfaces with hypochlorite or NaDCC and assessed the spread and inactivation of *C. difficile* spores [205]. They point out that most of the contamination (3 log from initial 10^6 cfu) was already removed from the surface by the wiping procedure and the disinfectant failed to prevent the spread of residual spores and to inactivate them even after 60 min incubation time (disinfectant evaporated earlier) [205]. This example highlights again the problematic situation of ineffective

decontamination in hospitals as well as the demand of accurate standard validation methods that reflect in-use practices [206].

In the previously mentioned study of Block et al. [186], they also exposed *C. difficile* and *B. atrophaeus* spores to Perasafe® and NaDCC using PVC flooring substrates (2 × 2 cm) without wiping and found that inactivation was aggravated with maximum 2.7 to 6 log compared to the set-up with stainless steel discs. This tendency appears also in my study comparing carrier tests with PVC field tests, where in contrast to Block et al. organic burden was additionally included.

Since this was the first test of this kind, there are no possible comparisons with other plasma approaches. Despite of that, it is possible that a direct surface treatment such as with a FE-DBD source would be more effective than the indirect treatment with a SMD device, as charged species from the micro-discharges would improve the inactivation effect and clinical surfaces are made of robust materials that proved to withstand strong liquid disinfectants. Another approach would be to shorten the distance with the given SMD device and/or to increase the plasma power. However, movement along rough surfaces could be hindered and life-time of the electrode would be reduced critically. Furthermore, you could think of using handheld SMD devices which are under development [154] together with pre-moistured wipes, in order to “activate” water by acidifying it for disinfection [115, 134]. Creating plasma through the wipe tissue during cleaning process might also be worth considering, since SMD plasma is active through various fabrics [121, 207]. However, all of these suggestions are based on hypotheses and would need to be reasoned in detail.

Indeed, surface decontamination is nowadays a well-accepted task in the conflict against nosocomial pathogens such as *C. difficile*, MRSA, VRE or norovirus [91, 208, 209], despite the lack of scientific evidence proofing the benefits a decade ago [210,

211]. Beside the debatable effectiveness, the application of conventional hypochlorite involves serious drawbacks: corrosion, low tolerance to organic matter, reduced effectiveness in cleaning surfaces, and requiring two operational steps, which is time-consuming [212]. Notably, conventional disinfectants such as quaternary ammonium compounds, hypochlorites and phenolics render a risk to the safety of employees and the environment by causing skin irritation and asthma; and benzalkonium chloride is one of the leading allergens in healthcare personnel [213]. In addition, commercial production of liquid disinfectants comes along with a lot of residual waste, which has to be disposed and causes environmental pollution. For these reasons, the investigation of alternative decontaminating agents is mandatory also in respect of the toxic nature and processing of agents. For instance, SMD air plasma is per se toxic, otherwise it would not possess any antimicrobial activity, but the technology does not produce any waste. The plasma utilizes ambient air molecules, consumes some electric energy and afterwards decomposes to air again which makes this technology sustainable.

However and without doubt, my SMD air plasma prototype is not competitive in this form for surface disinfection purposes and would need improvements as suggested earlier. A prerequisite for considering SMD plasma application would be the combination with cleaning processes among other aspects such as safe handling and an objective evaluation of essential measures (e.g. in efficacy, maintenance, handling, waste, toxicity, applicability, etc.) compared to conventional liquid disinfectants and other uprising air-borne decontaminants. A comprehensive list of advantages and disadvantages of common disinfecting and sterilizing agents is provided by Rutala and Weber [214].

4.7 Influence of Tyvek and other factors

Previously in my work, higher degrees of inactivation were obtained by the treatment of endospore samples wrapped in Tyvek coupons compared to samples without the wrap. Therefore, I investigated this phenomenon in detail and revealed that Tyvek actually functions as a diffusion barrier and mitigates the plasma effect as expected. Zimmermann et al. have demonstrated a similar barrier effect for treating bacteria on agar through textiles and envelope materials [207]. However, it does not explain the big difference in the reduction between treated samples without and with wrap. Wintenberg et al. treated as well *G. stearothermophilus* samples within Tyvek coupons and did not report any remarkable difference [28]. In contrast to spores, the treatment of vegetative bacteria did not result in distinct reductions during my work (data not shown). This could be attributed to a higher load (10^8 cfu) and density which did not allow big log reductions anyway. I did not carry out though comparing experiments with lower load. In line with my finding, Cotter et al. did not observe variations of the CAP effect upon treating wrapped or unwrapped MRSA biofilms [124].

In further experiments, I could exclude that the volume inside the Tyvek coupon or the contact to Tyvek surface were responsible. However, results indicate that the way of insulating the bare sample from the grounded bottom plate was important for the resulting reduction. When insulated, plasma was effective. It was also effective, when the sample was closer to the plasma electrode or with rising plasma power. These findings suggest that the electric field of the SMD electrode and its charging potential of surfaces could be the key. Moreover, the plasma effect cannot be assigned merely to the ozone dose, since an enhanced plasma power resulted in a lower dose.

Hence, other plasma components such as possibly the electric field support the sporicidal action of plasma.

Further investigations need to be conducted for a conclusive assessment and rationale of this phenomenon.

4.8 CAP research and applications in decontamination

My work addressed in depth the effect of CAP against bacterial species, vegetative and dormant ones. Nevertheless, it is not enough to proof the decontaminating behavior against such bacterial species. Other types of nosocomial pathogens, namely mycobacteria, fungi and viruses have to be included in decontamination studies, in order to cover the whole spectrum by testing mycobactericidal, tuberculocidal, fungicidal, yeasticidal and virucidal activity [91].

The fungal yeast *C. albicans* is a major cause of invasive infection. In our recent study, it was the hardest to inactivate by SMD air plasma in comparison with vegetative bacteria on agar [131]. In contrast to bacteria, the fungal cell wall consists of chitin/cellulose fibrils within a polysaccharide matrix. *C. albicans* can change its shape depending on the environment and growth phase, for instance its cell wall is thicker at lower than neutral pH. Furthermore, *C. albicans* produces dormant and environmentally resistant chlamydospores. As an eukaryotic cell, *C. albicans* has a nucleus containing a diploid genome and sheltered by the nuclear membrane as an additional diffusion barrier, which contribute to higher resistance to DNA damage [215]. These and other characteristics may enable *C. albicans* to be less sensitive to biocides [215]. Besides planktonic cell inactivation, encouraging results of inactivated *C. albicans* biofilms have been obtained recently with the same SMD device [130]. Planktonic and biofilm inactivation of *C. albicans* has also been demonstrated with

other DBD and APPJ systems [216-218]. Muranyi et al. achieved a significant reduction of the mold *Aspergillus niger* conidiospores by the direct treatment with a DBD system [104].

Non-enveloped viruses such as adenovirus or norovirus are also a common threat. Viruses cannot replicate by themselves and need the replication machinery of host cells, which they deplete, before they move to invade other cells and further attenuate the host. Zimmermann et al. demonstrated that SMD air plasma could inactivate adenovirus in small quantities of liquid within 4 min [125]. Similarly, M2 bacteriophage, which was used as surrogate for norovirus, was successfully inactivated with an APPJ [219] and bacteriophage Phi X 174 with another DBD system [105]. However, studies on the virucidal activity of CAP are at the moment rare.

Mycobacteria have a unique cell wall structure, which cannot be differentiated by gram stain and makes them very robust against environmental stress. *M. tuberculosis* and *M. leprae* are known for causing tuberculosis and leprosy, respectively. Only few studies have been conducted using mycobacteria. Venezia et al. inactivated *M. fortitum* by indirect treatment with a CAP source only described as PlasmaSol [220]. Another study applied pulsed electric fields through water containing *M. paratuberculosis* and showed an effect, which cannot convincingly be related to CAP [221]. In my work, tests with *M. terrae* and *M. avium* as surrogates provided by the IHPH were considered, but finally were not carried out due to the insufficient log reduction results of treated vegetative bacteria on dry carriers. Notably, tuberculocidity is technically approved after successful inactivation of *M. terrae* and mycobactericidity after inactivation of *M. terrae* and *M. avium*.

Overall, any validation of microbicidal activity introduced in this section requires a 4 log reduction in compliance with the European standard disinfectant methods [91].

All of these aspects have to be considered in addition to the content of my experimental work, in order to investigate the applicability of CAP sources for decontamination purposes. The disinfection testing with *C. difficile* endospores is not standardized yet [143], though it is important [91], since they gain higher prevalence in nosocomial infections at European [71] and American hospitals [222], and can be more resistant to disinfectants than surrogate species.

However, the prospective application of CAP is in particular promising in various medical settings. Examples are CAP systems that are under development for the decontamination of chronic wounds [64], medical endoscopes [223] or the root canal of tooth [224-226]. Other promising fields of application involve food processing [132] and planetary protection [106, 107].

4.9 Fundamental issues related to nosocomial infections

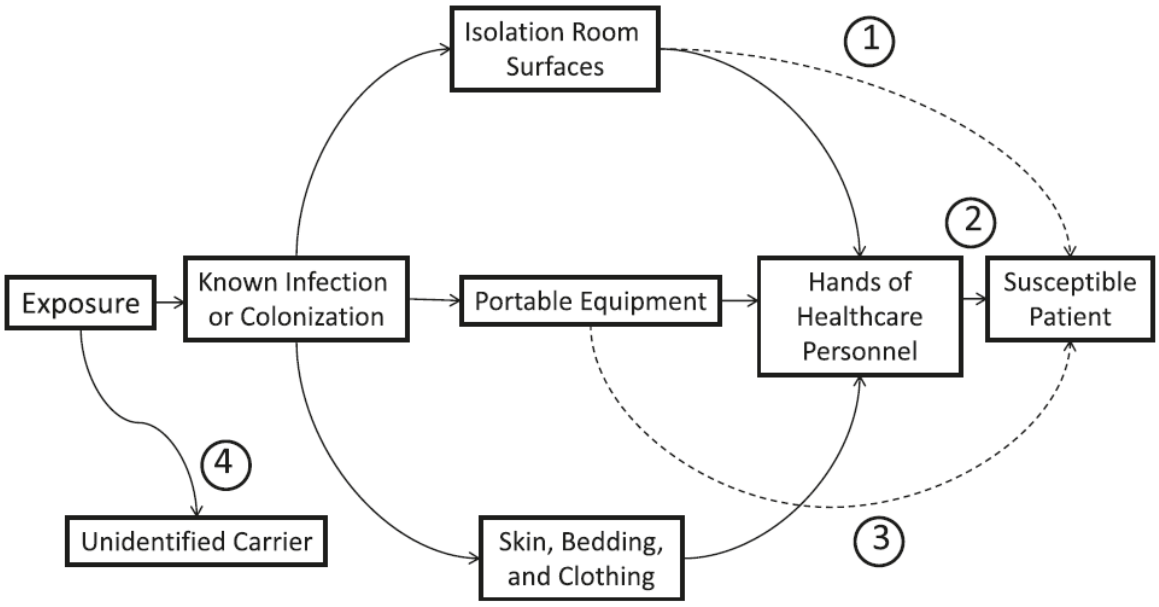

Figure 4.1: Overview of common routes of transmission of healthcare-associated pathogens (adapted from Donskey [208]).

An adequate hygienic practice in healthcare facilities is without doubt essential for the environmental control of nosocomial pathogens. However, there are many possible routes pathogens can take to invade susceptible patients which have to be blocked (Figure 4.1). Hence, some serious issues which are not directly linked to the actual decontaminating agent are associated with this topic and need consideration.

One issue arises from the fact that you do not see the microbial threat and thus, cannot really localize pathogens in the environment. For instance, healthcare workers have no real *ad hoc* control measures, if their hands are really free of considerable (harmful) microbial contamination after disinfection. Recommended hand disinfection procedures follow a certain step-to-step protocol and require at least 30 s [227]. Therefore, proper and continuous hygienic training is necessary for the compliance of hand hygiene. This demands extra time that the nursing personnel would have to invest for hand disinfection. As mentioned earlier, frequent disinfection of hands can lead to skin diseases [213]. In Germany, the trend towards less healthcare personnel, who are still responsible for the same number of patients, increases their working load and intensifies this issue. Further economic reasons force hospitals to shorten the duration of patients´ stay and to exploit their bed capacities at any time by hospitalizing as many patients as possible.

Furthermore, Figure 4.1 depicts the possible route via isolation room surfaces. In reality, many hospitals do not have the chance first of all to screen all patients that they hospitalize and second to isolate infected patients from other patients simply due to the lack of space. Many patients have to share a room and a bathroom, which further simplifies the spread of microbial pathogens among patients. Therefore, an insufficient clinical infrastructure can increase the risk for nosocomial infections. In addition, many people are asymptomatic carriers of potential harmful pathogens such

as *C. difficile* and contribute to the transmission [89, 228]. First reports about newborns that are colonized by multidrug-resistant and highly invasive microbial species such as hyper-producing ESBL *Enterobacteriaceae* are alarming [229-232].

In general, the concerns about antibiotic-resistant microbial pathogens are already justified without listing the complications for the affected individual arising from the actual infection at healthcare facilities. Once a nosocomial pathogen occurs, it is hard to eradicate it from the clinical ward and requires complex interventions [89, 208]. The same is valid for infected patients, since for instance in the case of *C. difficile* possible treatments are currently limited which are more or less effective in avoiding permanent recurrence of the infection [89, 233, 234].

In conclusion, the prevention of nosocomial infections should have highest priority, in order to maintain quality of medical services and reliability into medical facilities. This goal can be approached by improving the conditions and processes in healthcare facilities starting from the conscious use of antibiotics, modernization of clinical infrastructure such as provision of isolating rooms, appropriate clinical management and improvement of decontamination systems.

4.10 Conclusion

My work addressed different aspects of a CAP system based on the SMD technology and considered for the decontamination of medical devices and clinical surfaces. SMD air plasma has demonstrated its bactericidal and sporicidal potential in tests, according to European standard methods for sterilizing and disinfecting agents. Thereby, it was effective in the inactivation of conventional biological indicators as well as of endospores of *C. difficile*, a highly environmental resistant and fatal nosocomial pathogen. The synergy between various plasma species (such as ROS/RNS, electric field) is responsible for this effect. Furthermore, its microbicidal action is limited by the degree of surface contamination. High bacterial density or additional burden aggravate the access of gaseous plasma species and mitigate its chemical reactivity. Application at open condition further mitigated the microbicidal effect by side-diffusing species. For that reasons, SMD air plasma application is more attractive for the disinfection of pre-cleaned instruments in a closed volume rather than for surface disinfection. High ozone concentrations generated by plasma further suggest the operation in a closed chamber due to safety reasons. In addition, the oxidative nature of air plasma requires the use of inert device materials. This also implicates that air plasma, even it enables the treatment of heat-sensitive materials, can create complications, when chemical-sensitive surfaces are treated.

All in all, my work has improved the understanding about the decontaminating behavior of SMD air plasma. SMD air plasma has the potential due to its versatile properties to serve as an alternative to commonly used disinfecting or sterilizing agents and may contribute to the prevention of nosocomial infections in the future. Important will be to develop an up-scaled device, suitable for practical use, to solve

handling issues, to gain measurable additional effect compared to common methods and to validate its use in field studies.

4.11 Future perspectives

This work opens a new era in the research of SMD air plasma decontamination. Many starting points for follow-up research are already pointed out in various sections of the discussion.

One future objective will be to understand the radical chemistry step by step in a better way, in order to control and adjust the plasma chemistry specifically for an optimized decontaminating effect in the future. This includes the conduction of further plasma diagnostics, e.g. the determination of OH or NO radicals via spin-trapping followed by ESR spectroscopy, in combination with further kinetic studies, involving the treatment of fungal, mycobacterial and viral species on surfaces according to standards. Concerning the application, it is necessary to adjust the device set up to the needs of intended practical use and to evaluate and improve its actual applicability for the decontamination of more complex 3D objects. Furthermore, the investigation of various plasma-treated materials, e.g. from medical devices, will provide a better understanding, if and when undesired material alterations occur, which could lead to failure of function.

In the end, I would like to investigate the interaction between MO and plasma in more detail. Hence, I will continue to carry out confocal Raman imaging of plasma-treated bacterial endospores. This includes also the imaging of artificial peptidoglycan layer, a substantial cortex component in spores, and observing possible alterations in its chemical composition after plasma treatment. In addition, the photometric determination of the dipicolinic acid release from the spore core will clarify, if the plasma treatment causes leakages in the membranes and coats. Imaging of treated

spores by transmission electron microscopy will give some hints of morphological alterations in the structure of inner spore layers such as ruptures. Moreover, chromatographic investigations will reveal possible effects on DNA of treated spores. Sophisticated will also be single cell investigations as proposed for wet heat [183] that enables *in situ* measurements and treatments.

All the above future perspectives will further help to gain insight into the inactivation mechanism by unraveling the molecular mechanism of plasma treatment and its limitations, enabling its appropriate and alternative use in areas, where conventional decontaminating agents are not applicable.

5 ACKNOWLEDGMENTS

First of all, I want to thank Professor Gregor Morfill who supported me thoroughly, gave me freedom and his faith in my work at any time. Without his encouraging visions and energy, research in plasma medicine in such a great network would not have been possible. It was an honor to carry out my thesis in his group. I also would like to thank in particular Dr. Hans-Ulrich Schmidt, a great person and microbiologist, who has always been keen to discuss my project work, inspired me and motivated me with his ideas to stick to my research direction.

I also want to acknowledge my supervisor at the TUM Prof. Jürgen Schlegel and my mentor Prof. Claus Zimmer for their benevolent confidence in my work, Dr. Katrin Offe as the supportive coordinator of the Ph.D. program at TUM, and in general the TUM Graduate School.

I am also very grateful to the plasma medicine team at the MPE for their support throughout the whole time: From the scientific part Dr. Tetsuji Shimizu, Dr. Yang-Fang Li and Dr. Julia Zimmermann for their advices and for being available my questions, Dr. Roberto Monetti, Dr. Wolfram Bunk and Dr. Thomas Aschenbrenner for their efforts in SEM image data analysis of endospore morphologies, Dr. Mikhail Pustylnik for his time in sophisticated OES measurements, Dr. Satoshi Shimizu and Jin Jeon for good discussions, the student trainees Tanja Rosentreter and Andreas Oberauer and all others who were involved but I do not particularly mention here; from the non-scientific part the secretaries Angelika Langer and Birgit Boller, the technicians Katinka Hartmann and Bernd Steffes, Kurt Dittrich for his support in the use of the environmental chamber, the mechanical (Mr. Czempiel and coworkers), metal (Walter Schunn and coworkers), electric (Mr. Tarantik and coworkers) and polymer work shop (Franz Soller and coworkers), the drivers Toni Arturo and Erich

Rossa, and all administrative staff (Eva Kuhwald, Sylvia Goldbrunner, Wolfgang Karing, Mirko Grasemann, Mrs. Mayr-Ihbe, Tobias Baumann and coworkers) who were always a great support and who provided a great infrastructure for my project. My research project was funded solely by MPE and the research grant MTTA. Ext. 0002. Many thanks for a great atmosphere at MPE X6 building to my colleagues Pintu, Jayson, Philip, Jin, Guido, Thomas, Tanja, Arthur, Dong and Yang-Fang.

Furthermore, I want to thank Dr. Jürgen Gebel, Dr. Stefanie Gemein and Sylvia Koch (IHPH) for their contributions to the *Clostridium difficile* project; Toni Seis and Dr. Nicole Richter (Simicon GmbH) for their supportive communication regarding sterilization/disinfection; Prof. David Graves and Dr. Yukinori Sakiyama (UC Berkeley) for their kind help during my laboratory visit regarding the simulation of plasma-chemical reactions; Dr. Alexander Gigler (LMU), Dr. Melanie Kaliwoda (LMU) and Dr. Marek Janko (TU Darmstadt) for their support in confocal Raman microscopy imaging of bacterial endospores; Dr. Petra Rettberg and Simon Barczyk (DLR Bonn) for the microbiological insights into endospore culturing during my laboratory visit; Katja Rodewald (TUM) for sharing her expertise in SEM imaging of *E. faecium* and especially Dr. Martin Balden (IPP Garching) for his great expertise and support in SEM imaging of bacterial endospores. Overall, I want to thank all of them for the friendly cooperation. Moreover, I would like to express my great gratitude to Prof. Molly Shoichet (University of Toronto, Canada) and Prof. Olaf Hinrichsen (TUM) for their initial support in applying for the Ph.D. Program.

Last and most importantly, I would like to emphasize that all of this would not have been possible without the great support, patience and love of my parents and my whole family throughout my entire academic life; and in particular of my partner Maria

who shared with me every tough and good moment, always supported me the most and has made my life colorful. Ευχαριστώ!

6 REFERENCES

1. Mott-Smith HM. History of "Plasmas". Nature 1971; 233(5316):219.

2. Fridman A. Introduction to Theoretical and Applied Plasma Chemistry. Plasma Chemistry. New York: Cambridge University Press; 2008. p. 1-10.

3. Fridman A, Kennedy LA. Plasma Physics and Engineering. 1st ed. New York: Taylor & Francis; 2004.

4. Wagner H-E, Brandenburg R, Kozlov KV, Sonnenfeld A, Michel P, Behnke JF. The barrier discharge: basic properties and applications to surface treatment. Vacuum 2003; 71:417-36.

5. Fridman A, Gutsol A, Cho YI. Non-Thermal Atmospheric Pressure Plasma. Elsevier Academic Press. 2007:

6. Laroussi M, Kong MG, Morfill G, Stolz W, editors. Plasma Medicine. New York: Cambridge University Press; 2012.

7. Research TT. Available from: http://www.teslatechnologyresearch.com/model1.html.

8. Hoentsch M, von Woedtke T, Weltmann K-D, Nebe B. Time-dependent effects of low-temperature atmospheric-pressure argon plasma on epithelial cell attachment, viability and tight junction formation in vitro. Journal of Physics D: Applied Physics 2012; 45(2):025206.

9. Shimizu T, Steffes B, Pompl R, Jamitzky F, Bunk W, Ramrath K, Georgi M, Stolz W, Schmidt H-U, Urayama T, Fujii S, Morfill GE. Characterization of Microwave Plasma Torch for Decontamination. Plasma Processes and Polymers 2008; 5(6):577-82.

10. Kogelschatz U. Dielectric-barrier Discharges: Their History, Discharge Physics, and Industrial Applications. Plasma Chemistry and Plasma Processing 2003; 23(1):1-46.

11. Siemens W. Ueber die elektrostatische Induction und die Verzögerung des Stroms in Flaschendrähten. Poggendorff´s Ann Phys Chem; 102:66.

12. Fridman A. Plasma Chemistry. New York: Cambridge University Press; 2008.

13. Hautefeuille P, Chappuis J, editors. The search for gaseous compounds and the study of some ot their properties with the help of the spectroscope [De la recherche des composes gazeux et de !'etude de quelques-unes de leurs

proprietes a l'aide du spectroscope.] Translated from French. Proceedings of the Academy of Sciences; 1881; Paris.

14. Warburg E, Leithäuser G. About the analysis of nitrogen oxides by their absorption spectra in the ultrared [Über die Analyse der Stickoxyde durch ihre Absorptionsspektra im Ultrarot.] Translated from German. Annalen der Physik 1909; 28(4):313.

15. Warburg E. About the ozonation of oxygen by silent electric discharges [Über die Ozonisierung des Sauerstoffs durch stille elektrische Entladungen.] Translated from German. Annalen der Physik 1904; 318(3):464-76.

16. Warburg E. About the chemical effect of silent discharges. [Über die chemische Wirkung stiller Entladungen.] Translated from German. Zeitschrift für technische Physik 1925; 6(12):625-33.

17. Buss K. Electron-free discharge according to the measurement with the cathodic oscillograph [Die elektrodenlose Entladung nach Messung mit dem Kathodenoszillographen.] Tranlated from German. Archiv für Elektrotechnik 1932; 26(4):261-5.

18. Klemenc A, Hintenberger H, Höfer H. About the discharge process in an Siemens ozone apparatus [Über den Entladunsvorgang in einer Siemens-Ozonröhre.] Translated from German. Zeitschrift für Elektrochemie und angewandte physikalische Chemie 1937; 43(8):708-12.

19. Suzuki M. On the nature of chemical reaction in silent discharge. Proceedings of the Japan Academy 1950; 26(9):20-4.

20. Suzuki M, Naito Y. On the nature of the chemical reaction in silent electrical discharge. II. Proceedings of the Japan Academy 1952; 28(9):469-76.

21. Honda K, Naito Y. On the nature of silent electrical discharge. Journal of the Physical Society of Japan 1955; 10(11):1007-11.

22. Gobrecht H, Meinhardt O, Hein F. About the silent electrical discharge in ozonizers [Über die stille elektrische Entladung in Ozonisatoren.] Translated from German. Berichte der Bunsengesellschaft für physikalische Chemie 1964; 68(1):55-63.

23. Bagirov MA, Kurbanov MA, Shkilev AV. Study of Electrical Discharge in Air between Electrodes Covered by Dielectrics. Sov Phys Tech Phys [Zh Tekh Fiz] 1971; 16 [41](6):1011-21 [287-97].

24. Manley TC. The Electric Characteristics of the Ozonator Discharge Trans Electrochem Soc 1943; 84(1):83-96.

25. Becker H. About the extrapolation and calculation of the concentration and yield of ozone apparatus [Über die Extrapolation und Berechnung der Konzentration und Ausbeute von Ozonapparaten.] Translated from German. In: Harries CD, editor. Wissenschaftliche Veröffentlichungen aus dem Siemens-Konzern. Berlin: Springer-Verlag Berlin Heidelberg GmbH; 1922. p. 76-106.

26. Becker H. A simplified graphical presentation of the yield and concentration of ozone apparatus [Eine vereinfachte graphische Darstellung der Ausbeute und Konzentration bei Ozonapparaten.] Translated in German. In: Harries CD, editor. Wissenschaftliche Veröffentlichungen aus dem Siemens-Konzern. Berlin: Springer-Verlag Berlin Heidelberg GmbH; 1923. p. 243-7.

27. Otto M-P. The ozone and its applications [L'Ozone et ses applications.] Translated from French. Paris: Société française des électriciens; E. Chiron; 1929.

28. Kelly-Wintenberg K, Montie TC, Brickman C, Roth JR, Carr AK, Sorge K, Wadsworth LC, Tsai PPY. Room temperature sterilization of surfaces and fabrics with a One Atmosphere Uniform Glow Discharge Plasma. Journal of Industrial Microbiology & Biotechnology 1998; 20:69-74.

29. Fridman G, Peddinghaus M, Ayan H, Fridman A, Balasubramanian M, Gutsol A, Brooks A, Friedman G. Blood Coagulation and Living Tissue Sterilization by Floating-Electrode Dielectric Barrier Discharge in Air. Plasma Chemistry and Plasma Processing 2006; 26(4):425-42.

30. Eliasson B, Kogelschatz U. Modeling and applications of silent discharge plasmas IEEE Transactions on Plasma Science 1991; 19(2):309-23.

31. Eliasson B, Egli W, Kogelschatz U. Modeling Dielectric Barrier Discharge Chemistry. Pure and Applied Chemistry 1994; 66(6):1275-86.

32. Kogelschatz U. Filamentary, Patterned, and Diffuse Barrier Discharges. IEEE TRANSACTIONS ON PLASMA SCIENCE 2002; 30(4):1400-08.

33. Brandenburg R, Navratil Z, Jansky J, Stahel P, Trunec D, Wagner H-E. The transition between different modes of barrier discharges at atmospheric pressure Journal of Physics D: Applied Physics 2009; 42(8):085208.

34. Raether H. Development of the electron avalanche into the discharge channel [Die Entwicklung der Elektronenlawine in den Funkenkanal.] Translated from German. Zeitschrift für Physik 1939; 112(7-8):464-89.

35. Raether H. About the development of channel discharges [Zur Entwicklung von Kanalentladungen.] Translated from German. Archiv für Elektrotechnik 1940; 34(1):49-56.

36. Loeb LB, Meek JM. The Mechanism of Spark Discharge in Air at Atmospheric Pressure. Journal of Applied Physics 1940; 11:438-47.

37. Meek JM. A Theory of Spark Discharge. Physical Reviews 1940; 57(8):722-8.

38. Fridman A. Electric Discharges in Plasma Chemistry. Plasma Chemistry. New York: Cambridge University Press; 2008. p. 163.

39. Braun D, Küchler U, Pietsch G. Microdischarges in air-fed ozonizers. Journal of Physics D: Applied Physics 1991; 24(4):564-72.

40. Yoshida K, Tagashira H. Computer Simulation of Ozone Electrosynthesis in an N2/O2 Mixture-fed Ozonizer. Memoirs Kitami Institute of Technology 1986; 18(1):11-20.

41. Gibalov VI, Pietsch G. Dynamics of dielectric barrier discharges in different arrangements. Plasma Sources Sci Technol 2012; 21(2):1-35.

42. Eliasson B, Hirth M, Kogelschatz U. Ozone synthesis from oxygen in dielectric barrier discharges Journal of Physics D: Applied Physics 1987; 20:1421-37.

43. Herron JT, Green DS. Chemical Kinetics Database and Predictive Schemes for Nonthermal Humid Air Plasma Chemistry. Part II. Neutral Species Reactions. Plasma Chemistry and Plasma Processing 2001; 21(3):459-81.

44. Sieck LW, Herron JT, Green DS. Chemical Kinetics Database and Predictive Schemes for Humid Air Plasma Chemistry. Part I: Positive Ion–Molecule Reactions. Plasma Chemistry and Plasma Processing 2000; 20(2):235-57.

45. Capitelli M, Ferreira CM, Gordiets BF, Osipov AI. Plasma Kinetics in Atmospheric Gases. Heidelberg: Springer Verlag; 2000.

46. Becker KH, Kogelschatz U, Schoenbach KH, Barker RJ, editors. Non-Equilibrium Air Plasmas at Atmospheric Pressure. London: Insitute of Physics Publishing, Taylor & Travis, CRC Press; 2004.

47. Sakiyama Y, Graves DB, Chang HW, Shimizu T, Morfill GE. Plasma chemistry model of surface microdischarge in humid air and dynamics of reactive neutral species. J Phys D Appl Phys 2012; 45(42).

48. Samoilovich VG, Gibalov V, Kozlov KV, editors. Physical Chemistry of the Barrier Discharge. Düsseldorf: DVS-Verlag; 1997.

49. Kogelschatz U, Eliasson B, Hirth M. Ozone Generation from Oxygen and Air: Discharge Physics and Reaction Mechanisms. Ozone: Science & Engineering 1988; 10(4):367-78.

50. von Sonntag C, von Gunten U. Chemistry of Ozone in Water and Wastewater Treatment. London: IWA Publishing; 2012.

51. Eliasson B, Kogelschatz U. Electron impact dissociation in oxygen. Journal of Physics B: Atomic and Molecular Physics 1986; 19(8):1241-7.

52. Yagi S, Tanaka M. Mechanism of ozone generation in air-fed ozonisers. Journal of Physics D: Applied Physics 1979; 12(9):1509-20.

53. Kogelschatz U, Baessler P. Determination of Nitrous Oxide and Dinitrogen Pentoxide Concentrations in the Output of Air-Fed Ozone Generators of High Power Density. Ozone: Science & Engineering 1987; 9(3):195-206.

54. Stoffels E, Flikweert AJ, Stoffels WW, Kroesen GMW. Plasma needle: a non-destructive atmospheric plasma source for fine surface treatment of (bio)materials. Plasma Sources Sci Technol 2002; 11:383-8.

55. Kramer A, Hübner N-O, Assadian O, Below H, Bender C, Benkhai H, Bröker B, Ekkernkamp A, Eisenbeiß W, Hammann A, Hartmann B, Heidecke C-D, Hinz P, Koban I, Koch S, Kocher T, Lademann J, Lademann O, Lerch M, Maier S, Matthes R, Müller G, Partecke I, Rändler C, Weltmann K-D, Zygmunt M. Chances and perspectives of the plasma medicine by use of Tissue Tolerable Plasma (TTP). GMS Krankenhaushygiene Interdisziplinär 2009; 4(2):1-15.

56. Kong MG, Kroesen G, Morfill GE, Nosenko T, Shimizu T, van Dijk J, Zimmermann JL. Plasma medicine: an introductory review. New Journal of Physics 2009; 11:115012.

57. Demple B, Harrison L. Repair of oxidative damage to DNA: Enzymology and Biology. Annu Rev Biochem 1994; 63:915-48.

58. Graves DB. The emerging role of reactive oxygen and nitrogen species in redox biology and some implications for plasma applications to medicine and biology. Journal of Physics D: Applied Physics 2012; 45:263001 (42pp).

59. Stoffels E. ”Tissue Processing” with Atmospheric Plasmas. Contrib Plasma Phys 2007; 47(1-2):40-8.

60. Zhang XH, Li MJ, Zhou RL, Feng KC, Yang SZ. Ablation of liver cancer cells in vitro by a plasma needle. Applied Physical Letters 2008; 93:021502.

61. Keidar M, Walk R, Shashurin A, Srinivasan P, Sandler A, Dasgupta S, Ravi R, Guerrero-Preston R, Trink B. Cold plasma selectivity and the possibility of a paradigm shift in cancer therapy. Br J Cancer 2011; 105(9):1295-301.

62. Köritzer J, Boxhammer V, Schäfer A, Shimizu T, Klämpfl TG, Li YF, Welz C, Schwenk-Zieger S, Morfill GE, Zimmermann JL, Schlegel J. Restoration of sensitivity in chemo-resistant glioma cells by cold atmospheric plasma. PLoS One 2013; 8(5):e64498.

63. Arndt S, Wacker E, Li YF, Shimizu T, Thomas HM, Morfill GE, Karrer S, Zimmermann JL, Bosserhoff AK. Cold atmospheric plasma, a new strategy to induce senescence in melanoma cells. Exp Dermatol 2013; 22(4):284-9.

64. Heinlin J, Isbary G, Stolz W, Morfill G, Landthaler M, Shimizu T, Steffes B, Nosenko T, Zimmermann J, Karrer S. Plasma applications in medicine with a special focus on dermatology. Journal of the European Academy of Dermatology and Venereology : JEADV 2011; 25(1):1-11.

65. Lademann J, Kramer A, Richter H, Patzelt A, Meinke MC, Roewert-Huber J, Czaika V, Weltmann KD, Hartmann B, Koch S. Antisepsis of the follicular reservoir by treatment with tissue-tolerable plasma (TTP). Laser Phys Lett 2011; 8(4):313-7.

66. Kramer A, Hubner NO, Weltmann KD, Lademann J, Ekkernkamp A, Hinz P, Assadian O. Polypragmasia in the therapy of infected wounds - conclusions drawn from the perspectives of low temperature plasma technology for plasma wound therapy. GMS Krankenhaushygiene Interdisziplinär 2008; 3(1):Doc13.

67. Isbary G, Heinlin J, Shimizu T, Zimmermann JL, Morfill G, Schmidt HU, Monetti R, Steffes B, Bunk W, Li Y, Klämpfl T, Karrer S, Landthaler M, Stolz W. Successful and safe use of 2 min cold atmospheric argon plasma in chronic wounds: results of a randomized controlled trial. Brit J Dermatol 2012; 167(2):404-10.

68. Isbary G, Morfill GE, Schmidt HU, Georgi M, Ramrath K, Heinlin J, Karrer S, Landthaler M, Shimizu T, Steffes B, Bunk W, Monetti R, Zimmermann JL, Pompl R, Stolz W. A first prospective randomized controlled trial to decrease bacterial load using cold atmospheric argon plasma on chronic wounds in patients. The British journal of dermatology 2010; 163(1):78-82.

69. Isbary G, Stolz W, Shimizu T, Monetti R, Bunk W, Schmidt HU, Morfill GE, Klämpfl TG, Steffes B, Thomas HM, Heinlin J, Karrer S, Landthaler M, Zimmermann JL. Cold atmospheric argon plasma treatment may accelerate wound healing in chronic wounds: Results of an open retrospective randomized controlled study in vivo. Clinical Plasma Medicine 2013; In press - corrected proof.

70. Fridman A, Friedman G. Plasma Medicine. Philadelphia: John Wiley & Sons, Ltd.; 2013.

71. ECDC. Point prevalence survey of healthcare associated infections and antimicrobial use in European acute care hospitals. Stockholm: European Centre for Disease Prevention and Control 2013.

72. ECDC. Annual epidemiological report on communicable diseases in Europe. Stockholm: European Centre for Disease Prevention and Control (ECDC) 2010.

73. Pollack A. Rising Threat of Infections Unfazed by Antibiotics. New York Times. 2010.

74. CDC. Puplic Health Report. Centers for Disease Control and Prevention (CDC) 2007.

75. Coello R, Glenister H, Fereres J, Bartlett C, Leigh D, Sedgwick J, Cooke EM. The cost of infection in surgical patients: a case-control study. J Hosp Infect 1993; 25(4):239-50.

76. Cosgrove SE, Carmeli Y. The Impact of Antimicrobial Resistance on Health and Economic Outcome. Clinical Infectious Diseases 2003; 36(11):1433-7.

77. Leape LL, Brennan TA, Laird N, Lawthers AG, Localio AR, Barnes BA, Hebert L, Newhouse JP, Weiler PC, Hiatt H. The nature of adverse events in hospitalized patients. Results of the Harvard Medical Practice Study II. N Engl J Med 1991; 324(6):377-84.

78. Scott RD. The direct medical costs of healthcare-associated infections in U.S. hospitals and the benefits of prevention. Centers for Disease Control and Prevention 2009.

79. Bauer MP, Notermans DW, van Benthem BH, Brazier JS, Wilcox MH, Rupnik M, Monnet DL, van Dissel JT, Kuijper EJ. *Clostridium difficile* infection in Europe: a hospital-based survey. Lancet 2011; 377(9759):63-73.

80. Kuijper EJ, Coignard B, Tull P. Emergence of *Clostridium difficile*-associated disease in North America and Europe. Clin Microbiol Infect 2006; 12 Suppl 6:2-18.

81. Warny M, Pepin J, Fang A, Killgore G, Thompson A, Brazier J, Frost E, McDonald LC. Toxin production by an emerging strain of *Clostridium difficile* associated with outbreaks of severe disease in North America and Europe. Lancet 2005; 366(9491):1079-84.

82. McDonald LC, Killgore GE, Thompson A, Owens RC, Jr., Kazakova SV, Sambol SP, Johnson S, Gerding DN. An epidemic, toxin gene-variant strain of *Clostridium difficile*. N Engl J Med 2005; 353(23):2433-41.

83. Leggett MJ, McDonnell G, Denyer SP, Setlow P, Maillard JY. Bacterial spore structures and their protective role in biocide resistance. J Appl Microbiol 2012; 113(3):485-98.

84. Henriques AO, Moran CP, Jr. Structure, assembly, and function of the spore surface layers. Annu Rev Microbiol 2007; 61:555-88.

85. McFarland LV, Mulligan ME, Kwok RY, Stamm WE. Nosocomial acquisition of *Clostridium difficile* infection. N Engl J Med 1989; 320(4):204-10.

86. Kramer A, Schwebke I, Kampf G. How long do nosocomial pathogens persist on inanimate surfaces? A systematic review. BMC Infect Dis 2006; 6:130.

87. Speight S, Moy A, Macken S, Chitnis R, Hoffman PN, Davies A, Bennett A, Walker JT. Evaluation of the sporicidal activity of different chemical disinfectants used in hospitals against *Clostridium difficile*. J Hosp Infect 2011; 79(1):18-22.

88. Fawley WN, Underwood S, Freeman J, Baines SD, Saxton K, Stephenson K, Owens RC, Jr., Wilcox MH. Efficacy of hospital cleaning agents and germicides against epidemic *Clostridium difficile* strains. Infect Control Hosp Epidemiol 2007; 28(8):920-5.

89. Vonberg RP, Kuijper EJ, Wilcox MH, Barbut F, Tull P, Gastmeier P, van den Broek PJ, Colville A, Coignard B, Daha T, Debast S, Duerden BI, van den Hof S, van der Kooi T, Maarleveld HJ, Nagy E, Notermans DW, O'Driscoll J, Patel B, Stone S, Wiuff C. Infection control measures to limit the spread of *Clostridium difficile*. Clin Microbiol Infect 2008; 14 Suppl 5:2-20.

90. Hota B. Contamination, disinfection, and cross-colonization: are hospital surfaces reservoirs for nosocomial infection? Clin Infect Dis 2004; 39(8):1182-9.

91. Gebel J, Exner M, French GL, Chartier Y, Christiansen B, Gemein S, Goroncy-Bermes P, Hartemann P, Heudorf U, Kramer A, Maillard JY, Oltmanns P, Rotter M, Sonntag H-G. The role of surface disinfection in infection prevention. GMS Hygiene and Infection Control 2013; 8(1):Doc10.

92. Sehulster L, Chinn RY. Guidelines for environmental infection control in health-care facilities. Recommendations of CDC and the Healthcare Infection Control Practices Advisory Committee (HICPAC). MMWR Recomm Rep 2003; 52(RR-10):1-42.

93. Rutala WA, Weber DJ, HICPAC. Guideline for Disinfection and Sterilization in Healthcare Facilities. CDC. 2008:

94. Holy CE, Cheng C, Davies JE, Shoichet MS. Optimizing the sterilization of PLGA scaffolds for use in tissue engineering. Biomaterials 2001; 22(1):25-31.

95. Lerouge S, Tabrizian M, Wertheimer MR, Marchand R, Yahia L. Safety of plasma-based sterilization: surface modifications of polymeric medical devices induced by Sterrad and Plazlyte processes. Bio-medical materials and engineering 2002; 12(1):3-13.

96. Matthews IP, Gibson C, Samuel AH. Sterilisation of Implantable Devices. Clinical Materials 1994; 15(3):191-215.

97. Athanasiou KA, Niederauer GG, Agrawal CM. Sterilization, toxicity, biocompatibility and clinical applications of polylactic acid/polyglycolic acid copolymers. Biomaterials 1996; 17(2):93-102.

98. Feldman LA, Hui HK. Compatibility of Medical Devices and Materials with Low-Temperature Hydrogen Peroxide Gas Plasma. Medical Device & Diagnostic Industry. 1997:57-62.

99. EPA US. Health Effects Assessment Summary Tables (HEAST). Washington D.C.: U.S. Environmental Protection Agency 1997.

100. Angerer J, Bader M, Kramer A. Ambient and biochemical effect monitoring of workers exposed to ethylene oxide. International archives of occupational and environmental health 1998; 71(1):14-8.

101. Davies A, Pottage T, Bennett A, Walker J. Gaseous and air decontamination technologies for *Clostridium difficile* in the healthcare environment. J Hosp Infect 2011; 77(3):199-203.

102. Laroussi M. Sterilization of Contaminated Matter with an Atmospheric Pressure Plasma. IEEE Transactions on Plasma Science 1996; 24(3):1188-91.

103. Ehlbeck J, Schnabel U, Polak M, Winter J, von Wodtke T, Brandenburg R, von Hagen T, Weltmann K-D. Low temperature atmospheric pressure plasma sources for microbial decontamination. Journal of Physics D: Applied Physics 2011; 44:013002.

104. Muranyi P, Wunderlich J, Heise M. Sterilization efficiency of a cascaded dielectric barrier discharge. J Appl Microbiol 2007; 103:1535-44.

105. Gadri RB, Roth JR, Montie TC, Kelly-Wintenberg K, Tsai PP-Y, Helfritch DJ, Feldman P, Sherman DM, Karakaya F, Chen Z, Team UPS. Sterilization and plasma processing of room temperature surfaces with a one atmosphere

uniform glow discharge plasma (OAUGDP). Surface and Coatings Technology 2000; 131:528-42.

106. Cooper M, Fridman G, Staack D, Gutsol A, Vasilets VN, Anandan S, Cho YI, Fridman A, Tsapin A. Decontamination of Surfaces From Extremophile Organisms Using Nonthermal Atmospheric-Pressure Plasmas. IEEE Transactions on Plasma Science 2009; 37(6):866-71.

107. Shimizu S, Barczyk S, Rettberg P, Shimizu T, Klämpfl TG, Zimmermann JL, Hoeschen T, Linsmeier C, Weber P, Morfill GE, Thomas HM. Cold Atmospheric Plasma – a New Technology for Spacecraft Component Decontamination. Planetary and Space Science 2013; 90:60-71.

108. Von Woedtke T, Kramer A, Weltmann KD. Plasma Sterilization: What are the Conditions to Meet this Claim? Plasma Processes and Polymers 2008; 5:534-9.

109. Gebel J, Kirsch-Altena A, Exner M, Schwebke I. Prüfung der Wirksamkeit chemischer Desinfektionsmittel. In: Kramer A, Assadian O, editors. Wallhäusers Praxis der Sterilisation, Desinfektion, Antiseptik und Konservierung. 6 ed. Stuttgart, New York: Georg Thieme Verlag KG; 2008. p. 601-9.

110. Gemein S. Etablierung eines Testverfahrens zur Prüfung sporizider Flächendesinfektionsmittel mit dem Schwerpunkt *Clostridium difficile* Ribotyp 027. Bonn: University Bonn; 2011.

111. Tseng S, Abramzon N, Jackson JO, Lin WJ. Gas discharge plasmas are effective in inactivating Bacillus and Clostridium spores. Appl Microbiol Biotechnol 2012; 93(6):2563-70.

112. Morfill GE, Shimizu T, Steffes B, Schmidt H-U. Nosocomial infections - a new approach towards preventive medicine using plasmas. New Journal of Physics 2009; 11:115019.

113. Choi JH, Han I, Baik HK, Lee MH, Han D-W, Park J-C, Lee I-S, Song KM, Lim YS. Analysis of sterilization effect by pulsed dielectric barrier discharge. Journal of Electrostatics 2006; 64(1):17-22.

114. Leipold F, Kusano Y, Hansen F, Jacobsen T. Decontamination of a rotating cutting tool during operation by means of atmospheric pressure plasmas. Food Control 2010; 21(8):1194-98.

115. Oehmigen K, Hähnel M, Brandenburg R, Wilke C, Weltmann K-D, von Woedtke T. The Role of Acidification for Antimicrobial Activity of Atmospheric Pressure Plasma in Liquids. Plasma Processes and Polymers 2010; 7(3-4):250-7.

116. Joshi SG, Paff M, Friedman G, Fridman G, Firdman A, Brooks AD. Control of methicillin-resistant *Staphylococcus aureus* in planktonic form and biofilms: A biocidal efficacy study of nonthermal dielectric-barrier discharge plasma. Am J Infect Control 2010; 38(4):293-301.

117. Joshi SG, Cooper M, Yost A, Paff M, Ercan UK, Fridman G, Friedman G, Fridman A, Brooks AD. Nonthermal Dielectric-Barrier Discharge Plasma-Induced Inactivation Involves Oxidative DNA Damage and Membrane Lipid Peroxidation in *Escherichia coli*. Antimicrobial Agents and Chemotherapy 2011; 55(3):1053-62.

118. Mastanaiah N, Johnson JA, Roy S. Effect of Dielectric and Liquid on Plasma Sterilization Using Dielectric Barrier Discharge Plasma. PLoS One 2013; 8(8):e70840.

119. Montie TC, Kelly-Wintenberg K, Roth JR. An overview of research using the one atmosphere uniform glow discharge plasma (OAUGDP) for sterilization of surfaces and materials. IEEE Transactions on Plasma Science 2000; 28(1):41-50.

120. Schwabedissen A, Lacinski P, Chen X, Engemann J. PlasmaLabel – a New Method to Disinfect Goods Inside a Closed Package Using Dielectric Barrier Discharges. Contributions to Plasma Physics 2007; 47(7):551-8.

121. Eto H, Ono Y, Ogino A, Nagatsu M. Low-temperature sterilization of wrapped materials using flexible sheet-type dielectric barrier discharge. Applied Physical Letters 2008; 93:221502.

122. Eto H, Ono Y, Ogino A, Nagatsu M. Low-Temperature Internal Sterilization of Medical Plastic Tubes Using a Linear Dielectric Barrier Discharge. Plasma Processes and Polymers 2008; 5:269-74.

123. Hähnel M, Von Woedtke T, Weltmann KD. Influence of the Air Humidity on the Reduction of Bacillus Spores in a Defined Environment at Atmospheric Pressure Using a Dielectric Barrier Surface Discharge. Plasma Processes and Polymers 2010; 7(3-4):244-9.

124. Cotter JJ, Maguire P, Soberon F, Daniels S, O`Gara J, Casey E. Disinfection of meticillin-resistant *Staphylococcus aureus* and *Staphylococcus epidermidis* biofilms using a remote non-thermal gas plasma. Journal of Hospital Infection 2011; 78(3):204-7.

125. Zimmermann JL, Dumler K, Shimizu T, Morfill GE, Wolf A, Boxhammer V, Schlegel J, Gansbacher B, Anton M. Effects of cold atmospheric plasmas on adenoviruses in solution. J Phys D Appl Phys 2011; 44(50).

126. Shimizu T, Zimmermann JL, Morfill G. The bactericidal effect of surface micro-discharge plasma under different ambient conditions. New Journal of Physics 2011; 13:023026.

127. Boxhammer V, Morfill GE, Jokipii JR, Shimizu T, Klämpfl T, Li YF, Koritzer J, Schlegel J, Zimmermann JL. Bactericidal action of cold atmospheric plasma in solution. New Journal of Physics 2012; 14.

128. Maisch T, Shimizu T, Li Y-F, Heinlin J, Karrer S, Morfill GE, Zimmermann JL. Decolonisation of MRSA, *S. aureus* and *E. coli* by atmospheric plasma using a porcine skin model *in vitro* PLoS One 2012; 7(4):e34610.

129. Maisch T, Shimizu T, Mitra A, Heinlin J, Karrer S, Li Y-F, Morfill G, Zimmermann JL. Contact-free cold atmospheric plasma treatment of *Deinococcus radiodurans*. Journal of industrial microbiology & biotechnology 2012; 39(9):1367-75.

130. Maisch T, Shimizu T, Isbary G, Heinlin J, Karrer S, Klämpfl TG, Li Y-F, Morfill GE, Zimmermann JL. Contact-free inactivation of *Candida albicans* biofilm by Cold-Atmospheric Air Plasma. Journal of Applied and Environmental Microbiology 2012; 78(12):4242-7.

131. Klämpfl TG, Isbary G, Shimizu T, Li YF, Zimmermann JL, Stolz W, Schlegel J, Morfill GE, Schmidt HU. Cold atmospheric air plasma sterilization against spores and other microorganisms of clinical interest. Applied and Environmental Microbiology 2012; 78(15):5077-82.

132. Mitra A, Li Y-F, Klämpfl TG, Shimizu T, Jeon J, Morfill GE, Zimmermann JL. Inactivation of surface borne microorganisms and increased germination of seed specimen by Cold Atmospheric Plasma (CAP). Food and Bioprocess Technology 2013.

133. Pavlovich MJ, Chen Z, Sakiyama Y, Clark DS, Graves DB. Effect of Discharge Parameters and Surface Characteristics on Ambient-Gas Plasma Disinfection. Plasma Processes and Polymers 2013; 10:69 - 76.

134. Pavlovich MJ, Chang H-W, Sakiyama Y, Clark DS, Graves DB. Ozone correlates with antibacterial effects from indirect air dielectric barrier discharge treatment of water. Journal of Physics D: Applied Physics 2013; 46:145202 (10pp).

135. DIN EN ISO14937. Sterilization of health care products. General requirements for characterization of a sterilizing agent and the development, validation and routine control of a sterilization process for medical devices. German Version EN ISO 14937:2009.

136. DIN EN 14885. Chemical disinfectants and antiseptics - Application of European Standards for chemical disinfectants and antiseptics. German version EN 14885:2006.

137. Pearse RWB, Gaydon AG. The identification of molecular spectra. 4th ed. London: John Wiley & Sons, Inc. New York; 1976.

138. Molina LT, Molina MJ. Absolute absorption cross sections of ozone in the 185- to 350-nm wavelength range. Jorunal of Geophysical Research Atmospheres 1986; 91(D13):14501-08.

139. DIN EN ISO 11737-1. Sterilization of medical devices - Microbiological methods - Part 1: Determination of a population of microorganisms on products. German version EN ISO 11737-1:2006 + AC:2009.

140. Rutala WA. Principles of Disinfecting Patient-Care Items. Disinfection, Sterilization and Antiseptics in Health Care: Polyscience Publishers; 1998. p. 133-49.

141. DIN EN 12353. Chemical disinfectants and antiseptics - Preservation of test organisms used for the determination of bactericidal (including Legionella), mycobactericidal, sporicidal, fungicidal and virucidal (including bacteriophages) activity. German version EN 12353:2013.

142. DIN EN 13704. Chemical disinfectants - Quantitative suspension test for the evaluation of sporicidal activity of chemical desinfectants used in food, industrial, domestic and institutional areas - Test method and requirements (phase 2/step 1). German version EN 13704:2002.

143. CEN. N 783 WI Phase2-Step1 anaerobic spores. CEN TC 216. 2013: 1-52.

144. DIN EN 14561. Chemical disinfectants and antiseptics - Quantitative carrier test for the evaluation of bactericidal activity for instruments used in the medical area - Test method and requirements (phase 2, step 2). German version EN 14561:2006.

145. IHPH. SOP 112: Enrichment B. subtilis spores modified from Schaeffer - testing disinfecting agents. Institute for Hygiene and Public Health. 2004: 1-4.

146. Exner M, Vacata V, Hornei B, Dietlein E, Gebel J. Household cleaning and surface disinfection: new insights and strategies. J Hosp Infect 2004; 56 Suppl 2:S70-5.

147. DIN EN 16615:2013-06. Chemical disinfectants and antiseptics - Quantitative test method for the evaluation of bactericidal and yeasticidal activity on non-porous surfaces with mechanical action employing wipes in the medical area

(4-field test) - Test method and requirements (phase 2, step 2). German version prEN 16615:2013.

148. Gebel J, Exner M. Überprüfung der Wirksamkeit der Kombination von einem spezifizierten Wischtuch und einem Desinfektionsmittel im praxisnahen 4-Felder-Test. Hyg Med 2013; 38(6):252-6.

149. DIN 10113-1. Determination of surface colony count on fitment and utensils in foodareas - Part 1: Quantitative swab method. DIN 10113-1:1997-07.

150. DIN EN ISO 18472. Sterilization of health care products - Biological and chemical indicators - Test equipment. German version EN ISO 18472:2006.

151. Li Y-F, Shimizu T, Zimmermann JL, Morfill GE. Cold atmospheric plasma for surface disinfection. Plasma Processes and Polymers 2011; 8.

152. Morfill GE, Kong MG, Zimmermann JL. Focus on Plasma Medicine. New Journal of Physics 2009; 11:115011 (8pp).

153. Ayan H, Fridman G, Gutsol A, Vasilets VN, Fridman A, Friedman G. Nanosecond-Pulsed Uniform Dielectric-Barrier Discharge. IEEE Transactions on Plasma Science 2008; 36(2):504-8.

154. Isbary G, Köritzer J, Mitra A, Li Y-F, Shimizu T, Schroeder J, Schlegel J, Morfill GE, Stolz W, Zimmermann JL. *Ex vivo* human skin experiments for the evaluation of safety of new cold atmospheric plasma devices. Clinical Plasma Medicine 2013; 1(1):36-44.

155. Laroussi M, Leipold F. Evaluation of the roles of reactive species, heat, and UV radiation in the inactivation of bacterial cells by air plasmas at atmospheric pressure. International Journal of Mass Spectrometry 2004; 233:81-6.

156. Burleson GR, Murray TM, Pollard M. Inactivation of Viruses and Bacteria by Ozone, With and Without Sonication. Applied and Environmental Microbiology 1975; 29(3):340-4.

157. Victorin K. Review of the genotoxicity of ozone. Mutation Research/Reviews in Genetic Toxicology 1992; 277(3):221-38.

158. Menzel DB. Ozone: an overview of its toxicity in man and animals. J Toxicol Environ Health 1984; 13(2-3):183-204.

159. OSHA. Ozone. Occupational Safety & Health Organization; 2012; Available from: https://www.osha.gov/dts/chemicalsampling/data/CH_259300.html.

160. NIOSH. NIOSH Pocket Guide To Chemical Hazards. National Institute for Occupational Safety and Health. 2007:

161. Shimizu T, Sakiyama Y, Graves DB, Zimmermann JL, Morfill GE. The dynamics of ozone generation and mode transition in air surface micro-discharge plasma at atmospheric pressure. New Journal of Physics 2012; 14.

162. Muranyi P, Wunderlich J, Heise M. Influence of relative gas humidity on the inactivation efficiency of a low temperature gas plasma. J Appl Microbiol 2008; 104:1659-66.

163. Zhao G, Zhu A, Wu J, Liu Z, Xu Y. Mearurement of OH Radicals in Dielectric Barrier Discharge Plasmas by Cavity Ring-Down Spectroscopy. Plasma Science and Technology 2010; 12(2):166-71.

164. Kudrle V, Vasina P, Talsky A, Mrazkova M, Stec O, Janca J. Plasma diagnostics using electron paramagnetic resonance. Journal of Physics D: Applied Physics 2010; 43:13pp.

165. Kozlov KV, Wagner H-E, Brandenburg R, Michel P. Spatio-temporally resolved spectroscopic diagnostics of the barrier discharge in air at atmospheric pressure. Journal of Physics D: Applied Physics 2001; 34(21):3164.

166. Bruggeman P, Walsh JL, Schram DC, Leys C, Kong MG. Time dependent optical emission spectroscopy of sub-microsecond pulsed plasmas in air with water cathode. Plasma Sources Sci Technol 2009; 18(4):045023.

167. Stancu GD, Kaddouri F, Lacoste DA, Laux CO. Atmospheric pressure plasma diagnostics by OES, CRDS and TALIF. Journal of Physics D: Applied Physics 2010; 43:124002.

168. Lukas C, Spaan M, Schulz-von der Gathen V, Thomson M, Wegst R, Döbele HF, Neiger M. Dielectric Barrier Discharges with Steep Voltage Rise: Mapping of Atomic Nitrogen in Single Filaments Measured by Laser-Induced Fluorescence Spectroscopy. Plasma Sources Sci Technol 2001; 10:445-50.

169. Niemi K, Schulz-von der Gathen V, Döbele HF. Absolute Calibration of Atomic Density Measurements by Laser-Induced Fluorescence Spectroscopy with Two-Photon Excitation. Journal of Physics D: Applied Physics 2001; 34:2330-5.

170. Zimmermann JL, Shimizu T, Schmidt HU, Li Y-F, Morfill GE, Isbary G. Test for bacterial resistance build-up against plasma treatment New Journal of Physics 2012; 14:073037.

171. Leduc M, Guay D, Leask RL, Coulombe S. Cell permeabilization using a non-thermal plasma. New Journal of Physics 2009; 11:115021.

172. Bielski BHJ, Arudi RL, Sutherland MW. A study of the reactivity of perihydroxy radical/superoxide ion with unsaturated fatty acids. Journal of Biological Chemistry 1983; 258:4759-61.

173. Pompl R, Jamitzky F, Shimizu T, Steffes B, Bunk W, Schmidt H-U, Georgi M, Ramrath K, Stolz W, Stark RW, Urayama T, Fujii S, Morfill GE. The effect of low-temperature plasma on bacteria as observed by repeated AFM imaging. New Journal of Physics 2009; 11:115023.

174. Setlow P. Spores of Bacillus subtilis: their resistance to and killing by radiation, heat and chemicals. J Appl Microbiol 2006; 101:514-25.

175. Setlow P. I will survive: DNA protection in bacterial spores. TRENDS in Microbiology 2007; 15(4):172-80.

176. Mahfoudh A, Poncin-Épaillard F, Moisan M, Barbeau J. Effect of dry-ozone exposure on different polymer surfaces and their resulting biocidal action on sporulated bacteria. Surface Science 2010; 604:1487-93.

177. Mahfoudh A, Barbeau J, Moisan M, Leduc A, Segúin J. Biocidal action of ozone-treated polystyrene surfaces on vegetative and sporulated bacteria. Applied Surface Science 2009; 256:3063-72.

178. Stapelmann K, Fiebrandt M, Raguse M, Awakowicz P, Reitz G, Möller R. Utilization of Low-Pressure Plasma to Inactivate Bacterial Spores on Stainless Steel Screws. Astrobiology 2013; 13(7):597-606.

179. Ishizaki K, Shinriki N, Matsuyama H. Inactivation of Bacillus spores by gaseous ozone. J Appl Bacteriol 1986; 60(1):67-72.

180. Aydogan A, Gurol MD. Application of gaseous ozone for inactivation of *Bacillus subtilis* spores. J Air Waste Manag Assoc 2006; 56(2):179-85.

181. Yardimci O, Setlow P. Plasma Sterilization: Opportunities and Microbial Assessment Strategies in Medical Device Manufacturing. IEEE Transactions on Plasma Science 2010; 38(4):973-81.

182. Cortezzo DE, Koziol-Dube K, Setlow B, Setlow P. Treatment with oxidizing agents damages the inner membrane of spores of *Bacillus subtilis* and sensitizes spores to subsequent stress. J Appl Microbiol 2004; 97:838-52.

183. Kong L, Zhang P, Wang G, Yu J, Setlow P, Li Y-q. Characterization of bacterial spore germination using phase-contrast and fluorescence

microscopy, Raman spectroscopy and optical tweezers. NATURE PROTOCOLS 2011; 6(5):625-39.

184. Zhang P, Kong L, Wang G, Setlow P, Li Y-q. Monitoring the Wet-Heat Inactivation Dynamics of Single Spores of Bacillus Species by Using Raman tweezers, Differential Interference Contrast Microscopy, and Nucleic Acid Dye Fluorescence Microscopy. Journal of Applied and Environmental Microbiology 2011; 77(14):4754-69.

185. Mahfoudh A, Moisan M, Segúin J, Barbeau J, Kabouzi Y, Kéroack D. Inactivation of Vegetative and Sporulated Bacteria by Dry Gaseous Ozone. Ozone: Science & Engineering 2010; (32):180-98.

186. Block C. The effect of Perasafe and sodium dichloroisocyanurate (NaDCC) against spores of *Clostridium difficile* and *Bacillus atrophaeus* on stainless steel and polyvinyl chloride surfaces. J Hosp Infect 2004; 57(2):144-8.

187. Barbut F, Menuet D, Verachten M, Girou E. Comparison of the efficacy of a hydrogen peroxide dry-mist disinfection system and sodium hypochlorite solution for eradication of Clostridium difficile spores. Infect Control Hosp Epidemiol 2009; 30(6):507-14.

188. Perez J, Springthorpe VS, Sattar SA. Activity of selected oxidizing microbicides against the spores of *Clostridium difficile*: relevance to environmental control. Am J Infect Control 2005; 33(6):320-5.

189. Maillard JY. Innate resistance to sporicides and potential failure to decontaminate. J Hosp Infect 2011; 77(3):204-9.

190. Shenton MJ, Lovell-Hoare MC, Stevens GC. Adhesion enhancement of polymer surfaces by atmospheric plasma treatment Journal of Physics D: Applied Physics 2001; 34(18):2754.

191. Block C, Robenshtok E, Simhon A, Shapiro M. Evaluation of chlorhexidine and povidone iodine activity against methicillin-resistant *Staphylococcus aureus* and vancomycin-resistant *Enterococcus faecalis* using a surface test. Journal of Hospital Infection 2000; 46(2):147-52.

192. Pottage T, Macken S, Walker JT, Bennett A. Meticillin-resistant *Staphylococcus aureus* is more resistant to vaporized hydrogen peroxide than commercial *Geobacillus stearothermophilus* biological indicators. Journal of Hospital Infection 2012; 80(1):41-5.

193. Finnegan M, Linley E, Denyer SP, McDonnell G, Simons C, Maillard JY. Mode of action of hydrogen peroxide and other oxidizing agents: differences between liquid and gas forms. J Antimicrob Chemother 2010; 65(10):2108-15.

194. Khadre MA, Yousef AE. Sporicidal action of ozone and hydrogen peroxide: a comparative study. Int J Food Microbiol 2001; 71(2-3):131-8.

195. Otter JA, Yezli S, French GL. Impact of the suspending medium on susceptibility of meticillin-resistant *Staphylococcus aureus* to hydrogen peroxide vapour decontamination. J Hosp Infect 2012; 82(3):213-5.

196. Springthorpe VS, Sattar SA. Carrier tests to assess microbicidal activities of chemical disinfectants for use on medical devices and environmental surfaces. J AOAC Int 2005; 88(1):182-201.

197. Sattar SA. Promises and pitfalls of recent advances in chemical means of preventing the spread of nosocomial infections by environmental surfaces. Am J Infect Control 2010; 38(5 Suppl 1):S34-40.

198. Welz C, Becker S, Li Y-F, Shimizu T, Jeon J, Schwenk-Zieger S, Thomas HM, Isbary G, Morfill GE, Harréus U, Zimmermann JL. Effects of cold atmospheric plasma on mucosal tissue culture. Journal of Physics D: Applied Physics 2013; 46(4):045401.

199. Boxhammer V, Li YF, Koritzer J, Shimizu T, Maisch T, Thomas HM, Schlegel J, Morfill GE, Zimmermann JL. Investigation of the mutagenic potential of cold atmospheric plasma at bactericidal dosages. Mutat Res-Gen Tox En 2013; 753(1):23-8.

200. Meyer B, Exner M, Gebel J. Re: Spread and persistence of *Clostridium difficile* spores during and after cleaning with sporicidal disinfectants. J Hosp Infect 2012; 80(2):185; author reply 6.

201. Büttgen S, Gebel J, Hornei B, Engelhart S, Koch ONJ, Exner M. Comparison of chemo resistance of *Clostridium difficile* ribotype 027 spores and *Bacillus subtilis* spores against desinfectants. Hyg Med 2008; 33(12):513-7.

202. Horejsh D, Kampf G. Efficacy of three surface disinfectants against spores of *Clostridium difficile* ribotype 027. International Journal of Hygiene and Environmental Health 2011; 214(2):172-4.

203. Chatuev BA, Peterson JW. Analysis of the sporicidal activity of chlorine dioxide disinfectant against *Bacillus anthracis* (Sterne strain). Journal of Hospital Infection 2010; 74(2):178-83.

204. Büttgen S, Gebel J, von Rheinbaben F, Hornei B, Engelhart S, Exner M. Efficacy of surface and instrument disinfectants with sporicidal claims against spores of *Clostridium difficile* ribotype 027. Hyg Med 2008; 33(5):194-200.

205. Ali S, Moore G, Wilson AP. Spread and persistence of *Clostridium difficile* spores during and after cleaning with sporicidal disinfectants. J Hosp Infect 2011; 79(1):97-8.

206. Wilcox MH, Fraise AP, Bradley CR, Walker J, Finch RG. Sporicides for *Clostridium difficile*: the devil is in the detail. J Hosp Infect 2011; 77(3):187-8.

207. Zimmermann JL, Shimizu T, Boxhammer V, Morfill GE. Disinfection Through Different Textiles Using Low Temperature Atmospheric Pressure Plasma. Plasma Processes and Polymers 2012; 9(8):792-8.

208. Donskey CJ. Does improving surface cleaning and disinfection reduce health care-associated infections? Am J Infect Control 2013; 41(5):S12-S9.

209. Otter JA, Yezli S, Salkeld JA, French GL. Evidence that contaminated surfaces contribute to the transmission of hospital pathogens and an overview of strategies to address contaminated surfaces in hospital settings. Am J Infect Control 2013; 41(5 Suppl):S6-11.

210. Dettenkofer M, Wenzler S, Amthor S, Antes G, Motschall E, Daschner FD. Does disinfection of environmental surfaces influence nosocomial infection rates? A systematic review. Am J Infect Control 2004; 32(2):84-98.

211. Dettenkofer M, Spencer RC. Importance of environmental decontamination - a critical view. Jorunal of Hospital Infection 2007; 65(S2):55-7.

212. Dettenkofer M, Daschner FD. Detergent versus hypochlorite cleaning and *Clostridium difficile* infection. Journal of Hospital Infection 2004; 56(1):78-9.

213. Allerberger F, Ayliffe GAJ, Bassett M, Braveny I, Bucher A, Damani N, Daschner FD, Dettenkofer M, Ezpeleta C, Gastmeier P, Geffers C, Giamarellou H, Goldman D, Grzesiowski P, Gubina M, Haanen PEM, Haydouchka I, Hübner J, Kalenic S, Van Knippenberg-Gordebeke G, Kranenburg AMH, Krcmery V, Kropec A, Krüger W, Lemmen S, Mayhall CG, Meester M, Meetar S, Munzinger J, Muzlovic I, Ojajarvi J, Rüden H, Scott G, Shah P, Tambic-Andraszevic A, Unertl K, Voss A, Weist K. Routine surface disinfection in health care facilities: Should we do it? Am J Infect Control 2002; 30(5):318-9.

214. Rutala WA, Weber DJ. Disinfection and sterilization: an overview. Am J Infect Control 2013; 41(5 Suppl):S2-5.

215. McDonnell G, Russell AD. Antiseptics and disinfectants: activity, action, and resistance. Clin Microbiol Rev 1999; 12(1):147-79.

216. Rupf S, Lehmann A, Hannig M, Schäfer B, Schubert A, Feldmann U, Schindler A. Killing of adherent oral microbes by a non-thermal atmospheric plasma jet. J Med Microbiol 2010; 59:206-12.

217. Koban I, Matthes R, Hübner N-O, Welk A, Meisel P, Holtfreter B, Sietmann R, Kindel E, Weltmann KD, Kramer A, Kocher T. Treatment of *Candida albicans* biofilms with low-temperature plasma induced by dielectric barrier discharge and atmospheric pressure plasma jet. New Journal of Physics 2010; 12:073039.

218. Sun Y, Yu S, Sun P, Wu H, Zhu W, Liu W, Zhang J, Fang J, Li R. Inactivation of Candida Biofilms by Non-Thermal Plasma and Its Enhancement for Fungistatic Effect of Antifungal Drugs PLoS One 2012; 7(7):e40629.

219. Alshraiedeh NH, Alkawareek MY, Gorman SP, Graham WG, Gilmore BF. Atmospheric pressure, nonthermal plasma inactivation of MS2 bacteriophage: effect of oxygen concentration on virucidal activity. Jorunal of Applied Microbiology 2013; 115(6):1420-26.

220. Venezia RA, Orrico M, Houston E, Yin S-M, Naumova YY. Lethal Activity of Nonthermal Plasma Sterilization Against Microorganisms. Infect Control Hosp Epidemiol 2008; 29(5):430-6.

221. Rowan NJ, MacGregor SJ, Anderson JG, Cameron D, Farish O. Inactivation of *Mycobacterium paratuberculosis* by Pulsed Electric Fields. Applied and Environmental Microbiology 2001; 67(6):2833-36.

222. Lessa FC, Gould CV, McDonald LC. Current Status of *Clostridium difficile* Infection Epidemiology. Clinical infectious diseases 2012; 55(S2):S65-70.

223. Polak M, Winter J, Schnabel U, Ehlbeck J, Weltmann K-D. Innovative Plasma Generation in Flexible Biopsy Channels for Inner-Tube Decontamination and Medical Applications. Plasma Processes and Polymers 2012; 9(1):67-76.

224. Bussiahn R, Brandenburg R, Gerling T, Kindel E, Lange H, Lembke N, Weltmann K-D, Von Woedtke T, Kocher T. The hairline plasma: An intermittent negative dc-corona discharge at atmospheric pressure for plasma medical applications. Applied Physics Letters 2010; 96:143701.

225. Schaudinn C, Jaramillo D, Freire MO, Sedghizadeh PP, Ngyuen A, Webster P, Costerton JW, Jiang C. Evaluation of a nonthermal plasma needle to eliminate *ex vivo* biofilms in root canals of extracted human teeth. International Endodontic Journal 2013; 46(10):930-7.

226. Pan J, Sun K, Liang Y, Sun P, Yang X, Wang J, Zhang J, Zhu W, Fang J, Becker KH. Cold plasma therapy of a tooth root canal infected with

Enterococcus faecalis biofilms in vitro. Journal of Endodontics 2013; 39(1):105-10.

227. WHO. WHO Guidelines on Hand Hygiene in Health Care. World Health Organization. 2009:

228. Kachrimanidou M, Malisiovas N. *Clostridium difficile* infection: a comprehensive review. Crit Rev Microbiol 2011; 37(3):178-87.

229. Kothari C, Gaind R, Singh LC, Sinha A, Kumari V, Arya S, Chellani H, Saxena S, Deb M. Community acquisition of beta-lactamase producing Enterobacteriaceae in neonatal gut. BMC Microbiol 2013; 13:136.

230. Giuffre M, Cipolla D, Bonura C, Geraci DM, Aleo A, Di Noto S, Nociforo F, Corsello G, Mammina C. Outbreak of colonizations by extended-spectrum beta-lactamase-producing *Escherichia coli* sequence type 131 in a neonatal intensive care unit, Italy. Antimicrob Resist Infect Control 2013; 2(1):8.

231. Rettedal S, Lohr IH, Natas O, Giske CG, Sundsfjord A, Oymar K. First outbreak of extended-spectrum beta-lactamase-producing *Klebsiella pneumoniae* in a Norwegian neonatal intensive care unit; associated with contaminated breast milk and resolved by strict cohorting. Apmis 2012; 120(8):612-21.

232. Oteo J, Cercenado E, Vindel A, Bautista V, Fernandez-Romero S, Saez D, Padilla B, Zamora E, Campos J. Outbreak of multidrug-resistant CTX-M-15-producing *Enterobacter cloacae* in a neonatal intensive care unit. J Med Microbiol 2013; 62(Pt 4):571-5.

233. van Nood E, Vrieze A, Nieuwdorp M, Fuentes S, Zoetendal EG, de Vos WM, Visser CE, Kuijper EJ, Bartelsman JF, Tijssen JG, Speelman P, Dijkgraaf MG, Keller JJ. Duodenal infusion of donor feces for recurrent *Clostridium difficile*. N Engl J Med 2013; 368(5):407-15.

234. Kelly CP, LaMont JT. *Clostridium difficile* - more difficult than ever. N Engl J Med 2008; 359(18):1932-40.

7 APPENDIX

7.1 List of figures

7.2 List of tables

8 PUBLICATIONS

1. **T. G. Klämpfl**, G. Isbary, Tetsuji Shimizu, Y.-F. Li, J. L. Zimmermann, W. Stolz, J. Schlegel, G. E. Morfill and H.-U. Schmidt. 2012. Cold Atmospheric Air Plasma Sterilization against Bacterial Endospores and other Microorganisms of Clinical Interest. Appl Environ Microbiol, 78(15):5077-5082. doi:10.1128/AEM.00583-12.

2. **T. G. Klämpfl**, T. Shimizu, S. Koch, Y.-F. Li, M. Balden, A. Mitra, J. L. Zimmermann, J. Schlegel, J. Gebel, G. E. Morfill, H.-U. Schmidt. Decontamination of nosocomial pathogens including *Clostridium difficile* spores on dry inanimate surface by cold atmospheric plasma. ***Submitted to AEM***

3. A. Mitra, Y.-F. Li, **T. G. Klämpfl**, T. Shimizu, J. Jeon, G. E. Morfill, J. L. Zimmermann. 2013. Inactivation of surface borne microorganisms and increased germination of seed specimen by Cold Atmospheric Plasma. Food Bioprocess Technol. doi: 10.1007/s11947-013-1126-4.

4. T. Maisch, T. Shimizu, G. Isbary, J. Heinlin, S. Karrer, **T. G. Klämpfl**, Y.-F. Li, G. Morfill, J. L. Zimmermann. 2012. Contact-Free Inactivation of Candida albicans Biofilms by Cold Atmospheric Air Plasma. Appl Environ Microbiol, 78(12):4242-4247. doi: 10.1128/AEM.07235-11.

5. Y.-F. Li, J. L. Zimmermann, **T. Klämpfl** and G. E. Morfill. 2012. Guiding of Reactive Plasma Species by Micro-Channels. Plasma Processes Polym, 9:1001–1005. doi:10.1002/ppap.201100182.

6. G. Isbary, J. Heinlin, T. Shimizu, J. L. Zimmermann, G. Morfill, H-U. Schmidt, R. Monetti, B. Steffes, W. Bunk, Y. Li, **T. Klämpfl**, S. Karrer, M. Landthaler, W. Stolz. 2012. Evaluation of 2 min cold atmospheric argon plasma treatment in a prospective randomized controlled trial on chronic infected wounds in patient. Br J Dermatol. doi: 10.1111/j.1365-2133.2012.10923.x.

7. V. Boxhammer, G. E. Morfill, J. R. Jokipii, T. Shimizu, **T. Klämpfl**, Y-F. Li, J. Köritzer, J. Schlegel and J. L. Zimmermann. 2012. Bactericidal action of cold atmospheric plasma in solution. New J Phys, 14. 113042 doi:10.1088/1367-2630/14/11/113042

8. J. Köritzer, V. Boxhammer, A. Schäfer, T. Shimizu, **T. G. Klämpfl**, et al. (2013) Restoration of Sensitivity in Chemo - Resistant Glioma Cells by Cold Atmospheric Plasma. PLoS ONE, 8(5): e64498. doi:10.1371/journal.pone.0064498.

9. G. Isbary, W. Stolz, T. Shimizu, R. Monetti, W. Bunk, H.-U. Schmidt, G.E. Morfill, **T. G. Klämpfl**, B. Steffes, H. M. Thomas, J. Heinlin, S. Karrer, M. Landthaler, J. L. Zimmermann. 2013. Cold atmospheric argon plasma treatment may accelerate wound healing in chronic wounds: Results of an open retrospective randomized controlled study in vivo. Clinical Plasma Medicine, 1(2):25-30. doi:10.1016/j.cpme.2013.06.001.

10. S. Shimizu, S. Barczyk, T. Shimizu, **T. Klämpfl**, J. L. Zimmermann, G. E. Morfill, P. K. H. Weber, P. Rettberg, H. Thomas. 2013. Cold Atmospheric Plasma - a New Technology for Spacecraft Component Decontamination. Planetary and Space Science, 90:60-71. doi: 10.1016/j.pss.2013.10.008.